

See discussions, stats, and author profiles for this publication at: <https://www.researchgate.net/publication/266030906>

Processing of nanostructured polymers and advanced polymeric based nanocomposites

ARTICLE *in* MATERIALS SCIENCE AND ENGINEERING R REPORTS · NOVEMBER 2014

Impact Factor: 15.5 · DOI: 10.1016/j.mser.2014.08.002

CITATIONS

20

READS

429

5 AUTHORS, INCLUDING:



Laura Peponi

ICTP CSIC

54 PUBLICATIONS 548 CITATIONS

[SEE PROFILE](#)



Debora Puglia

Università degli Studi di Perugia

114 PUBLICATIONS 1,421 CITATIONS

[SEE PROFILE](#)

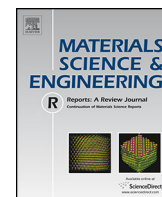


Jose M. Kenny

Università degli Studi di Perugia

631 PUBLICATIONS 10,191 CITATIONS

[SEE PROFILE](#)



Processing of nanostructured polymers and advanced polymeric based nanocomposites

Laura Peponi ^{b,*}, Debora Puglia ^a, Luigi Torre ^a, Luca Valentini ^a, José M. Kenny ^{a,b,c,*}

^a Materials Science and Technology Centre, University of Perugia, Loc. Pentima, 4, 05100 Terni, Italy

^b Institute of Polymer Science and Technology, ICP-T-CSIC, Juan de la Cierva, 3, 28006 Madrid, Spain

^c Institute of Macromolecular Compounds of the Russian Academy of Sciences, Bolshoy pr. 31, 199004 Saint-Petersburg, Russia



ARTICLE INFO

Article history:

Available online 14 September 2014

Guiding Editor: Philippe Dubois

Keywords:

Nanostructured polymers
Nanocomposites
Block copolymers
Processing
Carbon nanotubes
Graphene
Nanocellulose

ABSTRACT

The control of the nanostructure and the addition of nanoparticles to polymers have led to structural and functional property enhancements in a number of polymeric systems as a material answer to continuous requirements from advanced industrial sectors. The availability of new nanoparticles with extraordinary properties (i.e. carbon nanotubes, graphenes, but also nanoclays, nanocellulose, metals and ceramics) have determined new and exciting possibilities for a continuous enlargement of polymer markets. However, the potentialities of these new materials are still strongly dependent on the development and scaling-up of reliable processing routes. Therefore, the purpose of this report is to review the main processing approaches for nanostructured polymers and nanocomposites starting with a brief review of available nanoparticles and on their functionalization to promote a better polymer–particle interaction. Regarding processing, the review firstly addresses the bottom-up approaches typically adopted for nanostructured polymers, blends and copolymers. Then, the different technologies required by the top-down processing of thermoplastic and thermosetting polymer matrix systems are reviewed. Finally, the report addresses the recent applications of nanostructured polymers and nanocomposites as matrices of advanced composite materials. In all cases, the main processing approaches and the main structural and functional properties characterizing these materials and their potential and current industrial applications are specifically addressed.

© 2014 Elsevier B.V. All rights reserved.

Abbreviations and symbols: AFM, atomic force microscopy; APTS, aminopropyltriethoxysilane; ATRP, atom transfer radical polymerization; BC, block copolymer; BCC, body-centered cubic structure; BGY, Born–Green–Yvon theory; CEC, cation exchange capacity; CNC, cellulose nanocrystal; CNF, cellulose nanofibril; CNS, cellulose nanostructure; CNT, carbon nanotube; CNW, cellulose nanowhisker; CCVD, catalytic chemical vapor deposition; CVD, chemical vapor deposition; DDM, diaminodiphenyl methane; DDS, 4,4'-diaminodiphenylsulfone; DETA, diethylenetriamine; DGEBA, diglycidyl ether of bisphenol A; DMF, dimethylformamide; DPD, dissipative particle dynamics; DT, dodecanethiol; DTA, dodecyltrimethylammonium; E, Young's modulus; EFM, electrostatic force microscopy; FITC, fluorescein-5-isothiocyanate; FRP, fiber reinforced polymer; FTIR, Fourier transform infrared spectroscopy; GFET, graphene field-effect transistor; GFRP, glass fiber reinforced polymer; GNP, graphite nanoplatelet; GO, graphene oxide; GONP, oxidized graphite nanoplatelet; GRAPOSS, graphene-POSS hybrid; HDT, heat distortion temperature; HEX, hexagonal microphase (cylinders); HRR, heat release rate; ISO, International Organization for Standardization; ITO, indium tin oxide; kB, Boltzmann constant; LAM, lamellar morphology; MCDEA, 4,4'-methylene bis(3 chloro 2,6 diethylaniline); MFC, microfibrillated cellulose; MMT, montmorillonite; MWCNT, multiwall carbon nanotube; N, degree of polymerization; NMP, N-methyl pyrrolidone; NP, nanoparticle; PB, polybutadiene; PBT, poly(butylene terephthalate); PCL, poly(ϵ -caprolactone); PDMS, polydimethylsiloxane; PE, polyethylene; PEDOT, poly(3,4-ethyldioxythiophene); PEE, poly(phenylene ether); PEI, poly(ethylene imine); PEO, poly(ethylene oxide); PEP, poly(ethylene-alt-propylene); PLA, polylactide; PLLA, poly(L-lactide); PMMA, poly(methyl methacrylate); POSS, polyhedral oligomeric silsesquioxane; PPE, poly(phenylene ether); PPO, poly(propylene oxide); PPy, polypyrrole; PS, polystyrene; PSS, poly(styrene sulfonic acid); PTMO, poly(tetramethylene oxide); PU, polyurethane; PVA, poly(vinyl acetate); PVCH, poly(vinyl cyclohexane); P3HT, poly(3-hexylthiophene); rGO, reduced graphene oxide; RIFT, resin infusion under flexible tool; ROP, ring-opening polymerization; Rs, surface resistivity; RTM, resin transfer molding; SAXS, small angle X-ray scattering; SBS, poly(styrene-*b*-butadiene-*b*-methyl methacrylate); SBS, poly(styrene-*b*-butadiene-*b*-styrene); SCRIMP, Seemann® composites resin infusion molding process; SEBS, poly(styrene-*b*-ethylene-*b*-butylene-*b*-styrene); SEM, scanning electron microscopy; SBS, poly(styrene-*b*-isobutylene-*b*-styrene); SIS, poly(styrene-*b*-isoprene-*b*-styrene); SMMA, styrene-*b*-(methyl methacrylate); SWCNT, single walled carbon nanotube; T, temperature; TEMPO, 2,2,6,6-tetramethylpiperidine-1-oxyl; T_g, glass transition temperature; TGA, thermo gravimetric analysis; TGDDM, tetraglycidyl-4,4-diaminodiphenylmethane; TEM, transmission electron microscopy; TPE, thermoplastic elastomer; TPU, thermoplastic polyurethane; TRG, thermal reduced graphene; UV, ultraviolet; UV-vis, ultraviolet-visible; VARIM, vacuum assisted resin infusion method; VARTM, vacuum assisted resin transfer molding; wAB, interaction energy between monomers A and B; XRD, X-ray diffraction; Z, number of the nearest neighbors of the copolymer configurational cell; ϕ_A , volume fraction of component A; χ , Flory–Huggins interaction parameter; σ , tensile strength; 0D, zero-dimensional; 1D, one-dimensional; 2D, two-dimensional; 3D, three-dimensional.

* Corresponding authors at: Instituto de Ciencia y Tecnología de Polímeros, ICP-T-CSIC, C/Juan de la Cierva, 3, 28006 Madrid, Spain. Tel.: +34 912587424; fax: +34 915644853.

E-mail addresses: lpeponi@ictp.csic.es (L. Peponi), kenny@ictp.csic.es (J.M. Kenny).

Contents

1. Introduction	2
1.1. Top-down and bottom-up processing of polymer nanocomposites	2
1.2. Classification and properties of main nanoparticles	3
1.2.1. Nanoclays	3
1.2.2. Metal and ceramic nanoparticles	5
1.2.3. Carbon nanotubes	6
1.2.4. Graphene	7
1.2.5. Nanocellulose	7
1.3. Functionalization of nanoparticles	9
1.3.1. Covalent functionalization	9
1.3.2. Non covalent functionalization	11
2. Bottom-up nanostructuration	12
2.1. Nanostructured copolymers and their nanocomposites	13
2.1.1. Block copolymer thin films	15
2.1.2. Nanostructured block copolymers in solution	15
2.1.3. Nanocomposites based on BC	16
2.2. Nanostructured thermoplastics and blends	20
2.3. Nanostructured thermosets and blends	21
3. Top-down processing of thermosetting matrix nanocomposites	23
3.1. Dispersion of nanoparticles in thermosetting polymers	23
3.1.1. Dispersion of nanoclays in thermosetting matrices	23
3.1.2. Dispersion of carbon nanotubes in thermosetting matrices	23
3.1.3. Dispersion of graphenes, direct exfoliation and chemical reduction of graphite oxide in thermosetting matrices	24
3.1.4. Dispersion of nanocellulose in thermosetting matrices	24
3.2. Properties and applications of thermosetting matrix nanocomposites	25
3.2.1. Mechanical and electrical properties	25
3.2.2. Thermal properties	28
4. Top-down processing of thermoplastic matrix nanocomposites	29
4.1. Dispersion of nanoparticles in matrices	29
4.1.1. Dispersion of nanoclays in thermoplastic matrices	29
4.1.2. Dispersion of carbon nanotubes in thermoplastic matrices	30
4.1.3. Dispersion of graphenes, direct exfoliation and chemical reduction of graphite oxide in thermoplastic matrices	30
4.1.4. Dispersion of nanocellulose in thermoplastic polymers	31
4.2. Properties and applications of thermoplastic matrix nanocomposites	32
4.2.1. Processing of thermoplastic matrix nanocomposites	32
4.2.2. Main properties and applications of thermoplastic matrix nanocomposites	32
5. Processing of advanced composites with nanostructured matrices	34
6. Summary and perspectives	37
Acknowledgements	38
References	38

1. Introduction

1.1. Top-down and bottom-up processing of polymer nanocomposites

Nanostructured polymers and hybrid inorganic–organic nanocomposites have gained popularity in the last two decades due to their exciting bulk and surface properties. The control of the nanostructure of polymers and the addition of nanoparticles has led to structural and functional property enhancements in a number of polymer systems as a material answer to continuous requirements from advanced industrial sectors. The availability of new nanoparticles with extraordinary properties (i.e. carbon nanotubes, graphenes, but also nanoclays, nanocellulose, metals and ceramics) have determined new and exciting possibilities for a continuous enlargement of polymer markets. However, the potentialities of these new materials are still strongly dependent on the development and scaling-up of reliable processing routes. In fact, it has been already assessed that the bottleneck for the exploitation of the theoretical excellent properties of polymer nanocomposites is the complete dispersion of the nanoparticles in the matrix and the consequent development of a huge interfacial area. This complete dispersion will allow maximizing the available matrix–particle interphase optimizing then the organic–inorganic interaction, responsible of the enhanced properties of the final

material. So, most of the research efforts in this area have been focused on developing rational processing strategies for nanostructured polymers and nanocomposites and in promoting better matrix–particle interactions.

Since the extraordinary development of polymer nanocomposites, more than two decades ago, many reviews have been published in the scientific literature on this topic. Several of these reviews have been focused on the different processing aspects and on the processing–structure–properties relationships of these specific materials [1–13]. However, most of them are concentrated on a particular type of matrix or nanofillers and none of them report a comprehensive analysis of the physicochemical fundamentals affecting the processing behavior of polymer nanocomposites.

Bottom-up and top-down approaches have been typically reported for material nanotechnologies. In particular, it must be evidenced that polymer nanotechnologies are characterized by a predominant top-down approach. In fact, the application of typical processing technologies like extrusion (and other similar melt mixing processes) are clear top-down processes where ingredients (polymer and nanoparticles) are introduced and macroscopically melt mixed in the equipment. The quality of the dispersion is given by macroscopic processing factors like equipment design, mixing velocity, residence time, etc. with very limited possibilities for

processing optimization. On the other hand, self-assembling is not easily achieved in polymer materials due to the complex morphology of the polymer chains and to their complex interaction with nanoparticles. In fact, few bottom-up approaches have been reported and typically regard polymer and block copolymer nanostructuration by phase separation and reactive processing among others, with very few real applications.

Following the research priorities described above, the aim of this report is to review the main processing approaches for nanostructured polymers and nanocomposites starting with a brief review of available nanoparticles focusing our search on their functionalization to promote a better polymer-particle interaction. It is clear that nanostructured polymers and hybrid inorganic-organic nanocomposites are a very large subject. Numerous organic or inorganic nanoparticles can be used. Therefore, we have limited our subject to the most relevant nanoparticles and matrices in terms of availability, properties and relevant applications. In particular some important nanostructures as for example core-shell nanoparticles, liquid crystals, carbon black, some ceramic particles with advanced optical properties, etc. are excluded from this review in sake of a higher emphasis on how the processing approaches can provide a valid technological route to maximize the final properties of polymer matrix nanocomposites. Regarding processing, the review firstly addresses the bottom-up approaches typically adopted for the processing of nanostructured polymers, blends and copolymers. Then, the different technologies required by the top-down processing of different types of polymer matrices (i.e. thermoplastics, thermosets) are reviewed. Finally, the review focuses on the recent applications of nanostructured polymers and nanocomposites as matrices of advanced composite materials. In all cases, the main processing approaches and the main structural and functional properties characterizing these materials and their potential and current industrial applications are specifically addressed. The review ends with a summary, recommendations and future perspective of this relevant and continuously growing research sector. Evidently, this research topic is highly dynamic and continuous scientific and technological developments are reviewed and reported in the literature. As an example, during the preparation of the final version of this review new contributions have been published on the processing of carbon nanotube nanocomposites [14–16], graphene nanocomposites [16–18], clay

nanocomposites [19–22]. Environmental issues are also been continuously reviewed [23].

1.2. Classification and properties of main nanoparticles

1.2.1. Nanoclays

Among all the available nanofillers for polymer nanocomposites, those derived from layered silicates (nanoclays) are the most studied. LeBaron and co-workers [24], Giannelis and co-workers [25], Alexandre et al. [26] and, in more recent years, Pavlidou and co-workers [10] widely reviewed the processing and characterization of clay based nanocomposites, highlighting the benefits that nanoclays can produce to different polymeric matrices. In fact, compared with the pure polymers or conventional composites, by adding small amounts of clay nanofillers it is possible to achieve consistent increments of elastic modulus and strength, decrease the gas permeability, improve solvent and heat resistance and increase the flame retardancy characteristics. Clay minerals are generally composed by phyllosilicates that can be divided into four groups that mainly differ in the crystalline structure: kaolinite group, montmorillonite/smectite group, illite group and chlorite group [27,28]. Among them, montmorillonites are the most investigated for their potentially high aspect ratio and the unique intercalation/exfoliation characteristics [27].

Montmorillonites are clay minerals having 2:1 sheet-structure: an octahedral sheet of alumina is sandwiched between two silica tetrahedral sheets sharing with them an oxygen atom [27–29]. The silica tetrahedral sheet consists of SiO_4 groups linked to form a hexagonal network of repeating units of composition Si_4O_{10} ; the alumina sheet consists of two planes of close packed oxygen atoms or hydroxyls between which octahedral coordinated aluminum atoms are embedded in [30]. These three sheets form one clay layer called tactoid. Its thickness is around 1 nm and the lateral dimensions may vary from 300 Å to several microns depending on the particulate silicate, the source of the clay and the method of preparation. Therefore, the aspect ratio of these layers (ratio length/thickness) is particularly high, with values higher than 1000 [26,31,32]. The typical structure of the layered silicate is shown in Fig. 1 where it is possible to observe that each tactoid of the clay is separated from its neighbors by a van der Waals gap called gallery or interlayer that is usually occupied by cations. These cations counterbalance the negative charge generated by the isomorph

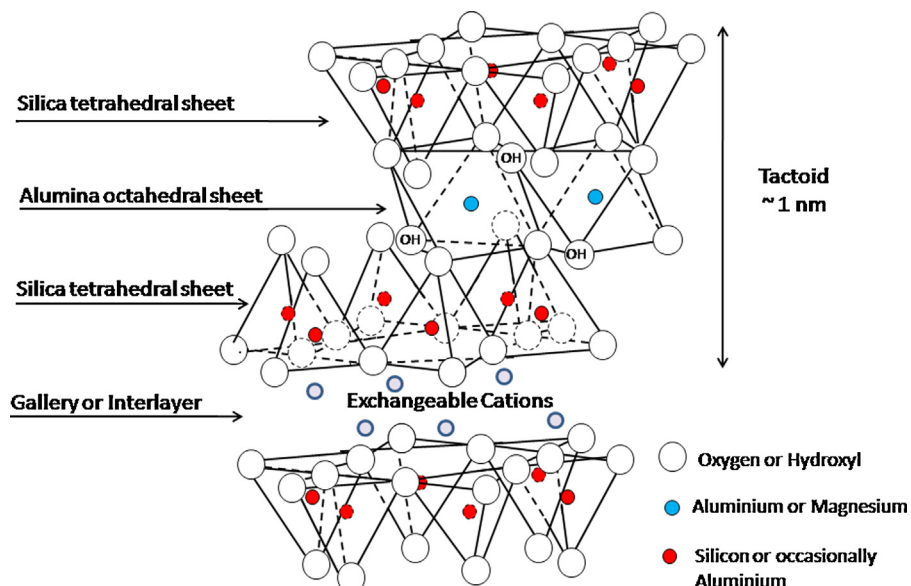


Fig. 1. Schematic structure of montmorillonite.

substitution of the atoms forming the crystal (for example in montmorillonite Mg^{2+} in the place of Al^{3+}) [33–36].

In pristine layered silicates, the interlayer cations are usually hydrated Na^+ or K^+ ions that make the clay hydrophilic and consequently incompatible with most polymers [37] that exhibit a hydrophobic behavior. Therefore, layered silicates first need to be organically modified to produce polymer-compatible clay (organoclay) [38]. In fact, it has been well demonstrated that the replacement of the inorganic exchange cations in the interlayers of the native clay silicate structure by alkyl-ammonium, sulfonium or phosphonium surfactants, can compatibilize the surface chemistry of the clay and the polymeric matrix [24,26,33,39]. Moreover, surfactants lower the surface energy of the clay enhancing the wettability. Since these cations arranged in the interlayers are generally longer and/or bigger than the originally cations, they increase the gap between the layers and facilitate the penetration of the polymer molecules [24]. Furthermore, alkyl ammonium or alkyl phosphonium groups can be linked to functional groups that can interact with the polymer or promote the polymerization of the monomer [3]; the result is an increment of the interface resistance between the tactoids and the polymer resulting in an improvement of the final characteristics of the nanocomposite [25].

The amount of surface charge present on the layers of clays, called cation exchange capacity (CEC), is another parameter that affects the interlayer space: generally, the gap grows with the growth of the CEC or the length of the organic tail of the “onium” ion surfactant. Pavlidou [10] reported that X-ray diffraction tests have demonstrated that different arrangements of the “onium” ions are possible in the interlayer: depending on the charge density of the clay (Fig. 2), the “onium” ions may lie parallel to the clay surface as a monolayer (Fig. 2a), or form a lateral bilayer (Fig. 2b), or form a mono- (Fig. 2c) or a bi-molecular inclined paraffin structure (Fig. 2d) [26].

However, any physical mixture of a polymer and silicate does not necessarily form a nanocomposite, because separation into discrete phases normally occurs and the formation of particle agglomeration tends to reduce the final properties of the material [1] that behaves as a traditional filled polymer (microcomposite) [37]. As just said, the organically modified clays allow the polymer

chains to penetrate within the galleries and to outdistance the single tactoids from one another. However, the ability of organic chains to intercalate within the interlayer of the montmorillonite principally depends on the nature of the components (polymer and clay) and on the method of preparation of the nanocomposite. Depending on the degree of polymer penetration into the galleries, it is possible to obtain two morphologies: intercalated or exfoliated (Fig. 3). If the penetration of polymeric chains leads up to a finite expansion of the silicate layers (less than 20–30 Å), the structure is defined intercalated: it consists of ordered multilayers of alternating polymer/silicate with a repeated distance of few nanometers. If the penetration of polymer leads to a delamination of silicate tactoids (separated by 80–100 Å or more), the final structure is defined exfoliated: individual tactoids are dispersed in the polymeric matrix [1,26,35,38]. These two types of polymer-layered silicate nanocomposites are schematically presented in Fig. 3. It is well known that the best combination of property improvements was observed in exfoliated nanocomposites [35,39] because of the high surface area of the single tactoid. However, modification of nanoclays is not enough to obtain a complete exfoliation of the layers; it strongly depends on the techniques used during the nanocomposite preparation.

Nowadays the principal methods of preparation can be summarized in four techniques: in situ template synthesis, intercalation of polymer from solution, in situ polymerization and melt intercalation.

The first one consists in the synthesis of the clay within the polymer matrix using mainly sol-gel techniques. The process consists in the nucleation and growth of the inorganic crystals in the polymer that become trapped within the layers as they grow [26,32]. In the second technique, the silicates are exfoliated into single layers using a solvent in which the polymer or pre-polymer are soluble: after the organoclay has swollen in the solvent, the polymer is added to the solution and intercalates between the clay layers. Finally, the solvent is removed and the inorganic sheets reassemble sandwiching the polymer and forming a nanocomposite structure [26,40–42]. In the in-situ polymerization, the modified layered silicate is swollen by a liquid monomer solution. The monomer migrates into the galleries of the layered silicate and

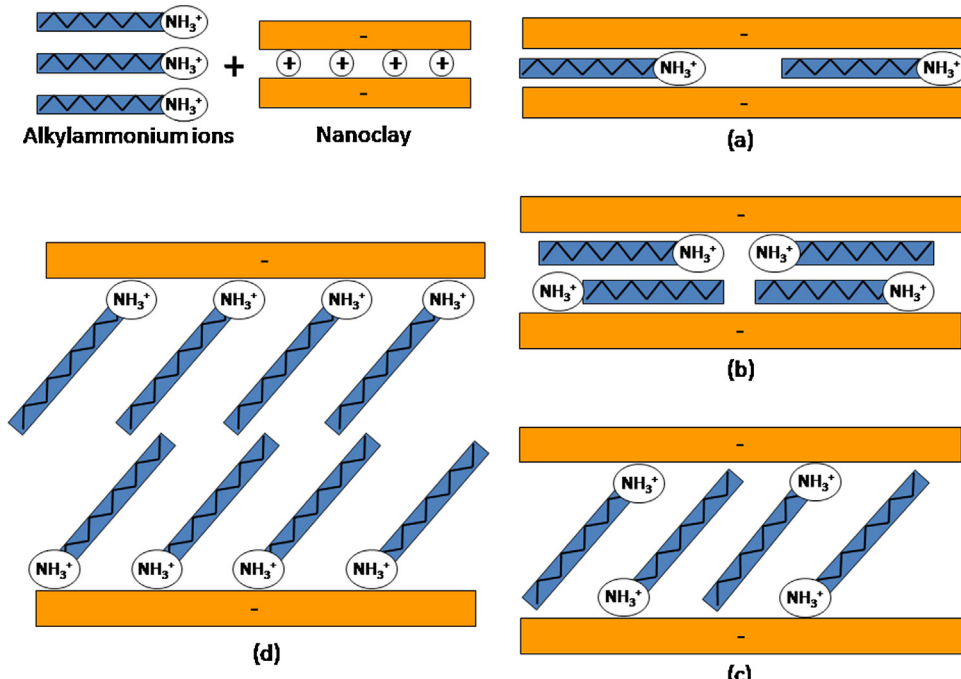


Fig. 2. Schematic representation of possible arrangements of “onium” ions in the nanoclay interlayer.

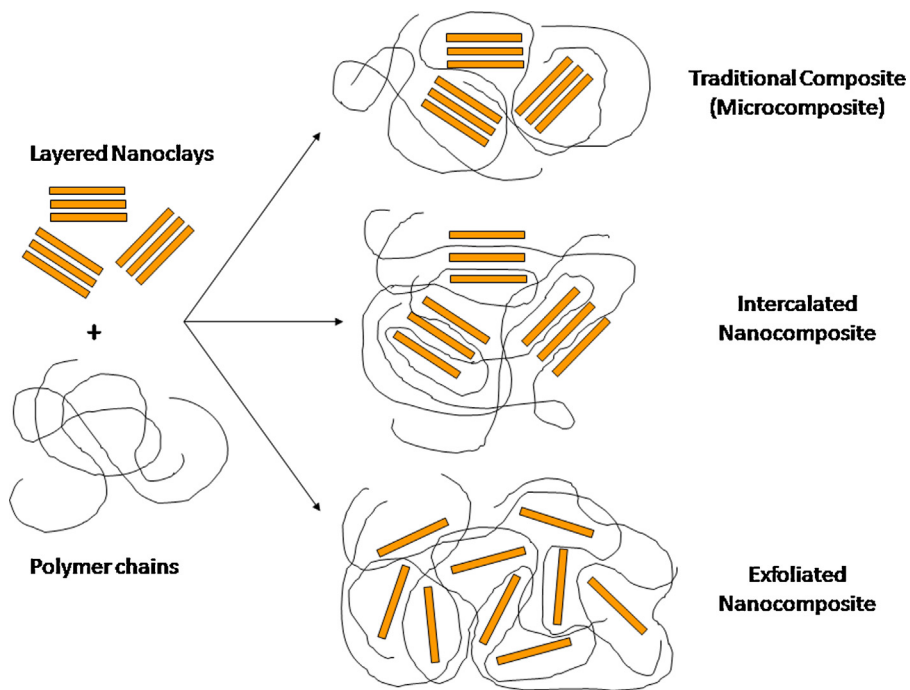


Fig. 3. Schematic representation of nanocomposite morphologies.

then the polymerization reaction occurs between the intercalated sheets producing long-chain polymers within the clay galleries. If intra- and extra-gallery polymerization rates are properly balanced, the clay layers delaminate and the resulting material possesses a disordered structure [26,31]. The last procedure consists of blending the layered silicate with the polymer matrix in the molten state. If the layer surfaces are sufficiently compatible with the chosen polymer, the polymeric chains can move into the interlayer space and form an intercalated or an exfoliated nanocomposite [26,31]. In order to evaluate if the processing method has led to a good intercalation/exfoliation of the layered silicates, two techniques are commonly used to characterize the structure of nanocomposite: X-ray diffraction (XRD) and transmission electron microscopy (TEM) [3,26,43]. The first one allows the determination of the spaces between structural layers of the silicate utilizing Bragg's law: in comparison with the spacing of the pristine organoclay, the intercalation of the polymer chains increases the interlayer spacing, leading to a shift of the diffraction peak to lower angles. Furthermore, the layer separation associated with exfoliated structures, breaks the layer stacking and results in a diffraction pattern in which no more diffraction peaks are visible [26,44]. On the other hand, with TEM analysis, it is possible to appreciate directly the internal structure, morphology and defect structures of nanoclays [44].

1.2.2. Metal and ceramic nanoparticles

Nanoparticles are used in a broad spectrum of applications, which require a precisely defined, narrow range of particle sizes distribution and dispersion. Therefore, carefully defined production and reaction conditions are crucial in obtaining such size-dependent particle features. Main parameters controlling particle size, chemical composition, crystallinity and shape include temperature, pH, concentration, chemical composition, surface modifications and process control. The basic top-down and bottom-up strategies for the production of nanoparticles already mentioned can be also applied to the manufacturing of metal and ceramic nanoparticles. Specifically in the top-down approach, the mechanical production approach uses milling to crush microparticles. This approach

traditionally applies to producing metallic and ceramic nanomaterials. For metallic nanoparticles, for example, traditional source materials (such as metal and metal oxides) are pulverized using high-energy ball mills that yield powders with a relatively broad particle-size ranges; so, in general, this method does not allow full control of the particle shape. In the bottom-up strategy, structures are built up by chemical processes and this approach produces selected, more complex structures from atoms or molecules, better controlling sizes, shapes and size ranges. It includes aerosol processes, precipitation reactions and sol-gel processes [45].

The synthesis methods of metal and ceramic nanoparticles can be also classified according to the nature of the process (physical, chemical, biological e.g. biomineratization) [45–50], the energy source (laser [51,52], plasma [53–56], ion sputtering [57], electron beam [58], microwave [53], hydrothermal [59], freeze drying [60], high-energy ball milling [61], combustion, flame [62,63], supercritical [64]) or the media (synthesis in gas [65], in liquid [66] or in solid [67,68]).

Metal nanoparticles have been extensively employed in polymer matrices to produce nanocomposites with several functional properties [69]. Nano-sized metals have special characteristics that can be exploited for a number of advanced functional applications. However, the difficult handling of these incredible small objects has represented a strong limitation to their use. In addition, most of nano-sized metals are very instable. They can aggregate because of the high surface free energy and can be oxidized contaminated by air, moisture, SO₂, etc. The embedding of metal nanoparticles into dielectric matrices represents a valid solution to the manipulation and stabilization problems [69,70].

Metals undergo the most considerable property change by size reduction, and their composites with polymers are very interesting for functional applications. The new properties observed in nano-sized metals (mesoscopic metals) are determined by quantum-size effects (i.e. electron confinement and surface effect). These properties are size-dependent and can be simply tuned by changing the nanoparticles dimension. Surface effects become predominant because with a decrease in size, matter consists more and more of surface atoms than of inner atoms. As a result,

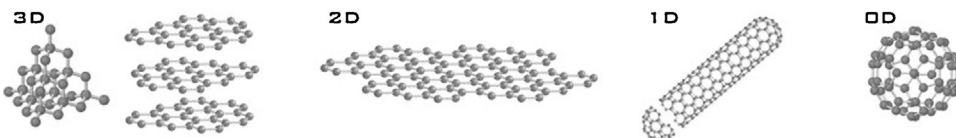


Fig. 4. Crystal structures of the different allotropes of carbon. From left to right: Three-dimensional diamond and graphite (3D); two-dimensional graphene (2D); one-dimensional nanotubes (1D); and zero-dimensional buckyballs (0D) (from Ref. [88]).

the matter properties slowly switch from that determined by the characteristics of inner atoms to that belonging to surface atoms. In addition, the surface nature of a nano-sized object significantly differs from that of a massive object. Atoms on the surface of a massive crystalline solid are principally located on basal planes, but they transform almost completely in edge and corner atoms with a decrease in size. Because of the very low coordination number, edge and corner atoms are highly chemically reactive, supercatalytically active and highly polarizable, in comparison with atoms on basal planes. Because of quantum-size effects, mesoscopic metals show a set of properties completely different from that of their massive counterpart. Particularly interesting are the size-dependent ferromagnetism and the superparamagnetism characterizing all metals (included diamagnetic metals like silver); the chromatism observed with silver, gold, and copper metals due to plasmon absorption; the photo and thermoluminescence; and the supercatalytic effect. Many of these unique physicochemical characteristics of nano-sized metals leave unmodified after embedding in polymers (e.g. optical, magnetic, dielectric, and thermal transport properties), and therefore they can be used to provide special functionalities to polymers. In the ex situ processes, metal nanoparticles are chemically synthesized and their surface are organically passivated. The derivatized nanoparticles are dispersed into a polymer solution or liquid monomer that is then polymerized. For the comprehension of mechanisms involved in the appearance of novel properties in polymer-embedded metal nanostructures, their characterization represents the fundamental starting point. Most metal clusters are characterized by the surface plasmon resonance, which is an oscillation of the surface plasma electrons induced by the electromagnetic field; consequently, their microstructure can be indirectly investigated by optical spectroscopy (UV-vis spectroscopy) [71–74].

The production of nanoparticles of practically all metals has been reported in the last decades, but the more diffused metals for polymer nanocomposites are silver, gold, platinum, iron, copper, etc., while the main functionalities developed for polymer matrix nanocomposites are conductivity [75,76], antibacterial [77,78], magnetic [79], catalytic [80], etc.

Examples of ceramic nanoparticles are nanocrystalline Al_2O_3 , ZrO_2 , SiC , Si_3N_4 , TiO_2 , titanates, ferrites and others (CeO_2 , Y_2O_3 , ZnO , AlN), but the most common, because of their larger-scale production, are undoubtedly silica (SiO_2), titanium dioxide (TiO_2) and zinc oxide (ZnO). They are used in many fields, including rheology (SiO_2), as active agents and additives in the plastics and rubber industries (SiO_2) [81,82], in sunscreens (TiO_2 , ZnO) [83,84] and in multifunctional paints and coatings (TiO_2) [85–87]. Some structures display interesting properties, allowing potential applications to be envisioned in various fields: sensors, optoelectronics, transducers, medicine as it will discussed later.

1.2.3. Carbon nanotubes

Between the elements in the periodic table, carbon is one of the most fascinating and it plays a crucial role in nature [88]. One of the most important capabilities of the carbon atom, which is fundamental for the existence of the known forms of life, is its trend to organize itself in special networks [89]. The different possible structures with carbon are numerous and their behavior

could be very complex. The most common studied hybridization of carbon atom are sp^3 (i.e. diamond) and sp^2 (i.e. graphite). Some of them such as nanostructured carbon materials, as fullerenes [90–92], carbon nanotubes (CNT) [93] and individual graphene sheets [94] were discovered 10–20 years ago and are currently a focus of attention for many physicists and chemists.

Thus, only three-dimensional (diamond, graphite), one-dimensional (nanotubes), and zero-dimensional (fullerenes) allotropes of carbon were known until few years ago. The two-dimensional form (graphene) was missing for long time, resisting any attempt at experimental observation even if, probably, it was the theoretically best-studied carbon allotrope. Only in the last decade, graphene was obtained in laboratory attracting a great deal of attention [94]. Fig. 4 shows the crystal structure of the different carbon allotropes.

With the dawn of nanoscience and nanotechnology now unfolding, we are still finding new properties for carbon nanostructures developing numerous applications in various areas such as material and biomedical sciences, electronics, optics, magnetism, energy storage, and electrochemistry. As it is well known, ultra small building blocks have been found to exhibit a broad range of enhanced mechanical, optical, magnetic and electronic properties compared to coarser-grained matter of the same chemical composition. In particular, composites based on carbon nanotubes represent the most promising class of new carbon-based materials for electronic and optic nanodevices as well as reinforcement nanocomposites.

For this kind of applications, we focus here on one special form of carbon that intrigued many scientists over the years: the sp^2 -hybridized carbon in the form of graphene and carbon nanotubes. The first goal in the field of nanocomposites has been to find appropriate solutions to treat CNT to improve their dispersion into solvents (to avoid the formation of bundles and aggregation) and into polymers and to find the best way to exfoliate graphene in order to have a one-layer thickness material. In addition, an appropriate choice of the deposition technique and the parameters linked to it are fundamental for a successful nanocomposite production.

Carbon nanotubes, as said before, are one of the allotropic forms of graphene [93]: a single walled carbon nanotube (SWCNT) can be considered as a graphene sheet rolled up into a cylinder (Fig. 4), with fullerene-like end cap with hexagonal and pentagonal faces. Depending on the chirality along the graphene sheet, they can be either semiconducting or metallic respect to the electronic states [95]. Both, experiments and theory have demonstrated that SWCNT possess high mobility (about $100,000 \text{ cm}^2/\text{V}\cdot\text{s}$) [96], high conductivity (up to $400,000 \text{ S/cm}$) and, for semiconducting nanotubes, tube diameter-dependent band gap ($E_{\text{gap}} \approx 1/R_{\text{tube}}$ more or less $0.6 \text{ eV}/d$) [97,98], while for metallic CNT a secondary band gap exists and varies with diameter as $1/R^2$ [99].

Physical properties of CNT and device integration of these nanoscale materials have been widely and deeply studied, while thin CNT films are a new field with high research interest and with the advantage of statistical averaging for better reproducibility [100–103]. For instance, films with thickness in the range of 10–100 nm show high optical transparency and electrical conductivity and can be used as a replacement for indium-tin-oxide (ITO) electrodes in polymer based flexible electronic devices [104,105].

1.2.4. Graphene

Graphene is the starting point for all calculations on graphite, carbon nanotubes and fullerenes [88]. At the same time, numerous attempts to synthesize these two-dimensional atomic crystals have usually failed, ending up with nanometer-size crystallites [106].

A flake of graphene was isolated for the first time in 2004 by a group of physicists from Manchester University, UK, led by Geim and Novoselov [94]. They used a top-down approach, which lead to a revolution in the field. From three-dimensional graphite they could extract a single sheet (a monolayer of atoms) using a technique called micromechanical cleavage [94,107]. In fact, graphite is a layered material and can be viewed as a stack of two-dimensional graphene crystals weakly coupled. By using this method and starting with large, three-dimensional crystals, the researchers avoided all the issues with the stability of small crystallites.

The atomic structure of graphene is characterized by two types of C–C bonds (σ ; π) constructed from the four valence orbitals (2s, px, py, 2pz), where the z-direction is perpendicular to the sheet. Three strong σ -bonds join a C atom to its three neighbors, giving rise to 120° C–C–C bond angles. In addition, the C–C bonding is enhanced by a fourth bond associated with the overlap of pz (or π) orbitals [108]. As said before, stacked layers of graphene constitute bulk graphite. A unit cell in graphite is represented by two layers. The 3D structure of graphite is therefore held together by a weak interlayer van der Waals force, giving a spacing of 0.335 nm. With no real chemical bonding in the c-direction, out-of-plane interactions are extremely weak [109]. This includes the propagation of charge and thermal carriers, which leads to out of plane electrical and thermal conductivities that are both more than 10^3 times lower than those of their in plane analogue. High in plane electrical of $\approx 10^4 \Omega^{-1} \text{ cm}^{-1}$ and thermal conductivity ($\approx 3000 \text{ W/mK}$) are reported for graphite [109].

As explained before, graphene exhibits exceptional properties due to its unique structure, a 2D honeycomb lattice composed by sp² hybridized carbon atoms. Graphene is a zero-gap semimetal and it shows an optical absorbance of just 2.3% [110,111]. The Young's modulus was found to be $E = 1 \text{ TPa}$ [112] and the breaking strength $\sigma = 42 \text{ N/m}$ [113].

Due to the hydrophobic nature of graphene, producing single-layer graphene by solution-based processes is a great challenge. The first works reported on the exfoliation of graphite were not related to pure graphene but to graphene oxide (GO) obtained by chemical modification of graphite to produce a water dispersible intermediary [114]. After oxidation by Hummers method (involving strong acids and oxidants), the resulting GO was a layered stack, which completely exfoliated in water upon the addition of mechanical energy [115]. The production of conductive films/composites using the insulating graphene oxide requires restoring its electrical conductivity. This major issue can be achieved by thermal annealing, UV irradiation or by treatment with chemical reducing agents, as hydrazine hydrate [116,117].

The advantage of using GO is the low-cost of chemically converted graphene suspensions that has permitted to investigate a large number of deposition techniques for film production [118]. Among these techniques, spray coating has been reported [119]. The production of a freestanding GO film with an extremely high tensile strength up to $\approx 42 \text{ GPa}$ has also been reported [120]. All these methods have been used to produce films with coverage ranging from evenly spaced single sheets to densely packed overlapping films. Ferrari et al. [121] produced reduced-GO films by spin-coating achieving a sheet resistance in the 10^2 – $10^3 \Omega/\text{L2}$ range and a transmittance $> 80\%$ over 400–1800 nm. GO films deposited by dip coating and reduced by thermal annealing, achieved a sheet resistances as low as $0.9 \text{ k}\Omega/\text{L2}$ and a 70% transmittance over 1000–3000 nm [122].

For what concerns polymer nanocomposites, reduced single graphene sheets were first used as additive for polystyrene-based composites [114]. The two-dimensional geometry led to an extremely low percolation threshold of only 0.1%, enhancing both the conductivity and strength of the matrix. The first example of transparent and conducting ceramic graphene-based composite was shown by Watcharotone [123], who prepared graphene-silica composite spun-cast thin films with a bulk conductivity of 0.45 S/cm.

The oxidation process results in the formation of structural defects that alter the electronic structure of graphene so much that the high conductivity of graphene can never be restored. Therefore, the liquid phase exfoliation of graphene without oxidation has been developed. The defect-free monolayer graphene can be produced in certain solvents, such as N-methyl-pyrrolidone (NMP), whose surface energy is well matched to that of graphene [124,125]. However, these solvents are expensive, require special care when handling and have high boiling points, making the deposition difficult. Liquid phase exfoliation in surfactant/water solutions has been also achieved by Lotya et al. [126]. Both, graphene exfoliated in NMP [124] and in water [126], have been tested as semi-transparent conducting films and in conducting composites; the best performance ($R_s = 22.5 \text{ k}\Omega/\text{L2}$ after annealing coupled with transparency $\approx 62\%$) was achieved for graphene prepared in aqueous solutions [126].

Some alternative methods to produce graphene films and composites have been also developed. Gilje et al. [127] produced stretchable transparent electrodes by direct synthesis of large-scale graphene films using CVD on thin nickel layers. The films, transferred via a PDMS stamp onto glass, showed $R_s = 280 \text{ k}\Omega/\text{L2}$ and 80% transparency in the optical range. Graphene-based polymer composites were also prepared with functionalized graphene sheets in poly(methyl methacrylate) (PMMA) [128,129], while expanded graphite was employed in PMMA/graphite nanosheet composites [130]. Solvent- and melt-based strategies to disperse chemically and thermally reduced graphene oxide in polymers have been reviewed by Kim et al. [131].

1.2.5. Nanocellulose

Cellulose, considered the most abundant renewable polymer on Earth, is a structural material naturally organized as microfibrils linked together to form cellulose fibers. A single filament of all plant-based natural fibers consists of several cells. These cells are formed out of cellulose-based crystalline microfibrils (Fig. 5), which are connected to a complete layer by amorphous lignin and hemicellulose [132]. These microfibrils are built from bundles of superfine fibrils, which have diameters in the nanoscale (10–30 nm) and indefinitely long containing 2–30,000 cellulose molecules in the cross section. Each nanofibril is composed to a large part (60–80%) by ordered crystallites and to a lesser part by disordered (mesomorphous and amorphous) domains. Individual cellulose chain passes through numerous crystallites and disordered domains and binds them together with 1,4- β -glycoside bonds. Since cellulose of various origins contains nanoscale fibrillar bundles, nanofibrils, nanocrystallites, and disordered nanodomains, this natural polymer can be defined as being nanostructured.

The nanostructured architecture of cellulose promotes isolation of nanoparticles and nanofibrils from initial fibers by various methods that facilitate breaking up of the glycoside bonds in the disordered nanodomains of nanofibrils and cleaving of interfibrillar contacts [133]. Comprehensive standard terms and definition for cellulose nanomaterial are proposed in a new TAPPI Standard that establishes and defines terms of the different forms of cellulose nanomaterials [134]. This document will provide standard definitions of cellulose nanomaterials. Definitions are

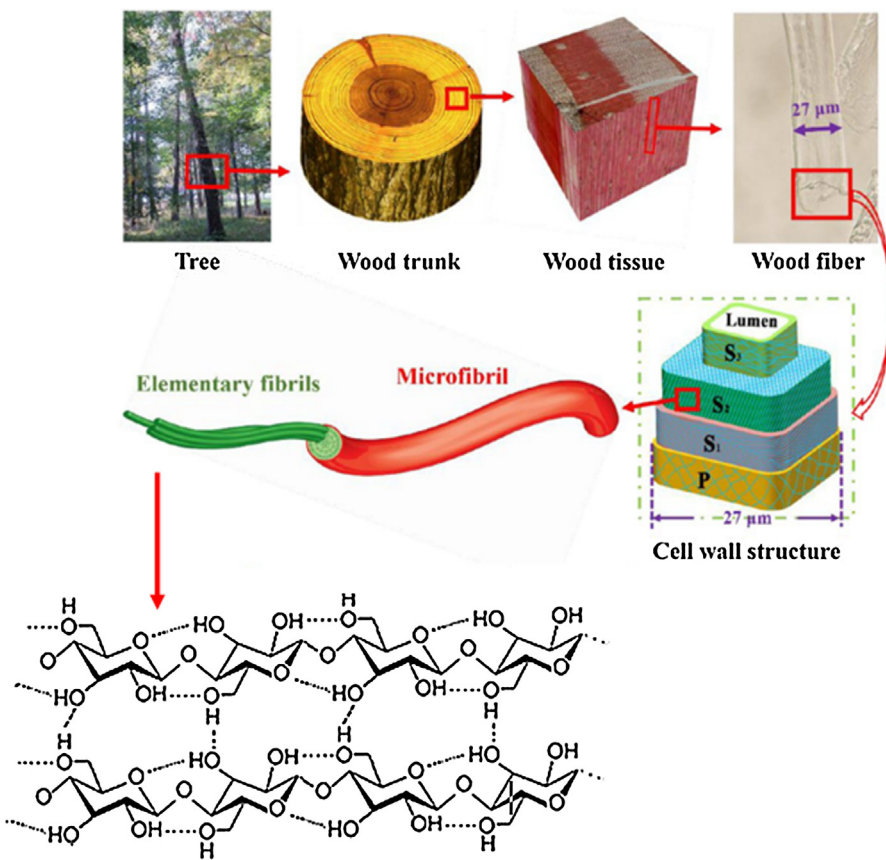


Fig. 5. Hierarchical structure from plant to cellulose chains (from [133]).

included for cellulosic nanomaterial, cellulose nanocrystal, and cellulose nanofibrils and are structured using terminology as defined by existing ISO standards for nanotechnologies and nanostructured materials. In these definitions, cellulose is a material consisting of linear polymer chains of one hundred to over ten thousand β-D-glucopyranose units linked by glucosidic bonds at their C1 and C4 positions. The word cellulosic encompasses cellulose that has been chemically or biologically derivatized, cellulose that has been broken down (or reduced in size) by chemical, mechanical, enzymatic or biological processes and cellulose from plant and non-plant sources. The term cellulose nanomaterials is synonymous of nanocellulose and denotes materials composed by cellulose nanocrystals (CNC), cellulose nanofibrils (CNF), cellulose microcrystals and cellulose microfibrils. Cellulose nanocrystal also known as nanocrystalline cellulose is a type of cellulose nanofiber with pure crystalline structure with dimensions of 3–10 nm in width and aspect ratio greater than 5 and usually less than 50, which are usually produced by acid hydrolysis, oxidation or other methods. The term cellulose nanowhisker applies to cellulose nanocrystals in aggregate or individual forms produced by acid hydrolysis. Finally, cellulose nanofibril is a type of cellulose nanofiber that contains both crystalline and amorphous regions with dimensions of 5–30 nm in width and aspect ratio usually greater than 50, reminiscent of elementary fibrils in plant cell walls. Cellulose nanofibrils are produced by either bacteria or mechanical treatment of plant material, possibly preceded by pretreatment; cellulose nanofibrils produced by mechanical treatment of plant materials usually contain hemicellulose.

Following these definitions, it can be easily derived that individual cellulose nanocrystals can be produced by breaking down the cellulose microfibers and isolating the crystalline regions

[135,136]. Even if several methods have been described and patented, the extraction of cellulose nanoparticles (i.e. elements having at least one dimension in the 1–100 nm range) from wood and natural fibers has traditionally been performed mainly by two routes: acid hydrolysis and mechanical treatment. Strong acid hydrolysis promotes transversal cleavage of non-crystalline fractions of cellulose microfibrils, leading to the so-called cellulose nanocrystals or whiskers, which are rod-like particles (Fig. 6).

Samir et al. [138] described cellulose crystals as nanofibers that have been grown under controlled conditions and that lead to the formation of high-purity single structures. The cellulose amorphous regions are randomly oriented in a spaghetti-like arrangement leading to a lower density compared to nanocrystalline regions [139] and they are susceptible to acid attack and eventual remotion, leaving intact crystalline regions. To produce colloidally stable CNC by sulfuric acid hydrolysis, the conditions regarding temperature, acid concentration, reaction time, and ratio of acid to cellulose source must be carefully controlled. The most commonly employed recipes use temperatures of 45 °C, 64 wt% sulfuric acid, 25–45 min reaction times and acid to cellulose ratios of 8.75–17.5 mL/g: Min et al. [140] were among the first researchers to study the effect of hydrolysis conditions on the properties of resulting cellulose nanocrystals. They proved that longer hydrolysis time leads to shorter monocrystals and to an increase in their surface charge. Beck-Candanedo et al. [141] studied the influence of hydrolysis time and acid-to-pulp ratio on the yield of cellulose nanocrystals.

This kind of cellulose nanostructure may find application as reinforcing components in different polymer matrices [142,143]; due to an abundance of hydroxyl groups existing on the surface of CNC, they can be modified with various chemical groups to facilitate their incorporation and dispersion into different polymer

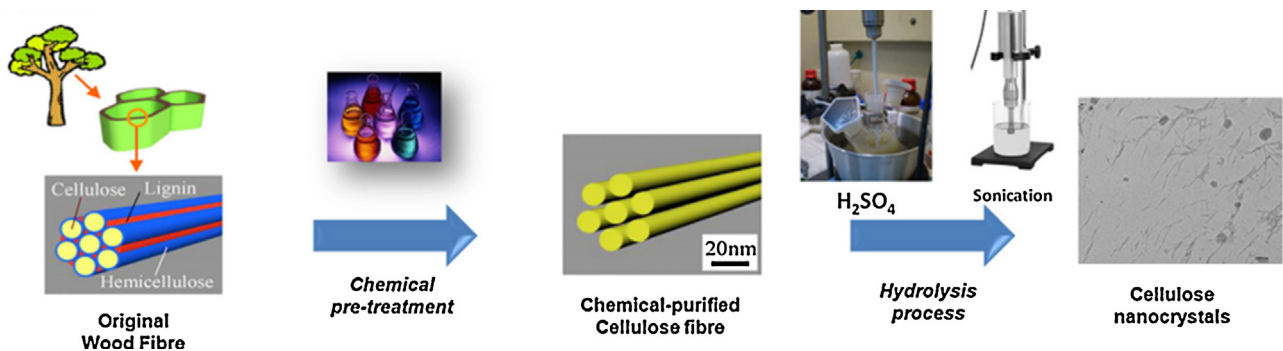


Fig. 6. Scheme of CNC extraction process (from [137]).

matrices [144,145]. Therefore, CNC are considered as one of the ideal nanoreinforcements for polymer matrices (including water-soluble and water-insoluble polymer systems) and have already been incorporated into many polymer matrices for different final applications such as high performance materials, electronics, catalysis, biomedical, and energy [146].

Differently from chemical extraction of cellulose nanocrystals, strong mechanical treatment that imposes high shear forces to cellulose fibers allows the extraction of microfibrils and microfibril aggregates with high aspect ratio that form highly entangled networks. This kind of nanocellulose is usually called microfibrillated cellulose (MFC) [147,148]; although widely used, the mechanical process developed for the production of MFC has an important drawback, which is the high-energy input involved (several passes through high-pressure homogenizers, which are frequently blocked). In the last years, enzymatic and chemical pretreatments have been proposed to reduce the energy input of the process [149–151]. Regarding MFC uses and potential applications, MFC has been mainly used as reinforcing phase in polymer nanocomposites [152].

Nanofibrillated celluloses or nanofibrils, (CNF) are indeed produced when specific techniques facilitating fibrillation are incorporated in the mechanical refining of wood and plants pulps. They ideally consist of individual nanoparticles with a lateral dimension around 5 nm [153]. The production of fully degradable or biocompatible nanocomposites, containing CNF with high aspect ratio and diameters below 100 nm, remains a challenging task because of the strong agglomeration tendency that occurs during drying of aqueous CNF suspensions or during compounding of CNF with hydrophobic polymers. This clustering is normally accompanied by an important decrease of the CNF aspect ratio and consequently results in a decrease or loss of some beneficial properties. In order to tackle this problem, one strategy involves the chemical modification of CNF's surface hydroxyl groups, in order to decrease the nanofiber surface hydrophilicity [153].

Finally, in recent years, the microbial synthesis of cellulose micro/nanofibers with specific bacteria has received great attention. Cellulose molecules are synthesized in the interior of the bacterial cell and spun out to form nanofibrils of ca. 2–4 nm in diameter, which then aggregate in the form of ribbon-shaped microfibrils of ca. 80 × 4 nm [154]. Its unique fibrillar nanostructure endows it with excellent physical and mechanical properties such as high porosity, high elastic modulus, and high crystallinity. Applications of bacterial cellulose [155] include reinforcement of polymer matrices [156,157].

1.3. Functionalization of nanoparticles

The production of polymer nanocomposites requires the formation of a controlled interface between the polymer and the nanofillers in order to allow the disaggregation and a uniform

dispersion of the nanofillers in the polymeric matrix. Normally, both components have a completely different chemical structure, which prevents a proper and desirable interfacial interaction. Therefore, with the purpose to improve the interaction of polymer matrices and nanofillers, different compatibilization strategies have been developed. Depending of the chemical structure of both components, typically these strategies can be represented by a chemical modification of the nanofillers surface (covalent functionalization) or by the promotion of physical interactions between the matrix and the filler including the eventual use of compatibilization additives (non-covalent functionalization). This section of the review is limited to carbon nanoparticles and nanocellulose, however, later in the text, some results from the literature on clays and silica nanoparticles are reported as well as on the use of surfactants. For example, the use of silanes as compatibilizers chemically attached to nanoclays and silica have been the subject of several reports, but for the sake of a higher simplicity, only covalent approaches regarding different carbon nanoparticles and grafting strategies for nanocellulose compatibilization are reviewed here.

1.3.1. Covalent functionalization

1.3.1.1. Carbon nanoparticles. From the chemical point of view, the graphene surface is chemically inert and interacts with other molecules mainly via physisorption (π - π interactions). However, the edges of graphene, carbon nanotubes and graphene nanoribbons are more chemically reactive (Fig. 7) and can indeed anchor different chemical groups including carboxyl (COOH), carbonyl, hydrogenated and amines. Therefore, the chemical activity of graphene-based materials can change dramatically at these edges, depending on their carbon termination (e.g. armchair or zigzag). The introduction of surface defects represents an effective way to make the graphene basal surface more chemically reactive (Fig. 7) [158].

An alternative route to make the graphene more reactive consists of adding fluorine. This process (called fluorination) has been known for decades. However, only recently graphene has been fluorinated using different techniques including plasma treatments and F_2 high temperature treatments [159,160]. From the materials point of view, fluorinated graphene can be homogeneously dispersed in different solvents to prepare polymer composites and further experiments are needed along this direction. It is also important to note that the electronic properties of graphene could be tuned via controlling the degree of fluorination, which modulates the energy band gap of the material [161].

Sofo and co-workers [162] predicted the possibility of reacting the graphene surface with hydrogen atoms; the sheet was termed “graphane” and it was reported experimentally by Geim and Novoselov [163].

Another way to fully functionalize the graphene surface is by oxygenation. The resulting material is known as graphene oxide

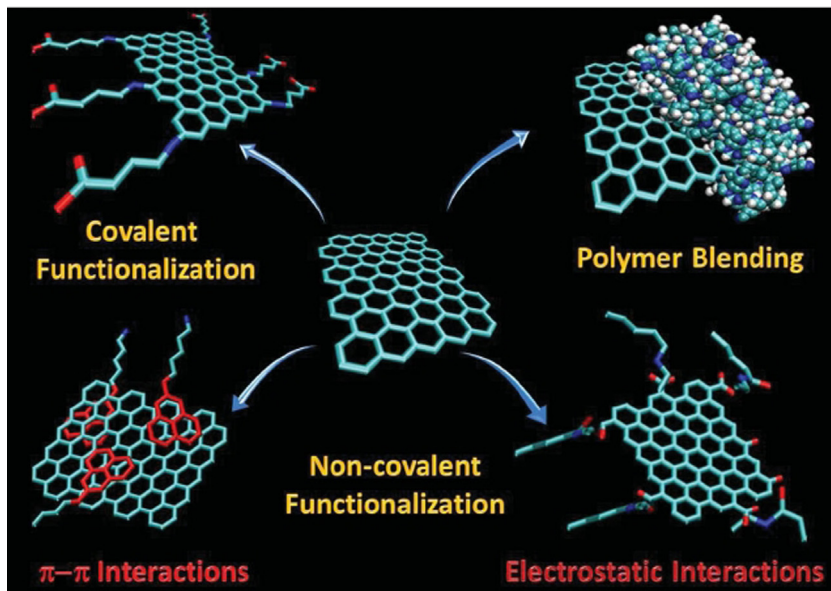


Fig. 7. Molecular models of sp₂ hybridized carbon (graphene) displaying different interactions with polymer matrices: non-covalent interactions (e.g. π–π interactions), covalent interactions, electrostatic interactions and polymer blending (from [158]).

(GO), and it contains different C–O functional groups (e.g. epoxy, carbonyl and carboxyl groups). These materials are remarkably hydrophilic and more reactive [120]. GO is usually synthesized via chemical routes and can be easily dispersed in different solvents for generating robust polymer composites [164]. These sheets contain a large number of defects, and further details about their preparation and applications could be found elsewhere [131,164].

Many concepts regarding the functionalization of graphenes started with or can be applied to CNT. The development of CNT based polymer nanocomposites has been indeed achieved thanks to approaches that have been used to exfoliate bundles of CNT through the interaction of the tubular surface with various species of polymers [165,166], aromatic compounds and surfactants [167,168]. For most of those methods, functionalization implies the formation of covalent bonds, made by addition reactions to CNT double bonds. The result is the formation of a new bond with simultaneous local destruction of the conjugation on the nanotube wall and a shift from sp₂ to sp₃ hybridization.

The direct fluorination of SWCNT and their subsequent derivatization provides a versatile tool for the preparation and manipulation of nanotubes with variable sidewall functionalities [169–174]. Furthermore, fluorine in SWCNT can be efficiently displaced by alkylamine functionalities [174,175]. The nucleophilic substitution offers an opportunity for SWCNT to be integrated into the structure of the epoxy systems through the sidewall amino functional groups [175,176].

The plasma treatment for the functionalization of carbon nanotubes represents a novel approach easy to scale up to industrial application. Several attempts to fluorinate carbon nanotube sidewalls in such manner have been reported [177–180]. The CF₄ plasma treatment of SWCNT sidewall was demonstrated to enhance the reactivity with aliphatic amines [179].

1.3.1.2. Nanocellulose. Multifunctional nanocomposites based on polymeric matrices and cellulose nanostructures (CNS) such as cellulose nanowhiskers (CNW), cellulose nanocrystals (CNC) and micro/nano fibrillated cellulose fibers (MFC/CNF) are of scientific and industrial interest for their notable performance improvement. Moreover, cellulosic nanoreinforcements have recently attracted much attention due to their renewable nature, the wide variety of source materials available throughout the world, their

low cost and density, their high surface functionality and reactivity. The exceptional mechanical strength together with high aspect ratio and large surface area enable these nanomaterials to reinforce a wide variety of polymers even at very low filler loadings. However, the hydrophilic nature of native cellulose generally limits the formation of CNS nanocomposites to water-soluble polymers [145,181,182]. In hydrophobic matrices, repulsive forces lead to aggregation and poor interfacial contact. Efforts to overcome this limitation are reported in the scientific literature and it is well recognized that methods involved in obtaining dispersion and strong matrix interactions for CNS in polymeric matrices are remarkably similar to that available for carbon nanotubes. Moreover, the higher presence of surface hydroxyl groups on reactive cellulosic surfaces with respect of carbon nanotubes may also permit further modification to alter its hydrophilicity. This latter characteristic facilitates the surface chemical modification of nanocellulose and grafting of chemical species allowing tailoring its surface chemistry to facilitate self-assembly and regular dispersion in a wide range of polymer matrices. However, it should be underlined that the surface chemistry of CNS is certainly governed by the extraction procedure from the cellulosic substrate and the introduced functionality could indeed, compromise the thermal stability of the CNS and their further use in polymer melt processing. As an example, sulfate ester groups randomly introduced on the surface during sulfuric acid hydrolysis, represent a problem due to the decreased thermal stability after drying of the CNS due to the formation of sulfate esters with high surface acidity [183,184], while hydrochloric acid hydrolysis results in hydroxylated surfaces [141]. TEMPO-mediated oxidation, in which carboxylate and aldehyde functional groups are added under moderate conditions onto the cellulose structure, employing an inexpensive oxidizing agent (such as sodium hypochlorite) in the presence of the 2,2,6,6-tetramethyl-1-piperidine-N-oxyl radical (referred to as TEMPO) and a bromide or a iodine as catalyst, is also used during CNS extraction. In Fig. 8, the main surface chemistries provided by the most common extraction methods are reported [185]. Other than surface modifications of CNS during their extraction, chemical bonding of molecules onto the surface of cellulosic nanostructures and no-covalent adsorption of molecules to the surface of the particles are the main adopted routes.

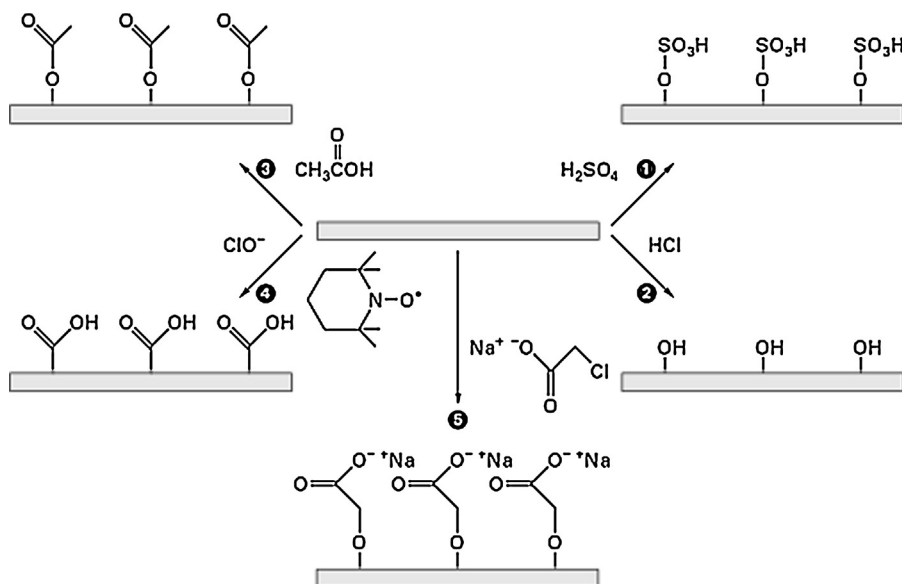


Fig. 8. Chemistry provided during CNS extraction by: (1) sulfuric acid hydrolysis; (2) hydrochloric acid hydrolysis; (3) acetic acid hydrolysis; (4) TEMPO-mediated treatment and (5) carboxymethylation (from [185]).

CNS possesses an abundance of hydroxyl groups on their surface, providing the possibility of extensive chemical modifications, most of them aiming at improving both the dispersability of CNS by reducing the hydrogen bonds, which cause the reaggregation of the crystals, and the compatibility in different solvents or matrices that are suitable for the production of nanocomposites. Due to the nature of polysaccharides, esterification, etherification and amidation are the most common approaches for the chemical modifications, but also other chemical modifications of CNS must be considered, as silylation [186], cationization [187], fluorescent labeling [188], carboxylation by TEMPO-Media oxidation [189], and polymer grafting by “grafting-onto” [190] and “grafting-from” methods [191,192] (Fig. 9 [192]).

All chemical functionalizations are mainly conducted to introduce stable negative or positive electrostatic charges on the surface of CNS to obtain better dispersion and tune the surface energy characteristics for improved compatibility [193], with the main challenge of conducting the process in such a way that original morphology and integrity of the cellulosic materials is preserved.

1.3.2. Non covalent functionalization

1.3.2.1. Carbon nanoparticles. Non-covalent functionalization routes for graphene include van der Waals interactions and $\pi-\pi$ stacking of aromatic molecules on its surface. These forms of functionalization do not disrupt the extended π conjugation on graphene and do not create sp^3 -hybridized carbons or defects. Polycyclic aromatic compounds like pyrene, perylene, anthracene, triphenylene and coronene (and certainly also graphene) can bond one onto another via π -orbital overlapping to form a $\pi-\pi$ interface, which is stronger than hydrogen bonding, van der Waals, or dipole-dipole interactions (though not as strong as covalent bonds). Therefore, most aromatic molecules exhibit $\pi-\pi$ interactions with graphene and can tune the electron density of the hybrid system via orbital hybridization. These are the interactions responsible for keeping graphene layers together in graphite. The higher the number of rings involved, the stronger the $\pi-\pi$ interaction.

Interfacing polymeric thin films to single layer graphene sheet can confer many desirable features, including mechanical strength

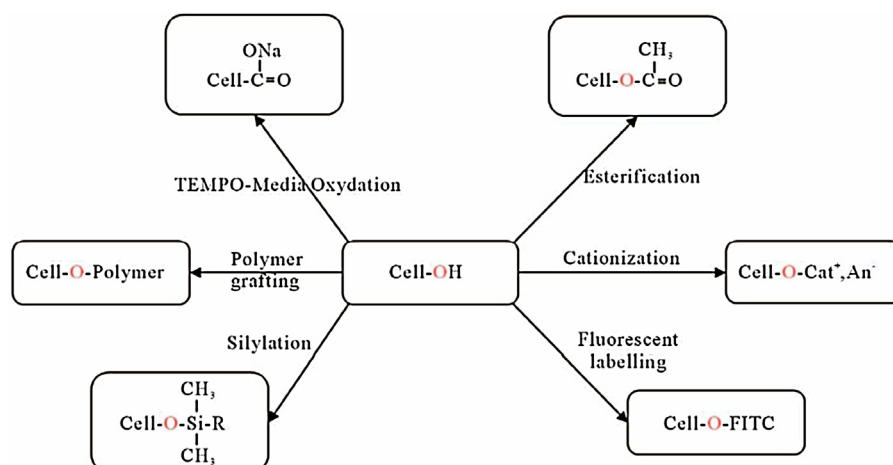


Fig. 9. Schematic diagram illustrating the various types of chemical modifications on nanocrystalline cellulose surface (FITC: fluorescein-5-isothiocyanate) (from [192]).

and/or flexibility [194], tunable changes in doping [195–197] and a large number of reactive functional groups [198]. In contrast to monomeric adsorbates, polymers form less-ordered, thicker layers that enable them to serve as environmental barriers and supporting or active layers. Polymers are also straightforward to introduce, usually via solution deposition, and may be patterned through a variety of lithographic techniques.

More exotic polymer films have also been used to impart improved performance or added function to graphene-based transistors. Ahn and co-workers utilized a block copolymer/ionic liquid gel gate electrode within field-effect transistors fabricated on flexible, transparent polymer substrates [199].

Szkopek and co-workers utilized a poly(ethylene imine) (PEI) layer to transform a graphene field-effect transistor (GFET) into a CO₂ sensor. The amines of the PEI layer reversibly bind CO₂, which induces a change in the single layer graphene conductance. Unfunctionalized GFET showed no measurable CO₂ response [200].

Functionalization through polymerization on the graphene surface has been also reported. For example, Zhou and co-workers used a soft lithographic approach to print 2 μm wide strips of methacrylic macroinitiators bearing both pyrene and bromostyrene side chains [198]. Polymerization under atom transfer radical polymerization conditions provided 100–300 nm thick polymer brushes in the patterned regions. The method was general to several monomer classes and graphene types (CVD, reduced graphene oxide, and graphene oxide). Dichtel and co-workers recently used single-layer graphene to crystallize oriented thin films of a class of 2D polymers known as covalent organic frameworks (Fig. 10) [201], which had been previously isolated as insoluble polycrystalline powders.

As alternative route, the non-covalent functionalization offers the possibility of attaching organic moieties without affecting the electronic network of the tubes. These interactions are of the same kind as those keeping the various graphite layers close one to another (π -stacking). In this regard, interactions between nanotubes and polynuclear species as well as pyrene-modified oxidized surfaces have been used for the assembly of single-walled carbon

nanomaterials [202]. Surfactants have been generally used for the purification and dispersing process of raw CNT [203]. Then, surfactant-stabilized dispersions of CNT have been used for their compatibility enhancement in the preparation of composite materials [204–206].

1.3.2.2. Nanocellulose. The interaction of cellulose with surfactants has been another way to stabilize cellulose suspensions into non-polar systems. These methods could include different chemical interactions between the surfactant and the cellulose surface and for simplicity are reviewed here. Some examples include acetylation of the CNS surface using mixtures of acetic acid and anhydride [207], stearic acid [208], cetyltrimethylammonium bromide [209], xyloglucan, xyloglucan block copolymers, mono- and diesters of phosphoric acid with alkylphenol tails [210,211]. These methods use the surfactants as stabilizing agents in which the hydrophilic end of the surfactant molecule adsorb on the surface of the CNS whereas the hydrophobic end may provide a non-polar surface that could be easily dispersed in non-polar organic media.

2. Bottom-up nanostructuration

Self-assembling is not easily achieved in polymer nanocomposites due to the complex morphology of the polymer chains, to the anomalous entropic and enthalpic contributions and to the wide variety of polymer–nanoparticle interactions. In fact, few bottom-up approaches have been reported and typically regard the use of block copolymer nanostructuration by phase separation, with few real applications. When two or more chemically different polymers are mixed together, they often tend to suffer macrophase separation due to the asymmetry in the energetic and entropic contributions of both materials. Block copolymers (BC) are a particular class of polymers that belong to a wider family known as “soft materials” [212–214] that, independently of the synthesis procedure, can simply be considered as being formed by two or more chemically homogeneous polymer fragments, the blocks, joined together by covalent bonds. Therefore, macroscopic scale

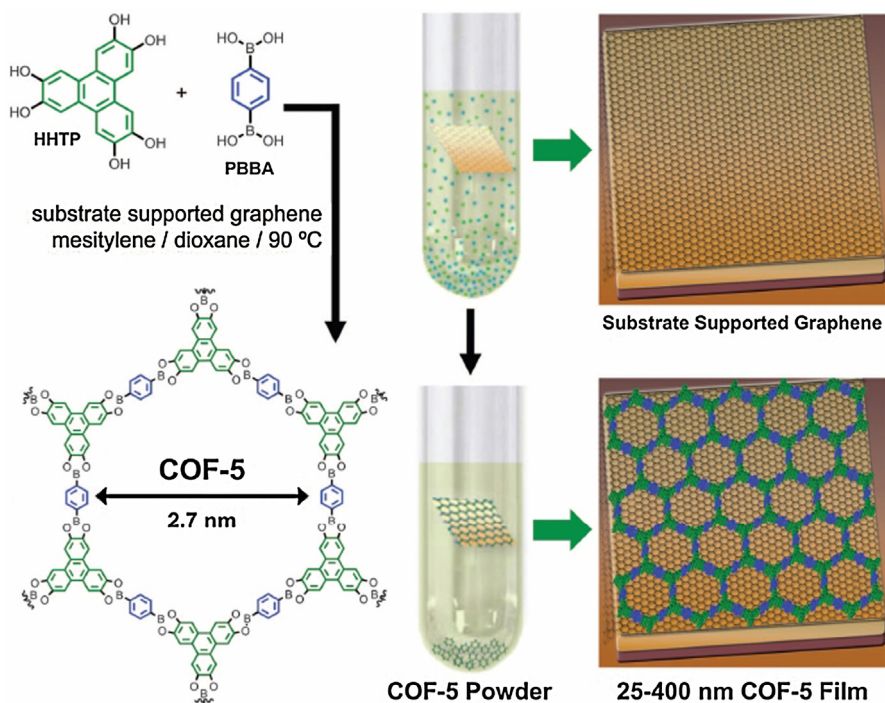


Fig. 10. Schematic representation of the solvothermal polymerization of hexahydroxytriphenylene and benzene-1,4-bis-boronic acid to form the 2D layered covalent organic framework network on single-layer graphene (from [201]).

separation of the two blocks is prevented a priori and the effects of the eventual incompatibility between them are limited to a local, ordered, segregation. It means that BC are able to self-assemble into well-defined, ordered structures potentially used as basis for several technological applications [215–220]. Consequently, BC are considered an example of bottom-up processing strategy, as they are able to generate, under appropriate conditions, the spontaneous formation of periodic nanostructures. The constituent blocks, covalently bonded together, can segregate at local level and their separation typically corresponds to the radius of gyration of the molecule thus forming self-assembled ordered nanostructures in the order of 5–100 nm. One of the main applications of BC, reviewed in this report, is their use as templates for the dispersion of nanofillers in polymer matrices.

2.1. Nanostructured copolymers and their nanocomposites

In general, BC can be considered as a kind of polymer alloy, and in the simplest case of two distinct monomers, conventionally named A and B, linear di-block (AB), tri-block (ABA), multi-block or star-block copolymers can be prepared.

Moreover, many different classes of BC are reported in the scientific literature. For example, regarding thermoplastic elastomers, BC can be formed by a rubbery matrix containing hard glassy domains. Thus, BC can be molded at high temperature as a thermoplastic but behaves as a rubber at ambient conditions. As reported by Peponi et al. [221], polyurethanes and poly (ester-urethanes) prepared by condensation polymerization of multi-block copolymers can be designed in order to show a desired multi-functionality, such as shape memory behavior. Moreover, BC can form micelles in solution with proper solvents. These micelles influence the structure as well as the flow characteristic of the BC solution leading to a material with different behavior than the corresponding homopolymers [217].

The synthesis strategies used in order to obtain BC are not so new and innovative, but are not trivial since high-purity starting monomers and high-vacuum procedures are required in order to prevent premature termination by impurities. In general, both anionic and living radical polymerization methods are using nowadays and it is important to note that the older anionic polymerization is still widely used in the industry of BC. For example, the first anionic polymerizations of block copolymers were conducted as early as 1956 [222] and it is still industrially used to prepare several classes of BC including thermoplastic elastomers and amphiphilic copolymers [217].

The main recent advances in the BC synthesis are represented by the use of the atomic transfer radical polymerization (ATRP), independently discovered by Sawamoto [223] and by Matyjaszewski [224]. This technique is one of the main used methods to prepare well-defined complex architecture polymers and, among them, nanostructured block copolymers. In fact, ATRP permits to define the architecture of the synthesized polymer by choosing the adequate initiator [225]. Many researchers have focused their attention on the synthesis of BC by ATRP thus obtaining AB di-block, ABA and ABC tri-block copolymers (based on polystyrene and various polyacrylates) [226].

Ring-opening polymerization has also been used to build blocks of the BC starting from cyclic molecules as reported by Peponi et al. [227] who have been able to correlate the chemical structure with the crystallization behavior of each block in poly(ϵ -caprolactone)-*b*-poly(L-lactide) di-block copolymers. Lee et al. studied the thermoresponsive phase transition of tri-block stereo-copolymers in aqueous solution, showing that there is a critical gel concentration and lower and upper critical gel temperatures at which the thermo-responsive phase transition occurs [228]. Moreover, Dove reviewed the application of poly(ester)s, obtained by

living/controlled ring-opening polymerization, as components of self-assembling block copolymers [229]. More recently, Chen et al. [230] reported the design of novel functional nanomaterials obtained by using these previous strategies. In fact, they reported the synthesis of hydrophobic polymer brushes based on a hard core of silica nanoparticles with a relatively soft shell of polystyrene-block-poly(ϵ -caprolactone) (PS-*b*-PCL) obtained by surface-initiated atom transfer radical polymerization (ATRP) of styrene, ring-opening polymerization (ROP) of ϵ -caprolactone and click reaction. At this regard, Hillmyer et al. have summarized the main BC synthesis techniques [231].

Probably, the most interesting aspect when working with BC is to understand their ability to self-assemble into nanodomains and to study their nanostructured ordered morphologies. Thus, their phase behavior has been the subject of numerous theoretical and experimental studies over decades [232–235]. However, in order to understand these phenomena and the morphological differences between the self-assembling of BC and the macrophase separation in the polymer blends, it is worth to refer to the Flory–Huggins interaction parameters and the thermodynamic fundamentals associated to the polymers mixing process. In fact, in polymer mixing the translational entropy is proportional to the number of molecules, while the interaction is proportional to the number of monomers or repetitive units. Due to the great number of monomers that are present in a polymer, even weak interactions between different monomers become relevant. Consequently, the product χN is the parameter that controls the thermodynamics of the blend, where χ is the Flory–Huggins interaction parameter and N is the characteristic length of the polymer or degree of polymerization. Taking into account that many monomers are chemically incompatible, the product χN has a strong tendency to be positive, leading to macrophase separation. Nevertheless, when two polymers chemically different are covalently linked together, the separation in a macroscopic scale is prevented a priori and their incompatibility leads to a separation at a local level driving the spontaneous formation of a periodically segregated structure. This self-assembling process is driven by an unfavorable mixing enthalpy and small mixing entropy, while the covalent bond connecting the blocks prevents macroscopic phase separation. Therefore, the microphase separation of block copolymers and in particular of di-block copolymers (the easier case of study), depends on the total degree of polymerization N ($N = N_A + N_B$), on the Flory–Huggins χ -parameter (which is a measure of the incompatibility between the two blocks) and on the volume fractions of the constituents blocks (ϕ_A and ϕ_B , $\phi_A = 1 - \phi_B$), as well as on the preparation conditions, which can affect drastically the final morphology of the BC.

In general, the phase separation process is governed by the free energy of Gibbs, which is directly related to both enthalpic and entropic terms. In the simplest case of (A-B)_n type block copolymers the interaction parameter χ_{AB} describes the free energy cost of the interaction among A and B monomeric units and, accordingly to the Flory–Huggins lattice theory [236–238] is defined by:

$$(2.1) \chi_{AB} = \left(\frac{Z}{k_B T} \right) \left[\frac{W_{AB} - (W_{AA} + W_{BB})}{2} \right]$$

where Z is the number of the nearest neighbors of the copolymer configurational cell, k_B is the Boltzmann constant, T is the temperature and w_{AB} is the interaction energy between A and B monomers. From this equation, it is easy to understand that the interaction parameter, inversely proportional to the temperature, reflects the interaction energy between different segments. Positive values of χ_{AB} , which occurs in most cases, indicate repulsion between A and B monomers and this repulsion leads to the copolymer segregation, while negative values of χ_{AB} would lead to the mixing of both of them. Therefore, as the entropic and enthalpic contributions to the Gibbs free energy are directly

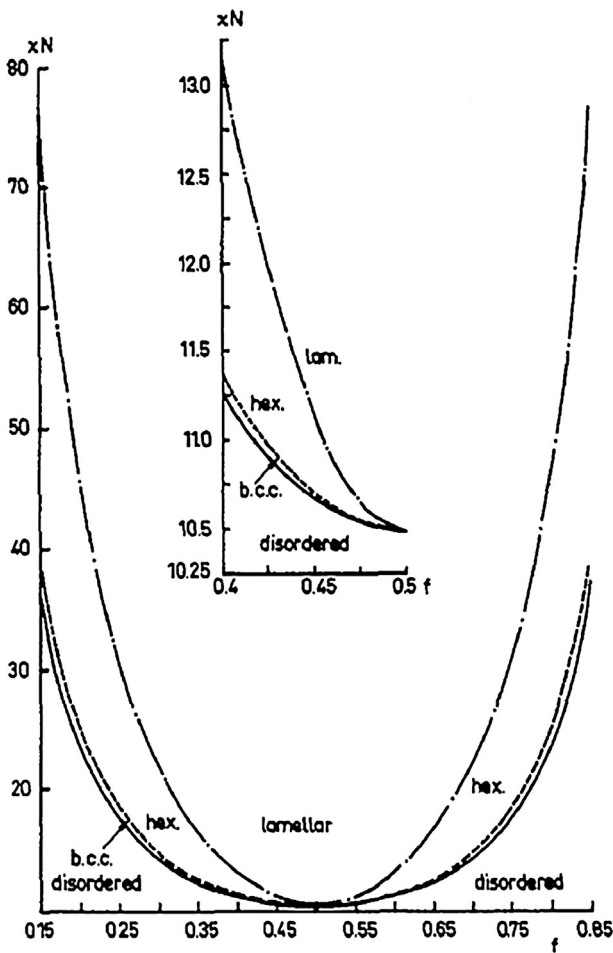


Fig. 11. Phase diagram for di-block copolymer in the weak segregation limit previously calculated by Leibler, from Ref. [243]. (LAM = lamellar morphologies, HEX = hexagonal microphase (cylinders), BCC = body-centered cubic microphase (spheres), ϕ_A = volume fraction of component A in the di-block copolymer).

proportional to $1/N$ and χ , respectively, the product χN is used to represent the block copolymers phase state. Moreover, as reported by Lodge et al. [239], it is evident the inversely proportional relationship between T and χN .

From the early 1970s, theoretical approaches for the phase separation of BC were developed. In particular, Helfand and co-workers [240–242] developed the self-consistent field theory to calculate the free energy, the composition profiles and chain conformations. Successively, in 1980, Leibler [243] presented a systematic analysis of the block copolymer phase diagram based on the expansion of the Landau free energy for a monodisperse A-B type di-block copolymer. He compared the free energy of different ordered phases with respect to the disordered phase and predicted

that for all di-block copolymers with asymmetric composition ($\phi_A \neq 0.5$), a microphase separation from the disordered into the body-centered cubic structure (BCC) occurs. According to the phase diagram in Fig. 11, a transition to the thermodynamically stable hexagonal and lamellar phases is expected upon further increase of the product χN . Only for symmetrical di-block copolymers ($\phi_A = 0.5$), a direct first-order transition from the disordered to the lamellar phase is expected.

In bulk, the minority block is segregated from the majority block forming regularly shaped and uniformly shaped nanodomains [244,245]. Fig. 12 shows the equilibrium morphologies documented for di-block copolymer [233]. The shape of the segregated domains in di-block is governed by the volume fraction of the minority block, ϕ , and the block incompatibility [244,245].

Numerous studies are reported in the literature in order to verify the formation of the different self-assembled nanostructured phases. In particular, a body-centered cubic spherical phase of the minority blocks (S, S' in Fig. 12) is formed in the matrix of the majority block when the volume fraction of the minority block is low, about 15–20%. Its nano ordered morphology changes to hexagonally packed cylinders (C, C' in Fig. 12) at an increased volume fraction of about 30%. At a volume fraction of around 35%, the minority block forms gyroid or perforated layers at moderate and high incompatibility, respectively (G, G' in Fig. 12). Alternating lamellae are formed when the two blocks have similar volume fractions (L in Fig. 12).

In the context of bottom-up nanostructuration, the interest has been paid also to segmented copolymers like thermoplastic polyurethane (TPU), poly(ether-*b*-ester) or thermoplastic elastomers (TPE) like poly(ether-*b*-amide). Also in these cases, their resulting polymeric chains form block-structures able to phase-separate in hard and soft segments. The practically unlimited amount of possible combinations obtaining by varying the structure and/or the molecular weight of the TPU components allows tuning their polymer structure to the desired final properties of the material [245–247].

Moreover, another important aspect to be considered when referring to bottom-up approaches and block copolymers structures is the role of the block polydispersity. In particular, these aspects are important when comparing phase diagrams obtained with BC synthesized by anionic or control free-radical polymerizations or when comparing di-blocks and segmented BC. In fact, Matsen recently indicated that, comparing a BAB tri-block copolymer with an AB di-block, the polydispersity induces shifts in the order-disorder transition of the tri-block copolymer system, attributed to a reduction of entropy in the A-rich domains due to the absence of chain ends [248].

From the discussion above, it is clear that the applications of self-assembling nanostructured BC are very eclectic but the common factor is to understand their phase separation behavior. Due to the complexity of the self-assembling theories, computer simulations have been used in order to study the BC self-assembling behavior.

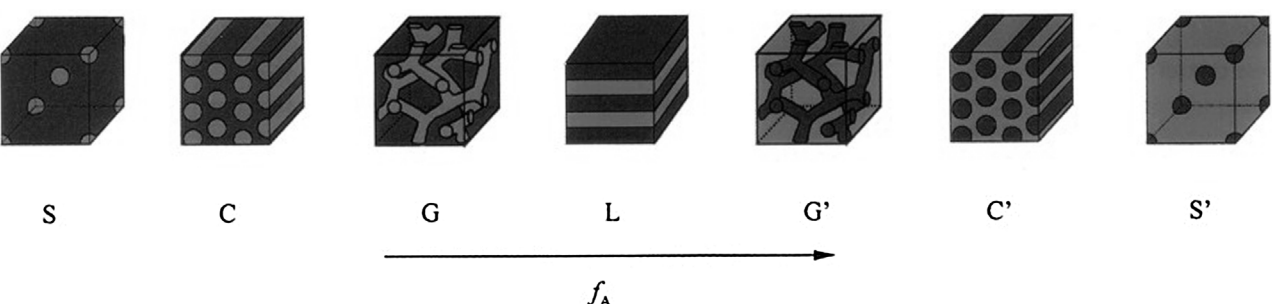


Fig. 12. Different microstructures of linear di-block copolymers [233].

For example, Banaszak et al. [249] have performed computer simulations for three symmetric ABA tri-block copolymers in order to study the microarchitectures as a function of the temperature, leading to the phase diagram for a symmetric ABA tri-block copolymer. They also obtained energy, specific heat, end-to-end distance and bridging fraction as a function of the reduced temperature.

Furthermore, different simulation calculation methods, among which Monte Carlo and dissipative particle dynamics (DPD) simulations, have been used in order to predict the phase diagram of block copolymers [250–260]. An example was reported by Gemma et al. [250], who used Monte Carlo simulations in order to study the morphology of ABC three-arm star-shaped copolymers with arm-length ratio 1:1:x thus studying the progression of the morphologies as a function of x . Moreover, they calculated the free energy of the system in the strong segregation limit for four kinds of simple phases, and obtained results consistent with the simulations. Another example of using the Monte Carlo simulations was reported by Cai et al. [251]. They studied the conformation and thermodynamic properties of both di-block and random square-well copolymers by the Born–Green–Yvon (BGY) theory and found that the BGY results for the end-to-end distribution of copolymers are in good agreement with Monte Carlo simulations when the attractive interaction between segments is not strong. More recently, Beardsley et al. evaluated the phase diagram for di-block copolymer melts with the lattice-based Monte Carlo simulations [252]. In particular, they found that the gyroid morphology could be spontaneously formed in place of the perforated-lamellar phase, even if still remains a small region where the perforated-lamellar phase appears to be stable. The same authors performed a similar study for a AB di-block copolymer melt with polydisperse A blocks and monodisperse B blocks correlating the order–order as well as the order–disorder transitions with the polydispersity of the block and temperature reporting that the polydispersity enhances the stability of the perforated-lamellar phase [253]. Song et al. [259] studied by lattice Monte Carlo simulation the phase behavior of symmetric ABA tri-block copolymers containing a semiflexible midblock. In fact, as the midblock evolves from a fully flexible state to a semiflexible state in terms of increasing its persistence length, different phase behaviors were observed. More recently, Hugouvieux et al. used lattice Monte Carlo simulations to study the phase behavior of amphiphilic multi-block copolymers with a large number of blocks in semidilute solutions studying also the different gel network structures obtained [260].

Regarding DPD simulations, Abu-Sharkh et al. [261] used the dissipative particle dynamics method to simulate the self-assembly of symmetric tri-block copolymers of the type ABA. They found that, depending on the volume fraction of the end blocks ϕ_A , several mesophases including lamellar, perforated lamellar, gyroid hexagonal cylinders and BCC spherical micelles could be obtained. Chou et al. [262] studied the morphologies and the internal structures of rod-coil copolymer in mixed selective solvents by DPD analysis, focusing the attention on their optoelectronic properties. Also Guo et al. [263] and Huang et al. [264] employed DPD simulations to study the phase behavior of paclitaxel loaded PEO-*b*-PLLA amphiphilic copolymer in two solvents, that is in water and N,N-dimethylformamide observing different ordered structures, and to analyze the molecular conformation of AB(2) miktoarm star copolymers, respectively. Also Han et al. [265] investigated more recently the formation of various micelle shapes of lipid-like amphiphilic AB(2) miktoarm star copolymers in solution. Furthermore, Khokhlov et al. [266] used dissipative particle dynamics, to study the microphase separation in the melt of amphiphilic/nonpolar di-block copolymers in the strong segregation regime showing that the phase

diagram for the copolymers with an amphiphilic block can be significantly different from that known for the conventional di-blocks. In fact, the surface activity of amphiphilic monomers forces them to be located in the regions of maximum concentration gradient. Xu et al. [267] found that the microphase-separation morphologies in graft di-block copolymers shift away significantly from that of the corresponding linear ones with the same component volume fractions. Yildirim et al. [268] recently used dissipative particle dynamics simulations in order to study the morphological properties of pyrrole and phenylene rod-coil di-block copolymers, two important conducting polymers classes. In particular, not only the interaction parameter and chain length of the blocks but also the chemical structure of the polymers must be considered to produce the phase diagram of the copolymers.

2.1.1. Block copolymer thin films

The self-assembling of BC has also been studied in **thin films** [269,270] due to their potential application as ultrafine filters or membranes [271], lithographically patterned semiconductors [272,273] and self-organization high-density data-storage media [274] among others. Thin films of BC can be prepared by spin coating, obtaining films with a very low surface roughness. The film thickness can be controlled through the spin speed, the concentration of the block copolymer solution or the volatility of the solvent, which also influences the surface roughness [275]. Dip coating as well as solvent casting techniques are other reliable methods for producing uniform thin films [276]. The nanostructured self-assembly morphologies that can be obtained in thin film are the same of those obtained in bulk except for the bicontinuous structures that cannot exist in 2-dimensions. Therefore, lamellar nanostructured films for symmetric BC as well as cylinder or spherical self-assembled morphologies for asymmetric BC can be obtained in thin films. Furthermore, Peponi et al. [277] have reported the nanostructuration of random PCL/PLA copolymer thin films. Other examples of nanostructuration in random copolymers were reported by Li et al. [278] and Wu et al. [279], whereas Houdayer et al. reported a computer simulation to obtain the phase diagram of random BC [280].

2.1.2. Nanostructured block copolymers in solution

Another BC system able to self-assemble in ordered nanostructures is represented by BC in solution. This refers to BC in solvent solution in which the solvent is selective for one block of the BC leading to the formation of BC micelles. In fact, in selective solvents, some block copolymers form micelle-like aggregates that consist of an insoluble polymeric core surrounded by a solvent swollen corona. The thermodynamically favored morphology and aggregate dimensions are determined by a force balance between the average degree of stretching of the core-forming block, by the steric crowding of chains in the corona and at the core–corona interface, and by the quality of the core–solvent interaction, which relates to the free energy contributions of the core, the corona, and the interface as deeply studied by Eisenberg [281–283].

Among others, Lodge et al. presented a deep study of BC in solution studying their phase diagrams [284]. The phase behavior of concentrated solutions can be mapped onto that of block copolymer melts [285]. The BC micelles can be used as surfactants, personal care products [286], in pharmaceutical applications especially in drug delivery [287–291] or as nanoreactors for the production of inorganic nanoparticles [292,293]. Hamley et al. proposed a study by small-angle X-ray scattering (SAXS) of the effects of the copolymer composition on the structure of micellar cubic phases of di-block copolymers in solution [294]. They also studied the micellar ordering obtained in a slightly selective solvent of di- and tri-block copolymers [295].

Finally, regarding the use of solvents, few words can be spent about reactive solvents that offer an interesting and flexible route to extend the processing characteristics of thermoplastic polymers beyond their existing limits [296] as well as regarding the nanostructuration of the thermosets as reported, among others, by Ruiz-Pérez et al. [297] and Tiiuta et al. [298].

Summarizing, block copolymers can be defined as the more important self-assembling materials due to their ability to allow controlling both “scalar” behaviors over self-assembling and advanced “vectorial” aspects regarding the application of the resulting nanostructured morphologies [244]. In particular, with BC it is possible to obtain a precise *control over length scale* of the dimensions of the nanostructured domains as well as a *control over morphology* by taking into account the phase diagram as well as a *quantitative prediction of the equilibrium structures*. Additionally, it is possible to obtain a *control over domain functionality and properties*, thus tailoring the materials for ultimate applications and finally, they maintain the traditional *advantages of polymeric materials* including cost effectiveness and flexibility. For example, the use of thermoplastic elastomers TPE is important in a variety of applications, but it is primarily the microphase separation of the segments that leads to robust and reusable elastomeric behavior, rather than any particular ordered structure [299]. Other examples of thermoplastic elastomers are presented by Cohn and coworkers referring to biodegradable multi-block copolymers [300].

In conclusion, due to the progress in the understanding self-assembly processes, and to the possibility to tailor BC morphologies as well as their functionality, they can be used as template for nanocomposites.

2.1.3. Nanocomposites based on BC

BC can be used as polymeric matrix for nanotechnology applications thus integrating the synergistic effect of both bottom-up as well as top-down approaches. In particular, the addition of nanoparticles to BC leads to the formation of hybrid nanostructured materials that show both ordered phase-separated domains at nanoscale and the functionality own of nanosized particles. Copious are the scientific works published on nanocomposite based on BC matrices, using nano-objects of different geometries yielding this topic very actual with continuously increasing scientific publications. Thus, in order to report some examples of the more recent publications about nanocomposites based on self-assembling BC, we underline the work of Giacomelli et al. [301] who published an interesting review on the recent advances in the fabrication of nanostructured materials using block copolymer chains as elementary building blocks, focusing the attention on the relationship between the physicochemical properties of the copolymer chains and the characteristics of nano-objects originated from their self-assembly in solution and in bulk. More recently, Capretti et al. [302] reported an interesting study on the use of BC self-assembling as a unique tool for realizing large-area ordered metamaterials with desired optical properties. Choi et al. [303] reported the interfacial assembly of amphiphilic heteroarm star copolymers on graphene oxide flakes at the air-water interface indicating that this non-covalent assembly represents a facile route for the control and fabrication of graphene oxide-inclusive ultrathin hybrid films applicable to layered nanocomposites. Horechyy et al. [304] proposed a novel step-wise approach for fabrication of periodic arrays of two different types of nanoparticles selectively localized at different block copolymer phases.

Regarding the localization of the NP, it is also important to remark that, when working with nanoclays and block copolymer structures, in general, the nanoparticles prefer to be hosted at the interface instead that in one phase as reported by Finnigan et al. [305] and Osman et al. [306] among others. These works

indicate the importance that nowadays is attributed to the nanostructuration of nanocomposites by using BC templates.

First of all when working with BC matrices the main goal is not only to obtain a good dispersion of the nanoparticles but also to reach the confinement of the nanoparticles into one block of the BC matrices. In order to achieve this goal two are the principal strategies to take into account. One is referred to the geometry of both the nanoparticles as well as of the self-assembly nanostructured domains of the BC, in order to avoid steric problems. On the other hand, it is necessary to drive the nanoparticles inside to only one block of the BC matrix. So, both surfactants and functionalization of the external surface of the NP can be used in order to achieve a good confinement of nanoparticles in only one block [307]. In fact, the major drawback when working with nanoparticles consists in obtaining good dispersion and absence of agglomeration into the polymeric matrix. Therefore, the inability to disperse NP in the matrix has been singled out as one of the main drawbacks when working with NP-composite materials and chemical modification of the NP surface and adsorption of polymers or surfactants provides useful dispersion techniques.

Following these drawbacks, in the last years, BC have been considered as potential candidates for the functionalization of NP [308,309], but in this review we will focus the attention on the confinement of NP into the BC matrices and, in particular, on how the confinement of NP can affect the self-assembly and phase separation of the BC matrices.

So, first of all the geometry of both nanostructured matrices as well as of the nano-objects must be correlated. At this regard, it must be considered that self-assembling BC nanostructures can form three main nanostructures such as lamellar, cylindrical and spherical domains while the geometry of NP can be classified into three main classes: 3D such as spherical nanoparticles with their three dimensions in the nanoscale range, 2D, such as nanotubes, that present 1 dimension not at nano-level, 1D, such as nanoplates, that present two dimensions not at nanoscale. The geometry relationship between BC nanophases and nanoparticles is reported in Table 1.

Intuitively, NP with 3D geometry can be incorporated into all the domains of the BC, while 2D nanoparticles theoretically can be introduced into cylindrical and lamellar domains, and 1D NP only into lamellar domains.

It is also important to underline that to control the confinement of NP in a single domain of the nanostructured phases of a BC, it is normally necessary to provide a proper chemical and/or physical functionalization of the nanoparticles. More specifically, when using a surfactant and working with BC, the surfactant not only can

Table 1
Relationship between BC morphologies and nanoparticle geometry [278].

BC morphologies→			
Nanoparticle geometry↓	OK	OK	OK
	OK	OK	OK
	OK	OK	NO
	OK	NO	NO

act as a bridge between the hydrophobic/hydrophilic materials but due to its selectively with one of the blocks, it can drive the NP into the selected block. Therefore, in nanocomposites based on BC matrices, it is very interesting to study the morphological changes produced in the BC matrix due to the confinement of the nanoparticles and to correlate them with the variation in the final properties of the nanocomposites. Peponi et al. studied the minimum surfactant concentration necessary to avoid affecting the mechanical as well as the rheological properties of the BC-based nanocomposites reinforced with silver NP [310]. Also Adhikari et al. studied the effects of surfactant treated boehmite NP on the thermal and mechanical properties of BC [311].

Numerous are the example reported in the scientific literature about the incorporation of metal spherical nanoparticles (3D), into the BC matrices. In particular, Horiuchi et al. [312] described a simple dry process to assemble metal nanoparticles in polymer films in two- and three-dimensions in multi-length scales. They used a bottom-up approach for the construction of well-ordered polymer/metal nanocomposites, as well as developed a top-down approach that enables the assembly of nanoparticles by UV photolithography. Bae et al. focused their research on the preparation of gold nanoparticles decorated with thiol-terminated polystyrene for PS-based thin nanocomposite films to fabricate organic memory devices exhibiting switching behaviors [313]. Hu et al. [314] studied the thermal and spectroscopic properties of polystyrene matrix nanocomposites with gold nanoparticles. Haupt et al. [315] presented a multistep procedure, based on the self-assembly of metal-loaded poly(styrene-*b*-(2-vinylpyridine)) micelles for creating nanohole-patterned gold films.

Peponi et al. [316] studied the morphological changes in the micelles of nanocomposite gels based on poly(styrene-*b*-butadiene-*b*-styrene) SBS block copolymer and Ag nanoparticles, when 1 wt% Ag NP were added to the physical gel of SBS. Zhou et al. studied the assembly of silica nanospheres in BC matrices [317], while Suntivich et al. [318] reported a study on the growth of gold NP in poly(styrene/(2-vinyl pyridine)) star-shaped block copolymer monolayers.

Moreover, Gutierrez et al. used the sol-gel technique in order to generate nanocomposites based on TiO₂ nanoparticles dispersed in poly(styrene-*b*-(methyl methacrylate)) and they observed by atomic force microscopy (AFM) that the addition of different amounts of nanoparticles caused strong variations in the self-assembled morphology of the TiO₂/SMMA nanocomposites with respect to the block copolymer [319]. Also Buzdugan et al. [320] used sol-gel processes to generate silica and to disperse it in hybrid composite materials based on radial styrene-butadiene block polymers.

Zhao et al. [321] studied the order-disorder transition in nanocomposites based on Pd nanoparticles dispersed in poly(styrene-*b*-isoprene) microdomain or in poly(styrene-*b*-(methyl methacrylate)) [322]. Peponi et al. [323–325] also studied the influence of the addition of Ag NP into the self-assembly morphologies of block copolymer of poly(styrene-*b*-isoprene-*b*-styrene) SIS. In particular, they added different amount of NP starting from 0.5 wt% up to 10 wt%. In Fig. 13 is reported the morphological changes. In this case, the Ag NP were treated with dodecanethiol, DT, a surfactant selective for the PS block of the SIS BC used.

Therefore, by increasing the amount of the treated Ag NP confined in the PS block, a gradient of PS phase was created, and this gradient was able to move horizontally along the phase diagram yielding to design different nanostructured morphologies. In particular, from a cylindrical neat SIS BC nanostructured phase, lamellar phase has been obtained adding up to 1 wt% treated Ag NP. Thus, by increasing the amount of treated AgNP up to 5 wt% the inverted cylindrical phase was obtained. For increasing the amount of treated Ag NP up to 10 wt%, disordered structures were obtained even if, as can be noted in the image, the treated Ag NP are well dispersed into the BC matrix and no agglomerations are observed. Consequently, performing the confinement of nanoparticles into the BC blocks not only can lead to a polymer matrix with a desired nanostructure, but also it will be possible to design functional nanocomposites with different properties depending on the properties of the NP confined (optical, electrical, magnetic, etc.) and well dispersed into the BC.

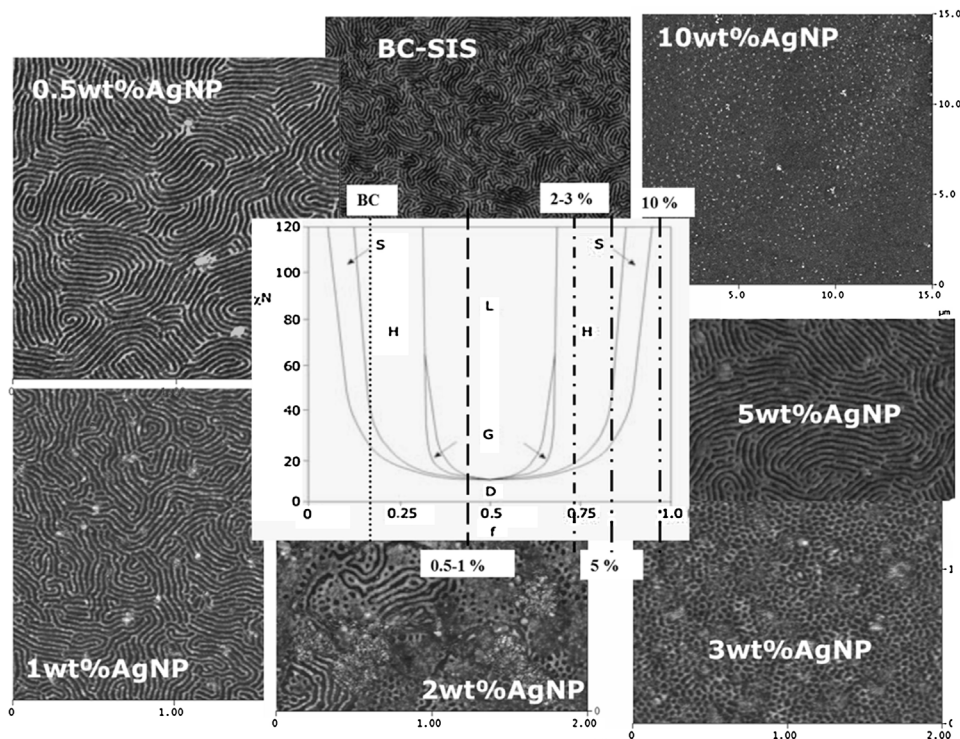


Fig. 13. Different nanostructured morphologies obtained adding different amount of Ag NP into the PS block of the SIS BC matrix.

Peponi et al. [326] studied the conductive response on nanocomposite based on poly(styrene-*b*-butadiene-*b*-styrene) SBS BC and Ag nanoparticles by electrostatic force microscopy (EFM). In particular, they analyzed the conductive abilities of SBS-Ag nanocomposites able to act as template for conductive materials. At this regard, the surface potential of the samples were measured by EFM and the localization of nanoparticles confined into the polystyrene cylinders was detected by applying a voltage of 5 V (Fig. 14).

Gutierrez et al. [327] studied also by EFM the conductive properties of nanocomposites based on TiO₂ nanoparticles and poly(styrene-*b*-(ethylene oxide)) BC matrices. Askari et al. [328] studied the optical properties of nanocomposites based on gold spherical nanoparticles dispersed in a cylindrical di-block copolymer. Garcia et al. reported a deep study on the nanostructuration of BC nanocomposites reinforced with modified magnetic nanoparticles [329].

As discussed previously, it is very important to well-understand the phase diagram of the BC and computational analysis can help to understand their phase separation behavior after the incorporation of nanoparticles into the BC matrices. Huh et al. [330] for example, investigated the influence of hard nanoparticles on the phase behavior of di-block copolymers and, by using Monte Carlo simulations, they obtained the phase diagrams as a function of the nanoparticle size and concentration. Fermeglia et al. [331] indicated that atomistic-based simulations such as molecular mechanics, molecular dynamics and Monte Carlo-based methods could be applied for industrial applications such as polymer-organoclay nanocomposites of a montmorillonite-polymer-surface modifier system, mesoscale simulation for di-block copolymers with dispersion of nanoparticles, polymer-carbon nanotubes system and applications of multiscale modeling for process systems engineering.

Regarding the confinement of 2D nanoparticles into the BC matrices, most of the scientific papers published on this topic are focused on the use of CNT as 2D nanoparticle. In particular,

Alberne et al. [332] studied the effects of the functionalization of multiwall carbon nanotubes on the morphology of the BC based nanocomposites prepared by solution casting. Zou et al. [333] presented a study on the dispersion of pristine both single-wall and multiwall carbon nanotubes using conjugated BC based on poly(3-hexylthiophene) (P3HT) and a polystyrene (PS) segment. The P3HT block forms pi-pi interactions with CNT, while the polystyrene block provides a good solubility to the debundled carbon nanotubes revealing that this approach is generic for carbon nanotube dispersion. Moreover, based on this approach they were able to functionalize also the CNT [334] and to create a superhydrophobic and conductive nanocomposite coating [335].

Bennett et al. [336] reported a novel approach that use block copolymer micelles to create large area arrays of iron-containing nanoclusters capable of catalyzing the growth of carbon nanotubes. Brostow et al. [337] created hybrids of functionalized single wall carbon nanotubes and multiwall CNT with a block copolymer of semicrystalline poly(butyl terephthalate) with amorphous oxytetramethylene studying their mechanical and tribological properties. Chakoli et al. [338] reported a study where poly(*L*-lactide-*co*- ϵ -caprolactone)-functionalized multiwall carbon nanotubes were synthesized by in situ ring-opening copolymerization. More recently, Chen et al. [339] reported another example of in situ polymerization between BC and CNT.

Datsyuk et al. [340] reported an investigation on nanocomposites based on amphiphilic BC and double walled carbon nanotubes obtained by in-situ polymerization. Gilmore et al. [341] studied the incorporation of CNT into the poly(styrene-*b*-isobutylene-*b*-styrene) SIBS BC, extensively used as a coating for medical devices in which it acts as a carrier for therapeutic drugs. Therefore, the incorporation of carbon nanotubes was investigated in order to modify both the electrical conductivity and the surface characteristics of the SIBS coatings to control and design the cell adhesion and proliferation characteristics of the coatings.

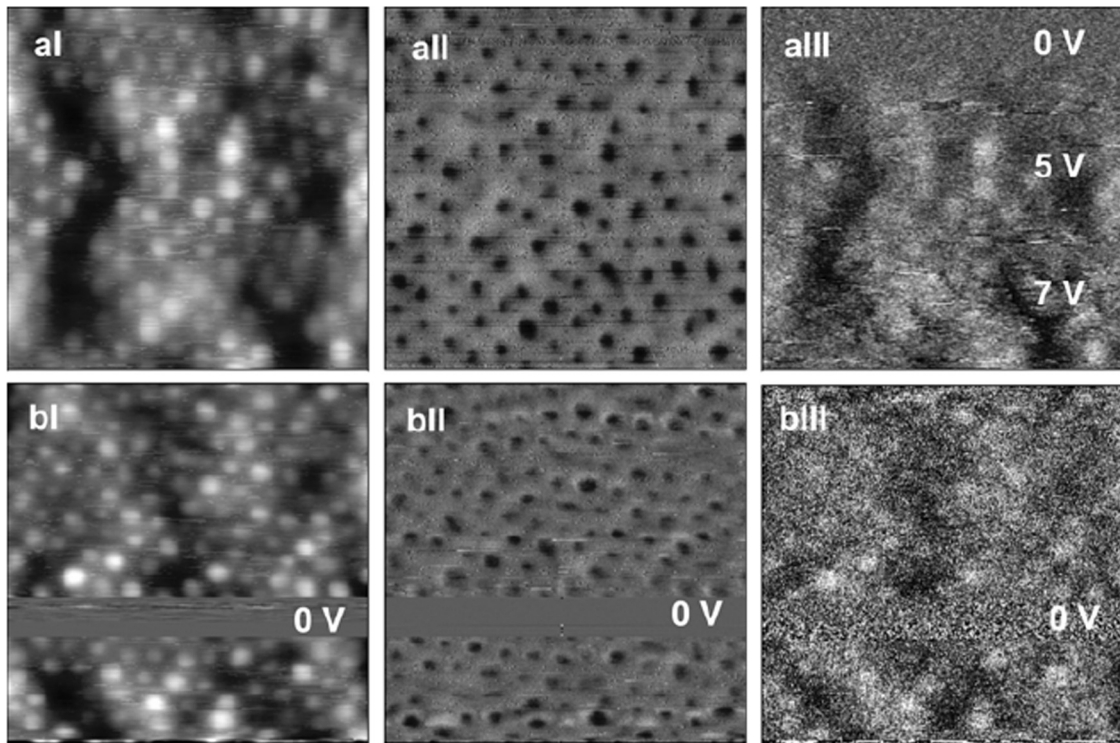


Fig. 14. 500 × 500 nm topographical, height and phase, I and II, respectively, and surface potential images, III, carried out on DT-Ag/SBS nanocomposite containing 7 wt% Ag nanoparticles. Reproduced with permission of John Wiley and Sons [326].

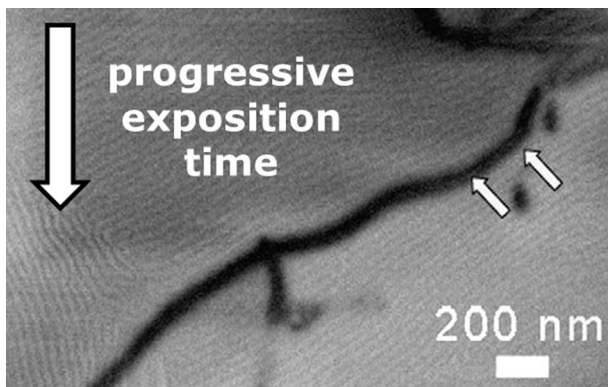


Fig. 15. FE-SEM image of the confinement of functionalized CNT into the PS block of the SIS BC (from [343]).

Li et al. [342] studied the final morphologies of fluorine containing poly(styrene-*b*-poly(2-vinylpyridine)) obtaining their phase diagram. The block composition, molecular weight, and the length of the fluorene side chain were varied to control the final morphologies, while the phase diagrams of the resulting block copolymers greatly depended on fluorene content. Depending on the number of pendant fluorene units, the block volume ratio, the solvent used to cast the samples, and thermal annealing history, spherical, hexagonally packed cylinders, lamellar, gyroidal, and hexagonally perforated lamellae could be found. The capability of these BC to host COOH-modified single wall carbon nanotubes (SWCNT) was also investigated and it was found that hydrogen bonding between COOH and one of the blocks favors miscibility of SWCNT within poly(2-vinylpyridine) domains.

Peponi et al. [343,344] studied the selective confinement of functionalized CNT in poly(styrene-*b*-isoprene-*b*-styrene) block copolymer matrix. They found that the functionalized CNT is able to well adapted to the lamellar morphology of the BC even in the cases where the lamellae is not straight, as reported in Figs. 15 and 16. Moreover, they reported the ability of electrostatic force microscopy to localize the CNT inside the PS domains of a block copolymer matrix (Fig. 16).

Also Garate et al. reported a study on the confinement of functionalized CNT on the SIS BC matrices [345], while Hernandez et al. [346] studied the relationships between the macroscopic deformation behavior and microstructure of a pure PBT-*b*-PTMO block copolymer and its polymer nanocomposite when 0.2% SWCNT was added.

Acharya et al. [347] presented a facile route to decorate the surface of networked single walled carbon nanotubes with silver nanoparticles by using copolymer micelles capable of stabilizing nanotubes in solution and subsequently forming a thin and uniform block copolymer/SWCNT composite film upon spin coating. Then, through the selective doping of silver acetate into BC domains in a thin composite film, the formation of Ag NP in the cores of micelles was obtained.

More recently, Enotiadis et al. [348] used a linear tri-block copolymer of the glassy-rubbery-glassy type for the development of novel polymer nanocomposite materials. Hybrid nanoadditives were prepared by catalytic chemical vapor deposition (CCVD) where carbon nanotubes were grown on the surface of smectite clay nanolayers. The hybrid clay-CNT nanoadditives were incorporated in the copolymer matrix by a simple solution-precipitation method increasing the mechanical behavior of the nanocomposites. More recently, Becker et al. [349] presented an interesting review on the recent advances in the use of surfactants and BC for dispersing and stabilizing CNT in several different media.

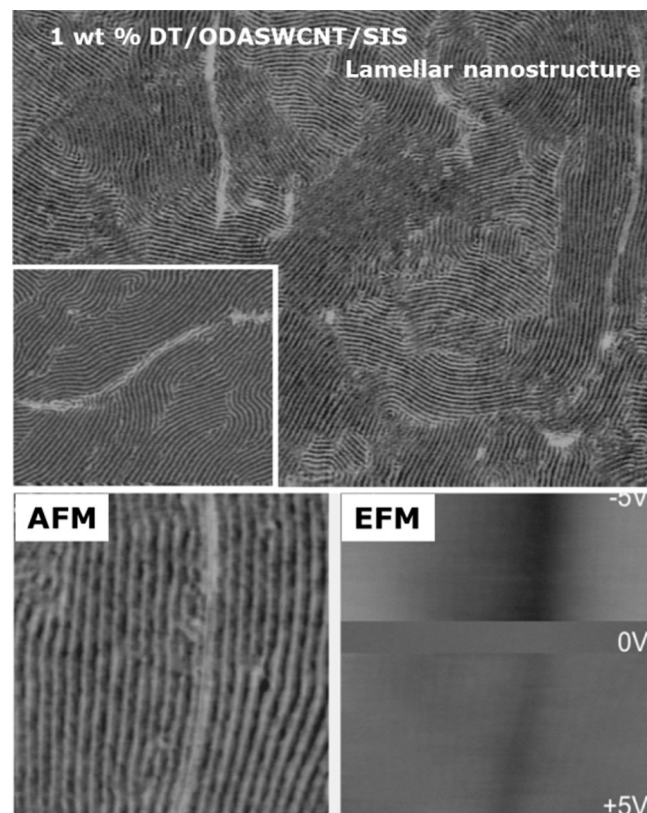


Fig. 16. AFM and EFM images of the confinement of functionalized CNT into the PS block of the SIS BC (from [344]).

Regarding the confinement of 1D nanostructures into the block copolymer matrix very few research works are reported, due to steric problems between the nanoparticles geometry and the nanostructure domains of the BC host. 1D nanoparticles are mainly represented by layered silicates and graphene.

At difference of 3D and 2D nanoparticles, for 1D NP few articles have been published in the last decade on the dispersion of layered silicates into BC matrices. For example, Adhikari et al. [350] studied the mechanical properties of nanocomposites based on a SBS tri-block copolymer and optimum dispersed organo-modified layered silicates prepared by solution casting followed by melt shearing. Ganguly et al. reported a study on the morphological mapping of thermoplastic elastomeric tri-block copolymers having different block lengths and their clay nanocomposites by using AFM. These nanocomposites exhibited well-ordered phase separated morphology [351]. Ganss et al. [352] investigated the influence on the mechanical response of the BC matrix nanocomposites of the incorporation of oligostyrene-modified montmorillonite (MMT) and oligostyrene-modified bentonite (BET) into star shaped styrene-butadiene block copolymers. Ha et al. [353] studied the deformation behavior of roll-cast layered-silicate/lamellar tri-block copolymer nanocomposites possessing a uniaxial texture in order to elucidate the effects of anisotropic particles upon deformation of the globally textured nanocomposite systems.

Vazquez et al. [354] analyzed the structural and ordering behavior in nanocomposite based on lamellar tri-block copolymer and different layered silicates. They verified by AFM that the nanosilicates were well-dispersed in the BC but not completely exfoliated.

Finally BC and layered silicates have been studied also in solution. Choi et al. [355] studied the generation of micelle-templated organosilicate nanostructures resulting from the self-assembly of a block copolymer/organosilicate mixture followed by

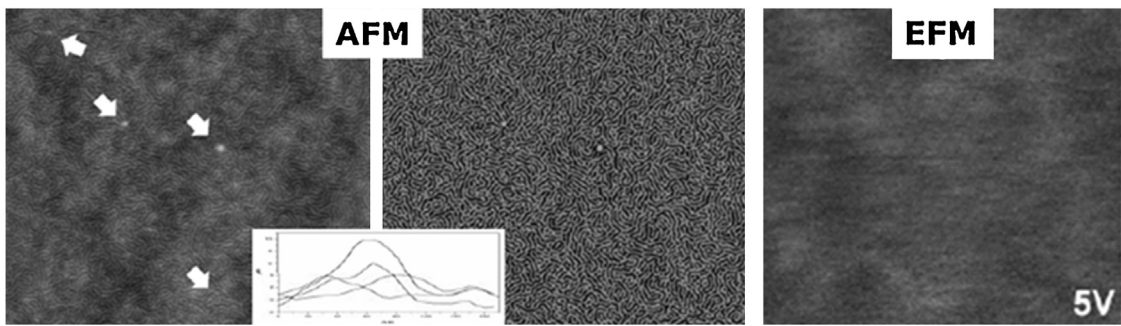


Fig. 17. Nanocomposite based on SIS and graphene nanosheets. AFM and EFM analysis (from [356]).

organosilicate vitrification and copolymer thermolysis by varying the solution conditions and the copolymer/organosilicate mixture composition.

In case of **graphene**, very few reports have been published on the confinement of graphene into the BC matrix. Peponi et al. [356] reported a study on the confinement of functionalized graphene sheets in the polystyrene domains of a nanostructured poly(styrene-*b*-isoprene-*b*-styrene) (SIS) block copolymer, also verifying by EFM the superficial electrical conductivity of the nanocomposites due to the presence of the graphene (Fig. 17).

In most cases, block copolymers are used to functionalize the graphene sheets as reported by Cao et al. [357]. They used click chemistry in order to functionalized graphene oxide sheets with poly(styrene-*b*-ethylene-*co*-butylene-*b*-styrene) (SEBS) tri-block copolymers and they incorporated the obtained SEBS-clicked-GO into polystyrene (PS) as reinforcing fillers. They obtained excellent compatibility with the PS matrix, and consequently, they achieved remarkably improved mechanical properties and thermal stability of the resulting composite films. Moreover, Chen et al. [358] modified non-covalently pristine graphene flakes with an amorphous-crystalline block copolymer, poly(vinylcyclohexane-*b*-ethylene-*b*-vinylcyclohexane) (PVCH-*b*-PE-*b*-PVCH) taking advantage of the fact that the PE block selectively crystallizes on the graphene surface, while the PVCH block extends freely and stabilizes the graphene flakes in aliphatic and aromatic solvents, which are generally viewed as nonsolvents for graphene. Zheng et al. [359] reported a study on a non-covalent modification of graphene oxide (GO) sheets with an amphiphilic double-crystalline block copolymer, poly(ethylene-*b*-(ethylene oxide)) (PE-*b*-PEO) with assistance of supercritical CO₂. Another example has been reported by Velusamy et al. [360]. In fact, they reported a simple but robust route to efficiently disperse very high concentrations of chemically reduced graphene oxides (rGOs) in various non-polar solvents and polymers based on the non-covalent, nondestructive modification of rGOs with a conjugated block copolymer, the poly(styrene-*b*-paraphenylene).

Furthermore, block copolymers can be used to obtain a direct exfoliation of graphite flakes as reported by Liu et al. [361]. They presented a method for the preparation of graphene/polymer composites by direct exfoliation of graphene from micro-sized graphite using a pyrene-functionalized amphiphilic block copolymer, in either aqueous or organic media. Skaltsas et al. [362] obtained the successful exfoliation of graphite to graphene sheets in a liquid phase via tip sonication using block copolymers to obtain a better aqueous solubilization of graphene.

In other cases, graphenes have been used to prepare special block copolymers nanotemplates. For example, Kim et al. [363] demonstrated that sufficiently reduced graphene served as a neutral surface modifier to induce surface perpendicular lamellae or cylinders in a block copolymer nanotemplate. On the other hand, Liu et al. [364] reported a process for fabricating dense

graphene nanoribbon arrays using self-assembled patterns of BC on graphene grown epitaxially on SiC, on the wafer scale. This process was developed combining both top-down and self-assembly steps to fabricate long graphene nanoribbon arrays with low defect counts.

2.2. Nanostructured thermoplastics and blends

When working with bottom-up nanostructured thermoplastic blends it is very important to take into account the compatibilization for improving the dispersability of nanoparticles into them, reducing interfacial tension, facilitating dispersion, stabilizing the morphology, enhancing adhesion between phases and improving the mechanical properties. In order to reach a good compatibilization, three mean solutions can be adopted: one is to select the most suitable blending technique; the second is the addition of a third homopolymer or block or graft copolymer or low molecular reactive compounds, which are miscible with any of the two phases, obtaining a non-reactive compatibilization; the third one is the reactive compatibilization applied when suitable functionalized polymers are used for specific interactions or chemical reactions. At this regard, block copolymers can play a double role, emulsify the disperse phase to give smaller particles as well as increase the interfacial adhesion between the phases. In particular, Macosko et al. deeply studied the effect of the reduction of the interfacial tension when block copolymers are used in polymer blends [365,366].

Moreover, an important application of block copolymers is their use as blend compatibilizer of otherwise immiscible homopolymers as deeply reviewed in the scientific literature [367–371]. In particular, blends of a block copolymer with a homopolymer, present interplay between macrophase separation (due to the presence of the homopolymer) and microphase separation (due to the BC). Which effect predominates depends on the relative length of the polymers and on the composition of the blend. In fact, BC can solubilize homopolymers up to a certain amount, beyond which, phase separation occurs. This ability to swell block copolymer microstructures is the basis of a number of potential and actual applications in optoelectronics. The limit for macrophase separation in blends of BC with homopolymer depends on the relative chain lengths as reported by Hashimoto et al. [372]. Another important aspect of adding homopolymer to a block copolymer is the ability to change morphology as indicated by Koizumi et al. [373].

Nanostructured blends of BC with two homopolymers can be obtained when BC act as compatibilizers by reducing the interfacial tension between homopolymers as analyzed by Hillmyer et al. [374]. It has been reported that BC can reduce the interfacial tension between homopolymers to the extent that polymeric microemulsions can be formed where the copolymer forms a continuous film between spatially continuous homopolymer

domains [375–377]. Although a theory for these compositions has not yet been developed, it should be considered that some properties of microemulsions such as elastic constants, composition profiles, etc., can be modeled [378–379]. Blends of different BC have been investigated in order to find the limit between macro and micro-phase separation as well as in order to induce morphological ordered nanostructures impossible to realize for the pure BC [380–382]. Frielinghaus et al. [383,384] studied the ABC tri-blocks morphologies just by blending AB and BC di-blocks with the block B, the polyisoprene, being the other two blocks polystyrene and poly(ethylene oxide). In this way, they can map their miscibility/immiscibility region.

It is also interesting to pay attention to structured thermoplastic blends of different polymers, and in particular of two important biopolymers, nowadays of great importance in the international scientific panorama. In particular, we refer to polylactide, PLA, widely used for different industrial applications, which presents brittleness as a main drawback. A successful approach used to strengthening and toughening brittle and stiff polymers is blending them with a soft or elastomeric second component. In fact, when the softer component forms a second phase within the more brittle continuous phase, it may act as a stress concentrator, enabling ductile yield mechanism and preventing brittle failure [367–370]. Poly(ϵ -caprolactone) (PCL) is a good candidate to toughen PLA. In particular, Lopez-Rodriguez et al. [385] and Simoes et al. [386] reported that there is a clear phase-separation of PLA/PCL blends at different mixing ratios in agreement with the work of Wu et al. [387], indicating that three typical immiscible morphologies, i.e. spherical droplets, fibrous and co-continuous structures, can be observed at various compositions of PLA/PCL blends.

2.3. Nanostructured thermosets and blends

The concept of nanostructured thermosets in a bottom-up approach refers to a thermosetting polymer nanostructured by blending with other polymers able to arrange into smaller components or nanostructures through complex assemblies. Nanostructuring of thermosetting systems using the concept of templating and taking advantage of the self-assembling capability of block copolymers is an exciting way for designing new materials for nanotechnological applications.

Epoxy is one of the thermosetting materials more widely used in the modern polymeric word even if its brittleness limits its use [388,389]. Many research approaches have been developed in order to improve the physical properties of thermosets through the incorporation of flexible elastomeric segments in the brittle epoxy network. But more efforts are needed considering that a typical drawback when using these approaches is the phase separation during the curing process, that generally results in micro irregular distribution of inclusions in the crosslinked networks. Therefore, in order to provide an efficient toughening effect, it is important to control the size and the distribution of these inclusions in the thermoset networks. Elliniadis et al. [390] reported a study on the phase diagram prediction for thermoset/thermoplastic polymer blends applied to an epoxy/polyarylsulfone blend paying particular attention to the competition between phase separation and cross-linking of the epoxy. Successively, Fine et al. [391] used a tri-block copolymer in order to compatibilize thermoplastic/thermoset blends of poly(phenylene ether) (PPE) as thermoplastic and using as the thermoset precursors a typical liquid epoxy formulation, diglycidyl ether of bisphenol A (DGEBA) and an aromatic diamine (4,4' methylene bis [3 chloro 2,6 diethylaniline], MCDEA). The tri-block poly(styrene-*b*-butadiene-*b*-methyl methacrylate), SBM was chosen because PS blocks interact very favorably with PPE; PMMA blocks remain miscible with the

thermoset during the whole curing process, and PB mid blocks cover the interface. Moreover, they found that the strong repulsion between PPE and PMMA blocks governed the organization of the blend before and during the curing process and demonstrated that the number of SBM micelles and their degree of dispersion was the main parameter controlling the mechanical properties of the resulting blends.

Indeed, the first example of a nanostructuring epoxy matrix was reported by Hillmyer et al. [392]. They reported a system formed by a low molecular weight bisphenol-A/epichlorohydrin epoxy system as a thermosetting precursor with amphiphilic di-block copolymers such as poly(ethylene oxide)-*b*-poly(ethyl ethylene) (PEO-PEE) and poly(ethyleneoxide)-*b*-poly(ethylene-alt-propylene) (PEO-PEP). They verified the miscibility of PEO with the epoxy precursor obtaining a system characterized by a negative Flory-Huggins interaction parameter and reported that the epoxy was able to swell the PEO domain without dissolving the other block, thus leading to an ordered hexagonally packed cylinder morphology of BC in the epoxy matrix. This behavior was preserved even after the crosslinking of the epoxy marking a clear difference with other epoxy-PEO systems where PEO was segregated. In this case, PEO-block acted as the bridge between the epoxy matrix and the other block of the BC as shown in Fig. 18 [392].

Starting from this study, numerous articles have been reported in the scientific literature regarding the use of BC for generating nanostructured epoxy or phenolic systems with long-range order in both uncured and cured states. Among them, Lipic et al. [393] studied a mixture of a low-molecular-weight poly(ethylene oxide)-*b*-poly(ethylene-alt-propylene) (PEO-PEP) di-block copolymer and a poly(bisphenol-A-*c*-epichlorohydrin) epoxy that selectively mixed with the PEO block, obtaining ordered structures of about 10 nm. They studied the corresponding morphologies with and without hardener and they found that without hardener, the phase behavior of BC/epoxy blends was similar to model BC/homopolymer blends and varied with changes in the blend composition and temperature obtaining lamellar, cubic bicontinuous, hexagonally packed cylinders, body-centered cubic packed spheres, and disordered micelles by increasing the epoxy concentration. While, when diaminodiphenyl methane, DDM, an aromatic amine hardener, was added to the blends, as the cured epoxy molecular weight increased, the PEO block segregated from the epoxy matrix, obtaining an increase in the principal spacing of the ordered structures and an order-order phase transitions at

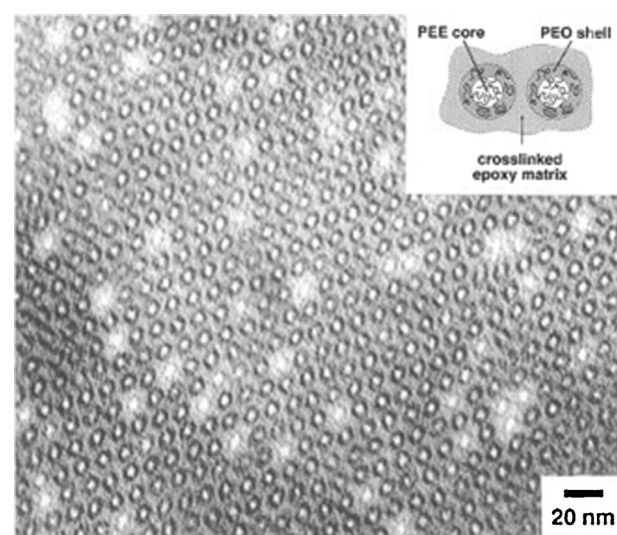


Fig. 18. TEM image of cured epoxy/PEO-PEP system. (The inset depicts the idealized nanostructure) (from [392]).

certain compositions. Chen et al. [394] reported a study on the phase separation process in blends of epoxy with poly(ϵ -caprolactone) finding a critical point in which macrophase separation occurs. Successively, they correlated this phase separation mechanism with the temperature and the curing process [395].

Larranaga et al. published a study on the microphase separation occurred in epoxy systems based on DGEBA and 4,4'-diaminodiphenylmethane cure agent blended with poly(ethylene oxide)-co-poly(propylene oxide)-co-poly(ethylene oxide) PEO-PPO-PEO tri-block copolymers [396]. Meng et al. [397] synthesized amphiphilic tri-block copolymer poly((ϵ -caprolactone)-*b*-butadiene-*b*-(ϵ -caprolactone)) (PCL-*b*-PB-*b*-PCL) via the ring-opening polymerization. The amphiphilic tri-block copolymer was further used to prepare nanostructured epoxy thermosets, taken into account that the PCL block is miscible with the epoxy remaining mixed with the cross-linked epoxy network. They reported a formation mechanism of the nanostructure in contrast to the strategy in which some equilibrium self-organized structures were preformed and the microphases were fixed via subsequent curing reaction.

Another interesting example was reported by Ritzenthaler et al. [398] where an epoxy precursor was blended with poly(styrene-*b*-butadiene-*b*-(methyl methacrylate)) tri-block copolymers and investigated before and after the epoxy-amine curing reaction. In Fig. 19 are reported the schematic description of the evolution of the tri-block organization in the DGEBA-MCDEA thermoset system before and after reaction.

Ocando et al. used a semifluorinated di-block copolymer in order to nanostructure thermosetting materials [399]. Tercjak et al. studied a thermally switchable nanostructured thermosetting material prepared by modification of an epoxy with 5 wt% of an amphiphilic poly(styrene-*b*-(ethylene oxide)) block copolymer and 30 wt% of a low-molecular-weight liquid crystal, 4'-(hexyl)-4-biphenylcarbonitrile [400]. Xu et al. [401] synthesized via the ring-opening polymerization poly((ϵ -caprolactone)-*b*-dimethylsiloxane-*b*-(ϵ -caprolactone)) tri-block copolymer (PCL-*b*-PDMS-*b*-PCL) to prepare nanostructured thermosetting blends and analyzed the obtained morphologies as well as their thermomechanical properties.

More recently, confirming the relevance of this topic in the scientific panorama, Romeo et al. [402] reported that it is possible to generate different nanostructures in a specific BC/epoxy blend simply by varying the cure cycle. Therefore, BC can be used as chemical compatibilizers with epoxy polymers but, when the BC blocks are not miscible with the epoxy, they must be functionalized by introducing suitable reactive groups in order to develop the covalent bonding for the epoxy network without the loss of long-range order in the resulting blends [403]. At this regard, one of the thermoplastic elastomers more used is the

poly(styrene-*b*-butadiene-*b*-styrene) (SBS) due to the fact that the PS block is immiscible with the epoxy and the PB can be chemically modified to turn it miscible with the epoxy as reported by Grubbs et al. [403]. For the chemical modification, one of the opportune methods is the epoxidation, which inserts oxygen atoms in the double bonds of the butadiene block [404]. Numerous examples are reported in literature regarding the use of epoxidized BC to nanostructured epoxy networks. Serrano et al. reported that epoxidized styrene-butadiene copolymers showed improved miscibility with epoxy monomers leading to self-assembled nanostructures in the uncured state [405]. Moreover, they obtained the nanostructuration of the thermosetting systems prepared by modification of an epoxy with 30 wt% epoxidized poly(styrene-*b*-butadiene) di-block copolymer [406,407] as well as using an epoxidized styrene-butadiene star block copolymer [408]. More recently, George et al. [409] reported a study on the mechanical characterization of the nanostructured thermoset system based on epoxidized SBS at several epoxidation degrees, while Ocando et al. [410] reported an approach to stiffen an epoxidized SBS thermoplastic elastomer by adding small amount of epoxy precursors.

Examples of nanocomposites based on thermoplastic/thermoset nanostructures blends are also reported in the scientific literature. In fact, Ocando et al. [411] obtained nanocomposite materials based on nanostructured epoxy system, SBS epoxidized tri-block copolymer and well-dispersed Al₂O₃ nanoparticles allowing an increase in fracture toughness maintaining the transparency and stiffness of neat epoxy.

Gutierrez et al. [412] prepared novel inorganic organic nanostructured thermosetting composites based on poly(styrene-*b*-ethylene oxide) BC used as templating agent and titanium dioxide (TiO₂) nanoparticles synthesized via sol-gel, studying the morphologies generated in the binary and ternary epoxy-based systems by AFM while confirmed the conductive properties of TiO₂ nanoparticles embedded in nanostructured thermosetting composites by using EFM measurements.

In addition to the epoxy system, attention has been focused also on unsaturated thermosetting polyesters. Some examples are reported by Serrano et al. [413], Mahaling et al. [414], Li et al. [415], Sinturel et al. [416], Builes et al. [417], Messori et al. [418]. More recently, Builes et al. [419] reported the relationship between the morphology of a nanostructured unsaturated polyester modified with a tri-block copolymer and its optical and mechanical properties.

In conclusion, multifunctional nanocomposite materials based on nanostructured thermosetting matrices with high transparency, improved mechanical and conductive properties, among others, can be obtained by mixing thermosetting system with block copolymers, which are able to phase separate within a nanometric scale, and nanoparticles.

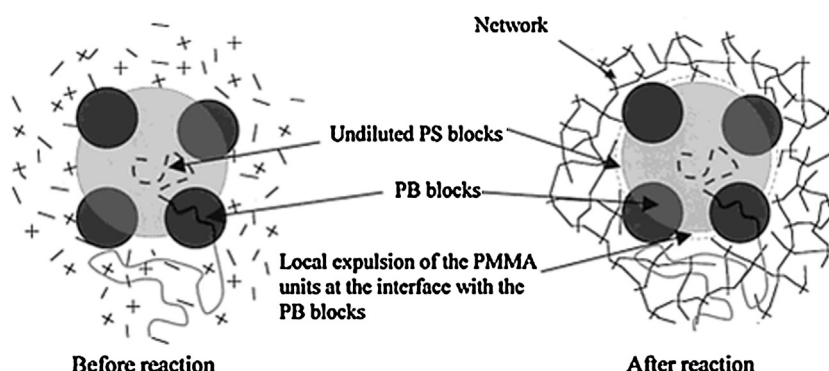


Fig. 19. Schematic description of the evolution of the tri-block organization in the DGEBA-MCDEA thermoset system before and after reaction (from [398]).

3. Top-down processing of thermosetting matrix nanocomposites

3.1. Dispersion of nanoparticles in thermosetting polymers

3.1.1. Dispersion of nanoclays in thermosetting matrices

Although the *in situ* intercalative polymerization exhibits some disadvantages, this is the only practicable technique for the preparation of thermoset-based nanocomposites [420–423]. In this case, the exfoliation ability of the organoclays is determined by their nature, as for example, the catalytic effect of the clay modifiers on the curing reaction, the miscibility with the curing agent, etc. As reported in literature [10,35,424], a curing competition between intra-gallery and extra-gallery monomer often occurs: if the intra-gallery polymerization occurs with a rate comparable to the extra-gallery polymerization, the curing heat produced is enough to exceed the attractive forces between the silicate layers and an exfoliated nanocomposite structure can be produced. If the extra-gallery polymerization is faster than the intra-gallery polymerization, or if intra-gallery polymerization is somehow delayed, the extra-gallery monomer will gel before the intra-gallery monomer that will produce not enough curing heat to lead the clay to exfoliate. Some factors can promote the curing reaction of the intra-gallery monomer and, consequently, facilitate the exfoliation of the clay. For example, the catalytic effect of the organoclay on the curing reaction, the capacity of curing agent to penetrate in the interlayer of the clay, the long chain of the organo-cations that allow the penetration of a greater amount of precursor in the gallery creating weaker attractive forces between the silicate layers [35,424]. For example, in the study of the *in situ* intercalative polymerization for epoxy-based nanocomposites, Messersmith et al. [425] found that the curing agent used in the polymerization process is determinant for the final structure of the nanocomposite. They analyzed the effect of different curing agents and curing conditions in the formation of nanocomposites based on the sonication of an epoxy monomer (DGEBA) and montmorillonite. When they used diamines as curing agent, intercalated epoxy-clay structures were obtained, while when other curing agents such as nadic methyl anhydride, boron trifluoride monomethylamine or benzylidimethylamine were added, delamination occurred as confirmed by XRD. Kornmann et al. [422] achieved an exfoliated structure in unsaturated polyester based on montmorillonite without the interlayer ion exchange but modifying the montmorillonite with silane coupling agent.

The intercalation of thermosetting polymeric species in the galleries of nanoclays and the successive exfoliation requires equipment able to generate high shear stresses. Sonication and intensive mixing, able to generate high shear mixing forces, are extensively used for the compounding of nanoclays. As reported by Bittmann and co-workers [426] sonication is a valid method to obtain a good dispersion of inorganic particles in a liquid medium: ultrasound waves can generate micrometric air bubbles that, when collapse, originate high shear loads allowing the separation of tactoids. Kahraman et al. [427] found that, for epoxy/nanoclay systems, the sonication process is more effective for the dispersion of the clay particles in comparison with intensive mixing process. The same result was found by Dean and co-workers [428]. On the other hand, Sriraman et al. [429] determined that more homogeneous epoxy/clay dispersions could be achieved by shear mixing in comparison with those processed by sonication. Natali et al. [430] achieved a good exfoliation of clays in a phenolic matrix using a high shear mixer. Another approach to disperse the nanoclays was presented by Yasmin et al. [431]; they produced good dispersion of clay particles in an epoxy matrix with short processing times with a three-roll mill: the dispersion was achieved by the shear forces

and the elongational flow generated between the adjacent corotating rolls.

3.1.2. Dispersion of carbon nanotubes in thermosetting matrices

The importance of the state of dispersion of solid nanofillers on the properties of the final cured nanocomposites has been widely recognized [432,433]. In thermosetting nanocomposites, the dispersion step is carried out in the liquid pre-polymer state. It is assumed that a high level of dispersion is required in this stage of the preparation of the nanocomposite, as the highly attractive forces between the nanoparticles can be expected to result in some degree of re-agglomeration during the process of cure. Effective dispersion of CNT is difficult to achieve due to van der Waals forces causing them to aggregate as a result of the large surface to volume ratio. The energy needed to disperse the CNT must be sufficiently high to overcome the van der Waals forces, but not so high to fracture the CNT. Several mechanical methods are used to accomplish dispersion including ultrasonication, calendering, ball milling and high speed stirring [434–436]. Solution mixing is another common method in which CNT are dispersed in a suitable solvent by mechanical mixing, magnetic agitation or sonication. The solvent can also dissolve the monomeric precursors. Subsequently, the dispersed CNT are mixed with polymer matrix at room or elevated temperatures. *In situ* polymerization is an efficient method to realize uniform dispersion of CNT in a thermosetting polymer. In this method, CNT are mixed with monomers, either in the presence or in absence of a solvent, and then these monomers are polymerized via addition or condensation reactions with a hardener or curing agents at an elevated temperature.

Recently, ionic liquids were used with advantage to disperse CNT in epoxies and to prepare composites with superior mechanical properties [437]. Furthermore, besides the physical approaches for the CNT dispersion, some other attempts including the use of surfactants and chemical functionalization of the CNT-surfaces are available in the literature as suitable methods able to alter the degree of dispersion and tailor the interface between the matrix and carbon nanotubes. The development of CNT based nanocomposites has been achieved thanks to approaches that have been used to exfoliate bundles of CNT through the wrapping of the tubular surface by various species of polymers, aromatic compounds and surfactants [438,439].

Different works have been dedicated to the effect of CNT on the cure kinetics of an epoxy matrix. Valentini et al. [440] stated that single wall carbon nanotubes accelerated the cure reaction of the diglycidyl ether of bisphenol A/diethylenetriamine (DGEBA/DETA) epoxy system studied by DSC analysis. The role played by the amine functional groups when they interact with the surface of the SWCNT has been considered as the origin of the modification of the cure behavior [441]. Similar results were reported by Xie et al. [442] they reported an acceleration effect in the case of carbon nanotubes dispersed in the tetraglycidyl-4,4'-diaminodiphenylmethane (TGDDM) and 4,4'-diaminodiphenylsulfone (DDS) epoxy system. In this case, the presence of hydroxyl groups on the surface of the tubes has been considered as the main catalyst for the epoxy ring opening.

Tao et al. [443] have observed a decrease of the onset temperature also in the SWCNT/diglycidyl ether of bisphenol-F/diethyl toluene diamine system. The modification of the cure behavior in its early stage can be attributed to surface functional groups on CNT or catalyst particles [444–447]. More in general it was found that [448] the acceleration of the curing time was related to the specific surface area of the filler considering the proportional relationship between the surface area and the peak temperature (the higher the surface area, the higher the temperature drop). Bae et al. [449] investigated the effect of CNT on the cure reaction of liquid crystalline epoxy. The authors

reported a retardation effect of CNT, indicating that the presence of CNT did not have a significant effect on the total heat of reaction if compared to that of the unfilled system.

3.1.3. Dispersion of graphenes, direct exfoliation and chemical reduction of graphite oxide in thermosetting matrices

Graphene composites can be produced via *in situ* intercalative polymerization of monomers [450]. Successful polymerizations of epoxy [451] with thermally reduced graphene have been reported. The production of electrically conductive epoxy [452] with graphene has been also reported. These materials can be used, for example, for electromagnetic shielding and antistatic coatings [453]. Superior thermal transport properties of graphene dispersion have potential for thermal management in miniaturized electronic devices [454].

When the platelets were oriented by extrusion or solvent casting, the conductivity was higher in the direction of graphite alignment than perpendicular implying macroscopic anisotropy [455]. Silane modification of exfoliated graphite was used to enhance the conductivity gain for an epoxy matrix; covalent bonding between the graphite surface and the polymer matrix may reduce the acoustic phonon scattering at the interface [456]. Moreover, graphite nano-platelets (GNP), prepared by intercalating graphite with metal ions or by acid treatment, followed by thermal exfoliation, represent two-dimensional layered structures that possess excellent electrical and thermal conductivities along with high modulus, which can be incorporated into thermosetting matrices. They have already shown promising results in the field of polymer composites as sensor, thermal interface materials and to create electrically conductive polymers [457,458]. Similar to other polymer nanocomposites, when used as filler in a polymer matrix, the glass transition temperature, modulus and fracture toughness of the polymer is improved upon addition of GNP [459]. The effect of the dispersion method on the properties of graphene nanoplatelet composites [460] such as the solvent assisted dispersion of GNP before their incorporation in the monomer, was also investigated [461]. Recently, roll milling and sonication combined with high-speed shear mixing have been considered as alternative method for the dispersion of GNP in epoxy system, obtaining better electrical and mechanical properties [462,463]. The use of graphene for the development of a strain and damage sensor has been also extensively evaluated. Specifically, a graphene epoxy based mixture was used as a conductive coating that was cured onto a carbon fiber reinforced composite. This methodology proved to be very effective where substantial changes in piezoresistivity (up to 400%) were found as a function of strain (up to 2%) [464,465]. Nevertheless, very few studies have so far been reported on the fabrication of graphene nanoplatelets carbon fiber reinforced preprints [466], in which the role of adding GNP into the matrix material, that will largely affect the impregnation of fibers and prepreg processing conditions, has been considered.

In a different way, in the case of electrically insulating graphene oxide, the easy dispersion in thermosetting matrices needs further reduction steps that are not always possible to perform during the processing of polymer nanocomposites [467–472]. In fact, GO obtained by the chemical modification of graphite, gives rise to the formation of graphitic layers highly oxidized with the presence of epoxy, alcohol and carboxylic acid groups on their surface [473–475].

Graphene oxide electrical resistance is exponentially higher than that of graphene, this is owing to the defects brought about by the existence of such oxygen containing units, which could cause a degradation of the electronic conjugation of graphene [476,477].

The structure of GO is characterized by sp₂ carbon clusters separated by sp₃ carbon sites that act as barriers for charge carriers

[478]. Recently it has been proposed a model where the dimension of the restored sp₂ clusters is directly proportional to the increase of the thermal reduction time [478]; accordingly, it has been shown that deoxygenation occurs in GO when it is heated above 100 °C resulting in a thermal reduction.

Photoreduction recently attracted great attention due to the observation that irradiation of graphite oxide in solution by UV radiation reduces it to graphene with negligible surface oxygen functionalities [479]. Therefore, the reduction of GO is definitely a key topic, and different reduction processes result in different properties that in turn affect the functional performance of polymer materials when used for coatings. Though the final target to achieve perfect graphene is hard to reach, research efforts made it closer. Here we report the emerging methods for the reduction of GO during the preparation of coatings with functional properties based on advanced polymer matrices. Chemical free methods for the reduction of graphene oxide have been obtained for example through photocatalytic action of TiO₂ [480]. Flash reduction of graphene oxide films and light radiation reduction of GO solutions were also reported [481,482]. These latter two works deal with the use of flash lamp energies that were around 0.1–2 J/cm² and/or laser treatment of GO solutions, respectively; the threshold of excitation light resulting in photolysis products corresponds to an energy of 3.2 eV and the conductivity of the GO layers was restored by exposure to UV light [483].

Reduced graphene oxide (rGO) produced by interactions with radiation has advantages over other techniques, mainly related to the lower level of impurities retained by rGO, which represents a typical drawback for chemically reduced GO. In this view, the preparation of polymer composites through UV curing presents several advantages, mainly related to the easiness of dispersing GO nanosheets into the liquid, low-viscosity monomers before curing. Actually, the UV curing technique is getting an increasing importance in the field of coatings due to its peculiar characteristics [484,485]: it induces the polymer formation with a fast transformation of the liquid monomer into a solid film with tailored physical-chemical and mechanical properties. Therefore, it can be considered an environmental friendly technique, being solvent free, and it is usually carried out at room temperature with energy savings.

The limiting factor in the adoption of polymer nanocomposites for specific applications regards mainly the tendency of the nanofiller to agglomerate. It is therefore very important to enhance the filler stabilization by the use of additives and exploring innovative dispersion and cross-linking methods. For this purpose, photocrosslinking systems can significantly help in achieving an adequate nanostructure. Since crosslinking times are very short, the nanofiller dispersion achieved in solution can be “frozen”, with a significant reduction of the filler re-agglomeration. The strategy of *in-situ* reduction of GO to rGO by UV exposure has been efficiently exploited during the UV-induced photopolymerization of polyethyleneglycol diacrylate monomer, for the preparation of highly dispersed graphene-polymer composites [485].

3.1.4. Dispersion of nanocellulose in thermosetting matrices

Cellulose nanocrystals (CNC) are reinforcing fillers of emerging interest for polymers due to their high modulus and potential for sustainable production. In recent years, numerous studies of CNC incorporation into a wide range of polymer matrices have been reported, much work has recently been devoted to the reinforcement of thermoplastic polymers with nanoscale cellulose, while, in comparison, few studies have also reported the reinforcement potential of cellulose nanoparticles on thermosetting matrices [486]. For example, tunicate cellulose whiskers (CNW) were reported to reinforce flexible, low glass transition temperature (*T_g*) epoxy crosslinked polymers [487]. In relatively higher *T_g* epoxies

(ca. 160 °C), a reinforcing effect was also reported with CNW especially above the polymer glass transition temperature [488]. More recent papers of the use of different cellulose based nanostructures can also be found. Specifically, the use of cellulose nanowhiskers and cellulose nanocrystals as reinforcing filler in polyurethanes (PU) synthesis has been reported [489–493]. Moreover, nanocrystalline cellulose was used as a modifier for waterborne polyurethane [494].

Due to the hydrophilic nature of CNS, some other studies also focused on thermosetting nanocomposites based on hydrophilic matrices. In fact, polycondensation polymers with prepolymers compatible and reactive towards cellulose, should be excellent candidates to develop cellulose nanocomposites. Indeed, CNS might be readily dispersed in the starting prepolymer leading to the formation of an interpenetrating network upon further polycondensation and crosslinking. Specifically, in the case of the polycondensation between phenol and formaldehyde, chemical reaction between the phenolic prepolymers and CNS is theoretically possible, with consequent modification of rheology and curing behavior [495–497]. The most important class of thermosetting systems in which the use of cellulose nanostructures was investigated was the one related to epoxy matrices: Eichhorn et al. [498] investigated the stiffness of cellulose whisker/epoxy system using Raman spectroscopy and highlighted the importance of the interface between matrix and nanofiller. Lu et al. [499] reported that the modulus increased approximately 6 times upon incorporation of 5% w/w microfibrillated cellulose (but not cellulose whiskers) into an epoxy matrix. Matos Ruiz et al. [487,500] studied waterborne epoxy coatings with low concentrations of tunicate whiskers, while Tang et al. [488] reported a solvent exchange process from aqueous into organic (DMF) dispersions as a suitable method to efficiently mix an oligomeric diglycidyl ether and a multifunctional amine cross-linker. In Takagi et al. [501] the preparation and characterization of a new type of natural fiber nanocomposite, which is composed of bacterial cellulose nanofibers in an epoxy matrix was reported.

Few examples of nanocomposites in which the cellulosic nanostructure is used in bio-based thermosets can be also found. Because these environment-friendly composites suffer from several limitations such as low mechanical properties due to low strength in reinforcement plus inadequate interfacial strength, and that cellulose nanostructures have been shown to have significant potential as reinforcement, the possibility of using cellulose nanofibers as reinforcements in a bio-derived polymeric system was revised. In Masoodi et al. [502], cellulose nanofibers were used as reinforcements in the forms of layered films, while in Lee et al. [503] the stability of the gas-soybean oil foam templates and the mechanical properties of the polymer nanocomposite foams are enhanced upon the addition of bacterial cellulose nanofibrils. Other examples of bio-based thermosets containing cellulosic nanostructures are the work of Shibata [504] in which the use of a bio-based epoxy was revised, as well as systems in which cellulose nanocrystals are incorporated in bio-based polyurethanes [505,506]. Few examples exist also in the literature on the polymerization of furfuryl alcohol in presence of CNS [507,508]; in these papers, the authors established the feasibility of producing furfuryl alcohol reinforced by cellulose nanowhiskers and montmorillonite using in-situ polymerization without using any solvent or surfactants. They found that sulfonic acid residues at the CNW surface, from the acid hydrolysis treatment, acted as catalysis for the polymerization reaction of furfuryl alcohol. The use of bio-based thermosets clearly represents an area of significant interest, since further combination of environmental friendly high performance materials with cellulosic nanostructures can surely give the opportunity of creating new high performance hybrids.

3.2. Properties and applications of thermosetting matrix nanocomposites

Traditional micrometric fillers must be added in large quantities in order to properly function as reinforcements and the use of conventional fillers, in the form of micrometric particles, has often led to a deterioration of properties, especially in terms of weight increase, brittleness, opacity, workability, etc. [26,509,510]. The development of nanocomposites in which the reinforcement exhibits at least one dimension in the range of nanometers, allowed obtaining polymeric materials with new characteristics, drastically reducing the amount of added filler and maintaining the mass or density of polymer unaltered. Analyzing the wide literature on polymer nanocomposites [10,24–26] it is clearly that the advantages that nanofillers can offer on the properties of un-modified polymers are numerous. The nanoparticles with a high potential for the enhancement of physical properties of thermosetting polymers are mainly nanoclays, carbon nanotubes, carbon nanofibers, graphene nanoplatelets and other ceramic particles such as silica, metallic oxides or carbides. Among the different matrices, epoxies, phenolics and unsaturated polyesters, generally used for the realization of conventional fiber-reinforced composites, have been widely reported in the literature as nanoreinforced matrices.

3.2.1. Mechanical and electrical properties

Regarding the mechanical properties of nanomodified matrices, generally the addition of a rigid nanofiller results in significant improvements of Young's modulus and maximum strength: when the bonding between the nanofiller and polymer is adequate, there is a good load transmission between the two phases and a significant part of the applied load is carried by the filler [511]. The larger is the surface area, the greater is the strengthening effect of the filler. Nanoclays are widely employed to modify thermosetting matrices. It was demonstrated that the modulus and the strength [512–514] of nanocomposites increase with the introduction of the filler. However many researches demonstrated that this behavior is true up to a specific amount of nanoclays added in the matrix [515]: too large amount of filler can lead to an incomplete intercalation/exfoliation of silicates or to an aggregation of the layers. Clay aggregates cannot act as reinforcement but as an inner defect that reduce the mechanical properties of the material [516] and the deformation to fracture. Regarding the toughness of nanocomposites, many works highlighted the role of the silicates in improving rigidity sacrificing toughness and elongation at break [26]: these results probably are due to the formation of microvoids originated by the debonding of clay platelets from the matrix; the voids coalesce and form larger cracks causing embrittlement.

The size of the nanoparticles could be another cause for the low toughening properties of the nanocomposites. In fact, according to some authors, nanoparticles are too small to provide a valid toughening mechanism and cannot effectively enhance crack-trajectory tortuosity [26]. Nevertheless, recent studies on BC toughened thermosets, have shown that it is possible to produce toughening effects through nanostructuration. For example, Liu et al. [517] have shown that the main mechanism of toughening for self-assembled block copolymers is micelle nanocavitation followed by matrix shear banding. Other factors influencing the toughening through nanostructuration regard crosslinking density that affects the size of BC particles [518]. Other works have shown that it is possible to obtain toughening using different nanosized elastomeric particles [519,520].

Furthermore, other investigations [514,521,522] have reported toughness improvements also upon clay dispersion. It is interesting to highlight the work of Zerda and co-workers [523] in which they showed that the yielding behavior of a glassy thermoset was

substantially modified by the formation of intercalated nanocomposites: the fracture behavior was improved in the intercalated system respect to the exfoliated configuration. According to them, the toughening mechanism was due to the spacing of regions of the intercalated filler that allowed the creation of additional surface areas for crack propagation.

Alumina and silica nanoparticles are also valid reinforcements for enhancing the properties of thermosets; their effects are more marked in the improvement of toughness and wear resistance. There is a wide literature concerning the effect of these materials in the form of nanospheres on the fracture mechanism: the nanoparticles enhance the crack-trajectory tortuosity leading to a higher toughness of the material [524–528].

Carbon based nanofillers, such as CNT and GNP, have assumed a more relevant role in the last years. Gojny et al. [529] demonstrated that a low amount of CNT can increase tensile strength and Young's modulus in epoxies. They also found an increased toughness respect to the neat material. Miyagawa et al. have obtained an improvement of the modulus without sacrificing impact strength adding a low amount of CNT in the epoxy matrix [530]. The same effect was found by Rafiee [531] using GNP instead of CNT. However, these kinds of nanofillers are especially appreciated for the interesting electrical properties they can confer to the polymeric matrices.

As widely reported in literature [532–534], the use of conductive nanoparticles such as carbon black, carbon nanotubes and carbon nanofibers can significantly enhance the electrical conductivity of the insulating polymer matrix in which they are embedded. In addition, the concentration to which this effect was evident (percolation threshold) was found to be very low [535]. The applications of electrically conductive thermosetting polymer nanocomposites are numerous [536–539]; a very interesting use of thermosetting films reinforced with conductive fillers was highlighted by Pham et al. [537] and by Chiacchiarelli et al. [539] using CNT and GNP, respectively. These researchers have found the potentially applications of these films for strain sensing in order to monitor the deformation state of the materials.

Nanocomposite thermosetting matrices have assumed a great importance in the last years especially for the production of traditional fiber-reinforced composites because nanoparticles give the opportunity to improve the bulk composite properties with the minimal deterioration of other properties of the composites. The incorporation of nanofillers can improve mechanical properties such as fracture toughness and the compressive strength [540].

Veedu et al. [541] reported significant improvements in the interlaminar fracture toughness, hardness, delamination resistance, in-plane mechanical properties, damping, thermoelastic behavior, and thermal and electrical conductivities adding CNT. Similar results were obtained by Gojny et al. [542,543] and by Zhao et al. [544] that demonstrated, moreover, the effect of CNT on the enhancement of strength and modulus of the composite materials. Hsiao et al. [545] and Meguid et al. [546] investigated the tensile and shear strength of nanotube-reinforced composite interfaces observing a significant increase in the interfacial shear strength.

Other investigators have found similar results using carbon nanofibers in thermosetting matrices. For example Iwahori et al. [547] reported an improvement on compressive strength in laminates. Joshi [548] observed that carbon nanofibers alter the interface behavior of the carbon fiber and the phenolic matrix, leading to an increment of mechanical properties. In terms of mechanical properties, GNP based nanocomposites, used as matrix for carbon fiber composites, as reported by Cho et al. [549], allowed obtaining enhanced compressive strength.

However, besides the use as mechanical reinforcements, these kinds of carbon fillers can create materials with fully new

properties, for example for applications in the field of electromagnetic interference protection [550,551] or to make conductive fiber composites [552]. Monti et al. [553] developed a glass fiber-reinforced nanocomposite based on unsaturated polyesters and carbon nanofibers. They found that the composite exhibited good sensing characteristics both when a continuous stress was applied and in the case of impact. In particular, regarding the impact load, a strong correlation was reported between the step increase in the electrical resistance of the sample and the impact damage.

Many works highlight the benefits of adding nanoclays or other ceramic nanoparticles in composite laminates. For example, Kormann et al. [554] found that layered silicates improved the interfacial bonding between the matrix and glass fibers and consequently the flexural strength of the composite. Similar results were obtained using modified montmorillonites in carbon fiber [555] and glass fiber [556] based composites. The results obtained by Wang et al. [557] and Siddiqui et al. [558] underline the role of layered silicate in the enhancement of the interlaminar fracture toughness. Zou et al. [559] found that, adding nanoclays into the phenolic matrix enhances the flexural properties. Similar benefits were obtained by other authors using ceramic nanoparticles. Hussain et al. [560] underlined the role of nanoalumina on the improvement of tensile modulus and strength in glass/epoxy composites; Wang et al. [561] considered the use of graphite and nano-SiO₂ to improve the friction and wear behavior of basalt fabric-reinforced phenolic composites while Lin et al. [562] investigated the thermal and mechanical properties of carbon fiber-reinforced phenolic/silica nanocomposite fabricated by sol-gel method: the incorporation of an inorganic phase into the matrix confirmed the increase in the flexural modulus of the fabricated composites. In the work of Hossain et al. [563], the effects of silicate nanoparticles in glass fiber-reinforced vinyl ester nanocomposites were investigated and an improvement in both mechanical and thermal properties was observed.

As in the case of thermoplastic polyurethanes [564,565], numerous scientific reports have addressed the use of nanoparticles in thermosetting polyurethanes. Nanocomposites based on sepiolite clay were studied by Hongxiang [566,567]. Sepiolite is a hydrous magnesium silicate with a microfibrous morphology where the fiber section consists of a series of tunnels and blocks. The blocks are composed of a three-layer structure, where two layers of silica surround a layer of magnesium oxide-hydroxide. The surface of these blocks is highly populated by silanol groups (Si-OH). The tunnels are populated by zeolitic water. Because pristine sepiolite is hydrophilic, organic modification of the surface must be performed in order to avoid particle agglomeration. Hence, the surface might be modified by quaternary ammonium salts, coupling agents and Lewis/Bronsted acids. The author used three different organic modifiers, aminopropyltriethoxysilane (APTS), hexadecyltrimethylammonium bromide and lauric acid. FTIR analysis proved that chemical links were formed with all modifiers and those with APTS were stronger. Optical analysis with SEM/TEM proved that homogeneous dispersion of the organo-sepiolite was obtained. In addition, mechanical tests showed an increase in ductility and tensile strength for modifier concentrations in the range of 1–5 wt%. Thermal degradation was also improved, showing an increase of approximately 15 °C of the onset degradation temperature. Of the previously mentioned properties, the APTS modifier achieved the best performance.

Polyurethane nanocomposites based on montmorillonite (MMT) were studied by Chang [568]. Three different organic modified MMT were used, hexadecylamine-montmorillonite (C₁₆-MMT), dodecyltrimethylammonium-montmorillonite (DTA-MMT), and Cloisite 25®. XRD measurements proved that the organic modifiers produced intercalation of the MMT (C₁₆-MMT achieved the highest intergallery spacing). SEM/TEM optical

analyses also supported those results. The fracture surface of all the hybrids showed voids, which were assumed to be formed by the agglomeration of the MMT layers. Thermal stability was shown to increase with onset degradation temperatures increasing up to 18 °C for the DTA-MMT. Mechanical properties were generally improved with the hybrids, but it depended on the type and concentration of the reinforcement. The best results were obtained with Cloisite 25®, where an increase in ultimate strength, modulus and elongation at break was found and it increased as a function of increasing reinforcement concentration (up to 4 wt%). Similar results were obtained in the work performed by Wang [569]. The MMT was organically modified with *N*-diamino octadecyl trimethylammonium chloride. XRD measurements proved that intercalation was achieved, showing an increase of the intergallery spacing from 1.5 to 3.2 nm. Mechanical properties were also improved, obtaining significant increments in tensile strength and elongation at break. These improvements also increased with an increment of reinforcement concentration (in the range 1–4 wt%). The authors proposed that the increment of mechanical properties was due to the proper intercalation of the MMT layers, forming a tortuous path for crack growth.

Polyurethane (PU) matrix nanocomposites based on MWCNT were studied by Mc Clory [570]. The PU system consisted of an isophorone diisocyanate and a polyether polyol, being both very hygroscopic. The MWCNT were synthesized with CVD and had diameters within 10–30 nm and lengths in between 1 and 10 μm. No additional surface treatment was performed. The preparation of the composite was done under vacuum and the precursors were all degassed for substantial times (8 h). SEM/TEM and XRD experiments proved that a high dispersion of MWCNT was achieved. Significant improvements in mechanical properties were obtained, for example, an addition of 0.1 wt% of MWCNT doubled the elastic modulus with a simultaneous increase in ductility and tensile strength. Raman spectroscopy was used to determine that a strong interaction was present between the matrix and the MWCNT. The resulting interface interaction was explained assuming that the defect sites of the nanotubes, which should contain either hydroxides (–OH) or carbamates (–COOH) groups, should be the cause of the excellent stress-transfer properties obtained.

Nanocomposites based on polymerization compounding of fumed silica were studied by Dubois [571]. Polymerization compounding is a process used to improve the inorganic–organic interface by the formation of a thin thermoset layer on the inorganic phase before it is blended in the organic phase. For example, for a PU matrix, a diisocyanate is reacted with the –OH or –COOH groups present on the surface of the inorganic phase. Then, a polyol reacts with the free isocyanate groups, leaving only unreacted –OH groups. The final entity chemically behaves as a polyol (Fig. 20). This method has the advantage of improving the dispersion of the nano-filler and the formation of a core–shell structure, in which the shell properties might be tailored to specific requirements. The final properties of the nanocomposite will ultimately depend on the chemical nature of the shell, for example, by using a long flexible polyol to form it, a simultaneous increase in elastic modulus, tensile strength and ductility was achieved.

Nanocomposites based on grafted nanosilica were studied by Chen [572]. A silane based coupling agent (3-aminopropyltriethoxysilane, APTS) was used to yield amine group functionalities on the silica surface. FTIR was used to corroborate that the concentration of Si–OH groups on the silica surface decreased as a function of increasing APTS concentration. TEM analysis revealed that a homogeneous dispersion of the grafted silica was obtained. No mechanical tests were performed.

Graphite oxide nanoplatelet nanocomposites were studied by Cai [573]. Oxidation of expanded graphite by direct ultrasonication in DMF produced exfoliation, forming nanoplatelets functionalized with oxygenated groups (GONP). These groups promoted covalent links with isocyanate, thus increasing interfacial strength. The resulting elastomeric composite showed a relevant increase in both hardness and elastic modulus. However, ductility and tensile strength decreased. Good dispersion of the nanoplatelets, studied with TEM, was obtained. In addition, the interaction of the GONP with the soft and hard segments of the PU chain was studied. It was shown that the GONP mainly bonded with the hard segment, thus decreasing the final crosslinking percentage. The exfoliation of graphene oxide nanoplatelets was also studied by Stankovich [574]. Isocyanate was used as exfoliation agent, which generated a stable dispersion in polar aprotic solvents (Fig. 21). The isocyanate

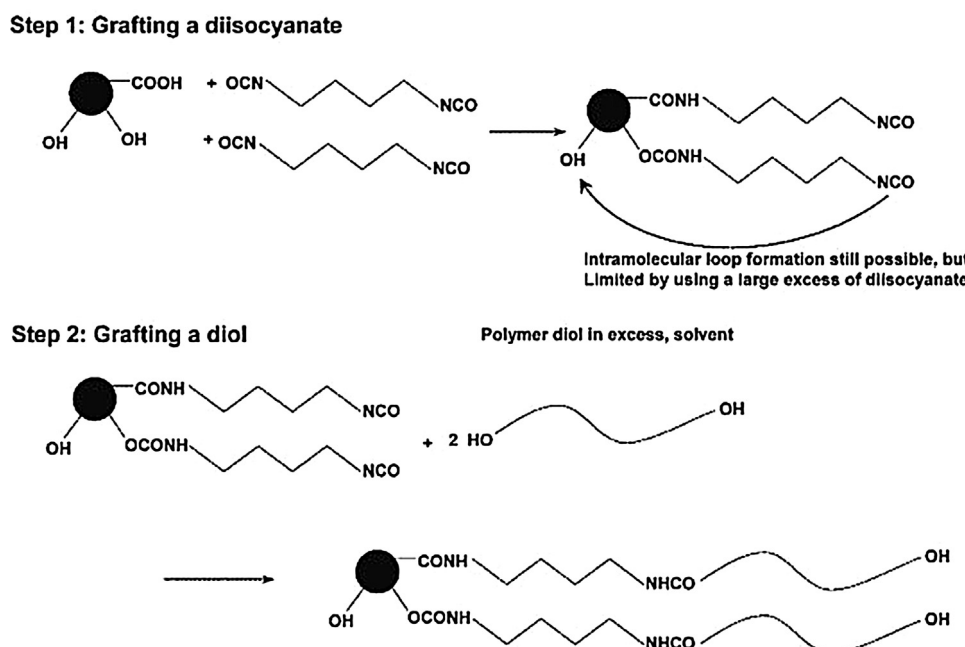


Fig. 20. Polymeric compounding technique for polyurethane matrix nanocomposites [571].

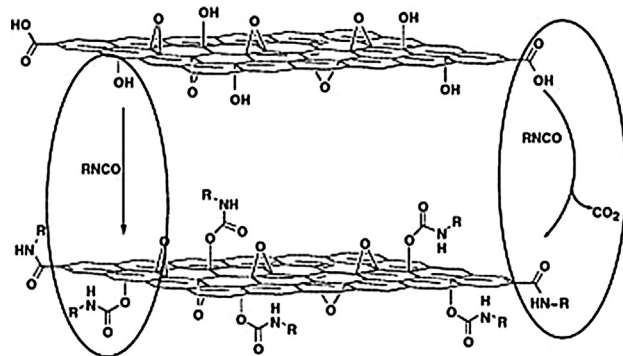


Fig. 21. Isocyanate treated graphene [574].

formed amide and carbamate links with the graphene surface [574].

Nanocomposites based on elastomeric PU and silicate layers were studied by Gorrasi [575,576], Tien [577,578], Wang [579] and Yao [580]. Elastomeric PU are characterized by a block copolymer structure $(AB)_n$, in which the blocks are designated as soft and hard segments. The soft segment is usually composed of a long and flexible polyester or polyether chain while the hard segment is a small molecule, which is formed by the reaction of an aromatic diisocyanate and a short chain polyol. From a thermodynamic point of view, phase separation is favorable, hence, microdomains are formed which have glassy (hard segments) and rubbery behavior (soft segments). Crosslinking occurs by hydrogen bonding between the hard segments of the copolymer chains. Reinforcement of elastomeric PU composites is usually performed to improve the thermal stability and barrier properties, while maintaining or increasing mechanical ones (shock absorption, flexibility, elasticity, abrasion resistance, etc.). Silicate layers of the montmorillonite type were used in all the publications cited above. In order to improve dispersion, the intergallery cations (generally Na^+) were exchanged with different molecules as summarized in Table 2, which also includes a summary of the properties obtained. From these data, it is possible to deduce that exfoliation is not necessary to obtain a simultaneous increase of all mechanical properties (yield stress, elastic modulus and ductility).

3.2.2. Thermal properties

One of the great limits of polymeric materials is their weak resistance to high temperatures. The use of thermosetting polymers is widely diffused in all those applications where a protection against fire is required because, compared to thermoplastics, thermosets can ensure insulation at higher working temperature. To improve the thermal stability and reduce the flammability of the material, flame retardant additives such as halogen-containing compounds or metallic hydroxides [581–584] are generally added to the matrix. However these compounds,

often lead to a deterioration of physical properties of the matrix [585,586]. By embedding specific nanoparticles in the organic matrix, it is possible to obtain nanocomposites with enhanced thermal properties minimizing the problems connected to the use of traditional fire retardant additives. Nanoclays revealed to be a new class of systems useful to enhance the flame retardancy and the thermal stability of many polymeric materials [587–589]. Silicates produce an increased heat resistance and they can act as a superior insulator and mass transport barrier to the volatile products generated during decomposition, also assisting in the formation of char after thermal degradation [590,591]. In cone calorimeter tests, the presence of silicates reduces the heat release rate (HRR) of the material. The carbonaceous char produced on the surface during combustion is reinforced by the silicates, creating an excellent physical barrier that protects the substrate from heat and oxygen, slowing down the escape of flammable volatiles [592–594]. Moreover, in lamellar nanocomposites, the thermal oxidation of the char is hindered by the oxygen barrier effect due to inorganic layer reassembling on the surface of the burning material. Many investigations underlined that to obtain a homogeneous residue, which can act as a surface protective skin, exhibiting the desired flame resistance and retardancy, it is critical to obtain a homogeneous nano-scaled dispersion of nanoclays [588,595]. Other investigations demonstrated the different thermal degradation behavior of the nanocomposites in oxidizing and in nitrogen atmospheres [596,597] using thermo gravimetric analysis (TGA). They experienced that, in a nitrogen environment, nanocomposite samples did not show difference of stability respect to the neat matrix. However, in an oxidizing environment, the presence of nanofiller led to a higher residue than that observed in a nitrogen environment. In addition, the organoclay shields the polymer from the action of oxygen, increasing the thermal stability under oxidative conditions.

In the case of heat fluxes and temperatures higher than those of obtainable by TGA or by cone calorimeter, nanoclays can change their shapes and experience sintering. The ceramic skin that forms on the surface of the burning material acts not only as a shield for heat and oxygen but it also allows re-radiating a substantial amount of energy proportional to T^4 . In this way, the increased re-radiation from the hotter ceramic surface is related to a reduced heat flux transferred into the material. Consequently, the mass loss rate is reduced and the fire resistance of the material is increased [588].

Applications of nanoclays in thermosets for enhancing thermal properties are numerous. For example, Gua et al. [598] demonstrated an enhancement of thermal stability of epoxy systems, evaluated by TGA, added with nanoclays; Zammarrano [599] pointed out that, the effect of nanoclays on the flame retardancy of epoxies strongly depends on the modification of the clays. The anionic clays showed improved performance in terms of self-extinguishing behavior and

Table 2

Cationic surfactants used for the ion exchange reactions and subsequent effects on nanocomposites mechanical properties.

Reference	Surfactant	Effects on nanocomposites mechanical properties
Tien [577,578]	3-amino-1-propanol 3-amino-1,2-propandiol tris(hydroxymethyl)aminomethane dodecylamine benzidine	Exfoliation achieved with an increase in ductility, yield strength and elastic modulus
Gorrasi [575,576]	(hydrogenated tallow alkyl)methyl bis(2-hydroxyethyl) ammonium ions 12-aminolauric acid	Exfoliation achieved only at low clay concentrations. Increase in strength and elastic modulus but decrease in ductility
Wang [579]	Alkylammonium ions $\text{C}_{12}\text{H}_{25}\text{NH}_3^+$ $\text{C}_{18}\text{H}_{37}\text{NH}_3^+$	Intercalation achieved for all formulations. Simultaneous increase in all mechanical properties (strength, elastic modulus and ductility). MMT exchanged with long chain onium ions showed good solvation in polyols
Yao [580]	Modified polyether polyol (Hyperlast®)	Intercalation achieved with an increase in strength and ductility

reduction of the heat release rate. A similar result was obtained by Camino and co-workers [587] that demonstrated that exfoliated nanoclays contributed to the reduction of the HRR in epoxy. The effect of exfoliation of nanoclays in epoxy was also pointed out by Schartel and co-workers [600]: they found that fire properties were enhanced with the increasing of exfoliation.

The use of ceramic nanoparticles as filler to enhance thermal properties was also evaluated; many authors [583,601,602] obtained a significantly reduction of the HRR adding silica nanoparticles in different polymeric matrices. As reported by Hsieh [603] the silica particles accumulated on the surface of the burning epoxy created a protective barrier that improved char stability in oxidative conditions. Natali and co-workers [604] demonstrated that well dispersed silica nanospheres in a phenolic matrix allowed obtaining an improved thermal stability in nitrogen as well as in air. Tibiletti et al. [605] demonstrated that alumina nanoparticles in a polyester matrix enhanced the thermal stability shifting degradation to higher temperatures. An enhancement of thermal stability was found also by Liu et al. [606] and by other authors [607,608] in epoxy-silica hybrid nanocomposites.

Kashiwagi et al. [609] investigated the flame retardant properties of CNT at high temperatures: CNT produce a continuous protective carbon network that works as a heat shield that slows down the mass loss rate and the material flammability. Moreover, CNT embedded in the charred surface re-emit the incident radiation reducing the transmission of heat flux into the inner layers and preserving the polymer degradation [610].

Matrices modified with nanoparticles, able to enhance the fire resistance, are much appreciated for the realization of fiber-reinforced composites. In fact, traditional fire retardant additives are not suitable for the realization of composite laminates since their particle dimensions are comparable to the fiber diameter. In such case, the fiber fabric behaves as a filter for the particles that cannot be homogeneously distributed in the composite (filtration effect). Conversely, the use of suitable nanoparticles in a matrix allows an improvement of the fire resistance properties without the drawbacks due to the filtration effect.

The use of nanomodified phenolics as matrices for fiber-reinforced composites represents a very promising way to maximize their fire retardant properties. Koo et al. [611] carried out a wide research in which a resole was mixed with several types of nanofillers such as carbon nanofibers, nanoclays and polyhedral oligomeric silsesquioxane (POSS). These nanocomposites were used to impregnate a carbon/phenolic composite [612]. Cone calorimeter tests were used to compare the performances of both the traditional composites and the nanocomposite based laminates [613]. The results showed that the nanostructured systems exhibited a lower heat release rate peak with respect to traditional carbon/phenolic composites.

Tate and collaborators [614] dispersed nanoclays in a water-based phenolic matrices using high shear mixing. The nano-modified phenolic was successfully used to produce E-glass-reinforced composites: cone calorimetry tests demonstrated that there was an improvement of the flammability properties by almost 33%. Bahramian et al. [615] used a layered silicate phenolic nanocomposite to impregnate asbestos fibers. They found that the material tested with cone calorimeter exhibited a lower value of HRR and a lower mass loss. In a recent work, Rallini and co-workers [616] tried to enhance the thermal properties of carbon fiber/epoxy composites using an epoxy matrix modified with boron carbide nanoparticles: it was found that, the peculiar behavior of boron carbide at high temperatures in oxidative atmosphere allowed to enhance the thermal stability of the composite and reduced the HRR. Moreover, the presence of boron carbide led to the conservation of a structural integrity of the laminate after burning.

4. Top-down processing of thermoplastic matrix nanocomposites

4.1. Dispersion of nanoparticles in matrices

4.1.1. Dispersion of nanoclays in thermoplastic matrices

Disregarding the sol-gel techniques, dispersion of nanoclays in thermoplastic polymers can be carried out using all the other three techniques presented in Section 1.2.1. Intercalation from solution is widely used to produce nanocomposites based on water-soluble polymers, such as poly(vinyl alcohol) [617], poly(ethylene oxide) [617], poly(acrylic acid) [618], poly(vinylpyrrolidone) [619]: the montmorillonite is dispersed in water and then the polymer is added. The blend is usually mechanical stirred at low rates to simplify the interaction between the polymer in solution and the nanoclays and then it is dried to remove the solvent. This technique can also be performed in organic solvents. For example poly(ethylene oxide) has been successfully intercalated in sodium montmorillonite and sodium hectorite by dispersion in acetonitrile [620], while poly(lactide) (PLA) and poly(*e*-caprolactone) (PCL) biodegradable nanocomposites [621,622] were prepared by dissolving either PLA or PCL in hot chloroform in presence of a given amount of the modified clay. Then the solvent was vaporized to obtain homogeneous films.

Nanocomposites based on polyolefin matrices can be also produced through in situ intercalative polymerization process. As reported by Tudor et al. [623] it is possible to use soluble metallocene catalysts to intercalate the polymer inside silicate layers and to promote the coordination polymerization of propylene. In another work [624], intercalated/exfoliated nanocomposites based on high-density polyethylene matrices have been synthesized by a technique called polymerization-filling technique. The surface of nanoclays is modified with a coordination catalyst, such as activated metallocenes, and then the in situ polymerization directly begins from the surface treated fillers.

However, in situ polymerization and intercalation from solution are limited because neither a suitable monomer nor a compatible polymer-silicate solvent system is often available. Consequently, the melt intercalation technique is the most used for the production of thermoplastic matrix nanocomposites. In order to facilitate the polymer intercalation, the mixture of melting polymer and nanoclays is subjected to high shear stress (for example in an extruder) that contributes to the delamination of silicate crystals. In the melt intercalation technique, no solvent is required and the layered silicate is mixed within the polymer matrix in the molten state [625,626]: a thermoplastic polymer is mechanically mixed by conventional methods such as extrusion and injection molding with organophilic clay at the polymer processing temperature. The polymer chains are then intercalated or exfoliated to form nanocomposites. As just said, exfoliated nanocomposites have higher phase homogeneity than the intercalated counterpart. Hence, the exfoliated structure is more desirable to enhance the properties of nanocomposites.

At this purpose, for the fabrication of exfoliated thermoplastic polymer nanocomposites, Dennis et al. [625] found that, increasing the mean residence time in the extruder generally promotes exfoliation, but excessive shear intensity or back mixing causes poor delamination and dispersion. Other authors [627–631] succeeded in silicate layer exfoliation in polyolefins, such as polypropylene and polyethylene, by the introduction of small amounts of polar groups to non-polar polyolefins. Regarding thermoplastic nanocomposites formed by melt, Dennis et al. [625] described how the extruder type and the screw design affects the degree of dispersion of nanoclays in a polyamide matrix: they found that, the use of non-intermeshing twin screw extruder led to the best delamination and dispersion. Moreover, they affirmed that

excellent delamination and dispersion can be achieved with co-rotating and counter-rotating, intermeshing types of extruders when a fully optimized screw configuration is employed. The melt-intercalation of nanocomposites has been scaled also up to an industrial level and applied to commercially available products and mainly in the automotive field.

4.1.2. Dispersion of carbon nanotubes in thermoplastic matrices

Effective use of nanotubes in polymeric composites with regard to enhancement of specific properties depends primarily on the ability to disperse homogeneously the nanotubes in the polymer matrix. However, CNT homogeneous dispersion is difficult to achieve due to the intermolecular van der Waals interactions between the nanotubes, thus resulting in the formation of aggregates [632–634].

Nanotubes can indeed be dispersed in solvent (colloidal suspension) or added directly to the dissolved polymer solution [635] or alternative solution is represented by in-situ polymerization, where the nanotubes are simply added to a system prior to polymerization [636]. The benefits of in-situ polymerization are the ability to form composites with polymers that are not easily solution blended or melt compounded. Furthermore, covalent functionalization that establishes chemical bonds between polymers and the surfaces of the CNT can be considered as a successful route for a good dispersion of carbon nanotubes in thermoplastics. Oxidative reactions with oxygen or various acid treatments made CNT can add –COOH and –OH functionalities to the surface of the CNT [637]. These treatments introduce functional groups to the surface of the nanotubes. Moreover, grafting of polymer to the surface of the nanotubes can be used for better dispersion [638]: grafting-from technique involves the chemical functionalization of a CNT surface to act as a macro initiator for polymerization, while the grafting-to methods involves the chemical attachment of functional polymers to the surface of CNT [639]. CNT can be pristine, oxidized or pre-functionalized depending on the functionality of the polymer to be grafted. Even if covalent functionalization approaches can improve nanotube dispersion, the chemical modification clearly introduces defects on the surface of carbon nanotubes. Therefore, the use of non-covalent functionalization approaches, that involves wrapping or adsorption of macromolecules to the surface of nanotubes through carbon-hydrogen group (CH)–π interactions, π–π stacking, or various other electrostatic and hydrophobic interactions [640] could be preferred.

Some time-consuming techniques, such as in situ injection molding method, magnetic field and in situ polymerization have been employed to align the carbon nanotubes in the polymer matrix [641,642]. More specifically, in the case of poly(methyl methacrylate)/nanotube nanocomposites huge efforts have been done in order to obtain the orientation of the tubes inside this polymer matrix [643]. The alignment of neat or carboxy-functionalized carbon nanotubes in polymers using electric fields has also been reported [644] and it was accomplished with an increase of the electrical conductivity of several orders of magnitude. Melt mixing can be surely considered as the preferred method for composite preparation, since it is expected that aggregates can be minimized by appropriate application of shear in melt mixing.

Among these methods, melt compounding is the most commonly used method for producing CNT/polymer composites. Although it requires specialized equipment, it is industrially relevant because it is simple, fast and capable of producing large volumes of sample. The polymer is heated to above its melting temperature and CNT are added to the melt. High shear mixing is then performed and the shear force generated in the compounder is responsible for breaking up primary aggregates and dispersing

nanotubes into the polymer. The primary disadvantage with this method is the suspected decrease of nanotubes aspect ratio upon application of high shear rates. In general, approaches to the manufacture of nanotube/thermoplastic composites cover a very broad range of processing technologies, including, in some cases, combinations of different methods.

4.1.3. Dispersion of graphenes, direct exfoliation and chemical reduction of graphite oxide in thermoplastic matrices

Despite the great interest in graphene nanocomposites, most of the work cited in the literature deals with thermoset nanocomposites. Today graphenes and nanometer-scaled graphite platelets are considered attractive alternatives to the rather expensive carbon nanotubes, and few examples of graphene based thermoplastic nanocomposites have been prepared by melt mixing [645–647]. On the other hand, thermoplastic matrix composites and nanocomposites are finding increasing interest in both academic and industrial research, mainly due to the advantages of thermoplastics in terms of manufacturing costs, impact resistance, and environmental compatibility. Many approaches towards fabrication of functionalized graphenes and graphene nanocomposites are exploiting graphite oxide (GO) as versatile intermediate. The GO functional groups provide a variety of surface-modification reactions, which can be used to develop functionalized GO-based materials [648–654].

For these reasons soluble alkylated GO nanosheets can be easily used as fillers in nanocomposites with polymeric matrices. The main motivation is because from an industrial point of view, wet-chemistry approaches are the most desirable methods for the large-scale integration of GO-based polymeric nanocomposites [655]. For this approach, the critical issue in terms of physical properties and coating uniformity remains the re-aggregation of the GO sheets after the dispersant evaporation. This issue is very critical mainly when the addition of such fillers have not to be detrimental for the optical transparency and conductivity of graphene/polymer composites as in the case of the development of transparent electrodes for applications in the area of optoelectronics.

Water-soluble poly(3,4-ethyldioxythiophene):poly(styrenesulfonic acid) (PEDOT:PSS) polymer represents one conjugated polymer that can be used as the active material in flexible organic electronics due to its remarkably high conductivity, transparency and environmental stability [656]. Furthermore, PEDOT:PSS often suffers from low conductivity; novel hybrid materials with high conductivity and transparency resulted when graphene was used in an appropriate form as filler for PEDOT:PSS [657,658]. Such chemically derived GO sheets gave stable water dispersion of extended layered sheets when they were exposed to the butylamine. From such material a blend of alkylated GO/PEDOT:PSS that gave conducting and transparent thin films has been obtained [659].

Polyhedral oligomeric silsesquioxanes (POSS) are organic-inorganic molecules, approximately 1 to 3 nm in diameter, with a general formula $(RSiO_{1.5})_n$ where R is hydrogen or an organic group, such as alkyl, aryl or any of their derivatives [660–662]. The incorporation of POSS molecules into polymeric materials leads to significant improvements in polymeric mechanical properties, thermal behavior and flame retardancy.

The approach involving a direct coupling of amino functionalized POSS with graphene oxide sheets to introduce amino groups via amide formation leads to a novel nanostructured hybrid material that merges the properties of the two starting nanomaterials, named GRAP POSS. In particular, thin films from solution casting of the resultant POSS-graphene were found to show hydrophobic properties with a reduced friction coefficient suitable for applications in lubricant coatings [663]. The successful

preparation of an “alkylated” graphene paper via the post-synthetic modification of “alkylated” graphene oxide paper has been recently used to develop POSS-modified graphene to be used as nanofiller in polymers (e.g. PMMA) to increase their glass transition and degradation temperatures [664].

GO readily exfoliates in water via hydrogen-bonding interaction [665]. Nanocomposites have been created with GO and water-soluble polymers such as poly-(ethylene oxide) [666] or poly(vinyl alcohol) [667]. Using GO after chemical modification with isocyanate or amine, composites have also been produced in aprotic solvents with hydrophobic polymers such as polystyrene [668], polyurethane [669] or poly(methyl methacrylate) [670]. Electrical conductivity can be restored via chemical reduction of the graphene oxide. This can also be done *in situ* in the presence of a polymer. For example, GO was added to sulfonated polystyrene and then reduced with hydrazine hydrate [671]. Without the sulfonated polystyrene, the reduced sheets rapidly aggregated. However, depending on polymer type and the reducing agent, this *in situ* reduction technique may result in polymer degradation.

Composites of chemical reduced graphene and thermal reduced graphene (TRG) have been made with a number of polymers via blending with organic solvents followed by solvent removal. Unlike chemically modified GO that retains some layered structure from GO, thermal expansion of GO leads to nearly complete exfoliation [672,673]. Therefore, dispersion of thermally reduced graphene can be easier while stacked layers of chemical reduced graphene have to be exfoliated by applying mechanical stress and via inter gallery polymer diffusion in solvents [674]. Graphene composites can be produced via *in situ* intercalative polymerization of monomers. Successful polymerizations of PVA [675], PMMA [676] and PU [677] with TRG have been reported. Especially for poly(arylene disulfide), graphene oxide was used as an oxidation agent which converts thiol salts to disulfide. However, so far, these monomers have only been polymerized in solvents. The high viscosity of even dilute dispersion of graphene makes bulk-phase polymerization difficult. If functional groups on the chemically modified graphene are reactive with the monomer, grafting of polymer chains onto graphene surfaces can occur. Chain grafting has been demonstrated with the polymerization of poly(2-(dimethylamino)ethylmethacrylate) [678] and PVA [679] and with PU formation [680]. The most economically attractive and scalable method for dispersing nanoparticles into polymers is melt blending. However, because of thermal instability of most chemically modified graphene, use of melt blending for graphene has so far been limited to a few studies with the thermally stable TRG. Successful melt compounding of TRG into elastomers [681] and glassy polymers [682] has been reported. Another challenge for melt compounding is the low bulk density of graphene like TRG, which makes feeding into melt mixers difficult. Torkelson and coworkers [683] have attempted to bypass all graphene synthesis steps by exfoliating graphite directly into polypropylene using the very high stresses generated in the solid-state shear pulverization process. Their X-ray diffraction and TEM data indicate, however, that the resulting composite is primarily small stacks of graphite.

Graphene oxide as stated above could not be used in advanced applications before repairing its defects [478]. So far, several reparation strategies cataloged as wet and dry methods, have been established. However, various chemicals, electrolytes, dangerous gases or high temperatures are required for the reparation.

Among the strategies to disperse graphene onto polymer matrix (i.e. solvent processing, *in situ* polymerization and melt processing), latex technology represents a novel method for manufacturing polymer/graphene nanocomposites [684–686]. While composites prepared from aqueous graphene dispersions mixed with polystyrene latex and subsequent compression molding were accomplished

with an increase of the electrical conductivity of several order of magnitude [687], more recently the morphological and physical properties of graphene oxide/polystyrene latex films deposited under an electric field assisted thermal annealing treatment have been reported [688,689]. It should be mentioned that the only one component of the hybrid composite able to be conductive is the reduced GO component that must be segregated forming a conductive pathway to avoid interruption of the electron charge carrier flow by the presence of intercalated insulating PS latex particles. The achievement of the electrical conductivity of such nanocomposites activated in temperature (i.e. above the glass transition temperature) by the application of an external electric [689] field suggest that: (i) the thermal annealing segregates the GO between the substrate/polymer interface leading to (ii) a percolation pathway for the electric current induced reduction of the GO film.

4.1.4. Dispersion of nanocellulose in thermoplastic polymers

Cellulose nanofibers and nanowhiskers derived from renewable biomass have attracted much interest as an alternative to micronized reinforcements in composite materials [690–698]. Homogeneous dispersion of cellulose nanoparticles in polymer matrices is difficult to achieve by means of traditional melt processing techniques due to the high tendency of cellulose nanofibers to form aggregates, because of the interactions between hydroxyl groups and high surface area of cellulose nanoparticles [699,700]. Proper dispersion and distribution of nanoparticles in the polymer matrix, as well as in the processing solvent, are the prerequisite for creating polymer nanocomposites that can display notable improvement of physical and mechanical properties [701]. In order to increase the dispersion of cellulose nanoparticles in non-aqueous polymer solution or suspension, several strategies have been adopted including the use of surfactants [702] and chemical modification on the particle surface [703–707]. However, the surface functionalization can reduce or even suppress the interactions between the nanoparticles, limiting their reinforcing effect [708,709]. Nevertheless, as previously described, these problems can be easily overcome by selective functionalization of cellulosic nanostructures.

On the basis of the approach discussed above, research on thermoplastic based cellulose nanocomposites was primarily focused on producing composites with reproducible properties, and this item was achieved by developing processing routes that were directed to maximize the dispersion of cellulosic nanostructures using functionalization procedures; general examples of these techniques are solution casting, melt-compounding, electro-spinning. In the first method, the CNS are dispersed within a solvent (water or different organic mediums) and then are mixed with the polymer solutions [710]. Nanocomposites can be produced from this mixture via three general techniques, casting on a suitable surface followed by evaporation, freeze-drying and compression molding, or freeze-drying, extruding, and then compression molding the mixture. As an example, to avoid the nanoparticle aggregation, Jonoobi et al. [711] mixed cellulose nanofibers with a small amount of PLA in acetone/chloroform mixture and then prepared composites by melt mixing the dried mixture with PLA in extruder. Various modifications of this method (e.g. CNS surface functionalization, etc.) have been developed to improve CNS dispersion [712]. The second useful method is the melt compounding where the incorporation of CNS into thermoplastic polymers is done by using compounding and extrusion of the melt mixture [713]. Careful control of processing parameters is needed to minimize CNS degradation resulting from shear stresses and temperatures involved in the process. The last method is the electrospinning, in which CNS are dispersed within a given medium and then mixed with the polymer solution and then

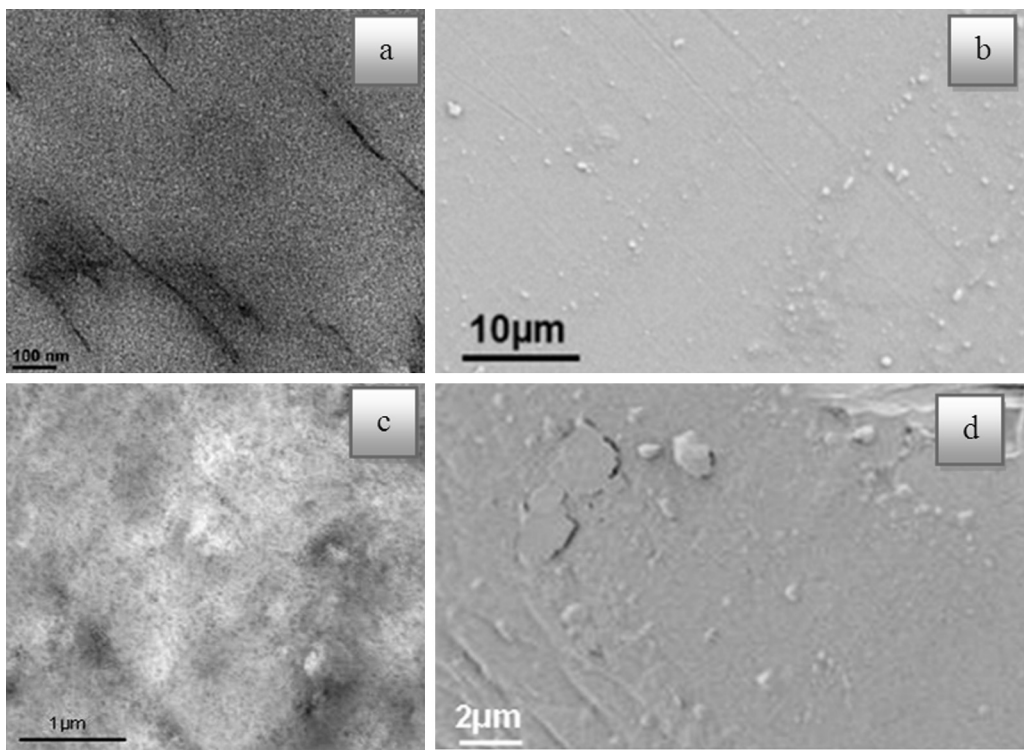


Fig. 22. Results of morphological investigation for PLA based nanocomposites containing 5 wt% of surfactant modified CNC obtained by solvent casting (a and b) and melt extrusion followed by a film formation process (c and d) (from [712,713]).

electrospun. Different morphologies and CNS distribution in the polymeric matrix are expected, as it is noticeable in Fig. 22.

The extensive and not exhaustive literature available on the use of cellulosic nanomaterials as reinforcing agents and fillers in thermoplastic composites, that considers and addresses the performance of many different cellulosic/thermoplastic materials combinations, is justified by the added benefits of abundance and biodegradability generated by the use of CNS and by the numerous approaches for interface modification that indefinitely expand the opportunities for new strong cellulose based nanocomposites.

4.2. Properties and applications of thermoplastic matrix nanocomposites

4.2.1. Processing of thermoplastic matrix nanocomposites

Nanomaterials reinforced thermoplastic nanocomposites have shown significant growth, consequently several methods reported in the literature aiming on the dispersability of the nanomaterials have been studied and revised, in order to enlarge the application windows of these specific materials. Although processing techniques of the nanocomposite are inherently different, all of them have to address the common issues of dispersion, alignment and functionalization that will directly affect the properties of the nanocomposite. Common processing techniques of polymer nanocomposites include melt blending, solution mixing, coating [714], in-situ polymerization [26] nanoinfusion, etc. [715]. The melt mixing of nanoparticles and thermoplastic polymers has been widely used through conventional processing techniques, such as extrusion, internal mixing, injection molding and blow molding due to the speed, simplicity and availability of these processes. These methods are beneficial because they are free of solvents and contaminants, which are indeed present in solution processing and in-situ polymerization. The main advantages of these two processes are that the reinforcing effect can be obtained at a molecular scale and provides an advantage of low viscosity, which

can facilitate mixing and dispersion. In addition, the pre-processing of nanoparticles is necessary to prepare the material for processing at a macroscopic scale. The pre-processing includes purification to eliminate the impurities, deagglomeration for dispersing individual nanoparticles, and chemical functionalization to improve the nanoparticle–polymer interaction and eventually the property enhancement [716].

4.2.2. Main properties and applications of thermoplastic matrix nanocomposites

Just as on the macroscale, the properties of the nanocomposite are dictated by the distribution, orientation and fiber/matrix interactions. Because nanoparticles tend to form clusters and bundles, the biggest challenges on the nanoscale are to fully disperse individual nanoparticles in the matrices and achieve good interfacial adhesion between them and polymer for load transfer capabilities. The important aspects of nanocomposite materials are their improved mechanical, thermal, gas-barrier, swelling, flame-retardant properties and these properties can be improved, in principle, only if a good dispersion of the nanoparticles (that have the potential to exhibit a combination of different properties such as physical, chemical, thermal, and mechanical) is achieved. As already described, different methods can be used to obtain nanocomposites with well-dispersed nanoparticles, in order to tune the specific properties of nanocomposites required for end-applications.

The nanocomposites prepared using the above mentioned methods has a huge potential for applications in automotive (seat frames, battery trays, bumper beams, load floors, front ends, valve covers, rocker panels and under engine covers, etc.) [717], aerospace (missile and aircraft stabilizer fins, wing ribs and panels, fuselage wall linings and overhead storage compartments, ducting, fasteners, engine housings and helicopter fairings, etc.) [718], optical devices [719], electrical and actuator devices and as flame-retardants.

Indeed, it is important to recognize that nanocomposites research is extremely broad, encompassing areas such as electronics and computing, data storage, communications, sporting materials, health and medicine, energy, environmental, transportation, and national defense applications. In some of these areas, fundamental studies of mechanical, electrical, thermal, optical, and chemical properties are required along with related research for real applications. Undeniably, without proper dispersion, the nanomaterial will not offer improved mechanical properties over that of conventional composites. Additionally, optimizing the interfacial bond between the particle and the matrix, one can tailor the properties of the overall composite, similar to what is done in macrocomposites. Reviewing the mechanical performance of thermoplastic nanocomposites containing different nanoreinforcements, it should be recognized that, from a mechanical point of view, a good adhesion at the interface would improve properties such as interlaminar shear strength, delamination resistance, fatigue, and corrosion resistance. In the case of CNT/polymer composites, the increase in CNT composition enhances the mechanical properties [720], such as the variation in CNT wall structures, length, diameter, and chirality along with a large variety of host polymers makes correlating mechanical properties challenging. Additionally, the variety of processing techniques will also have a significant influence on the mechanical properties of the CNT/polymer nanocomposite. Similarly, cellulose nanocrystals and nanofibrillated cellulose have a huge specific surface area and impressive mechanical properties, which make them ideal candidates to improve the mechanical properties of a neat matrix. In general, three main parameters have been reported as affecting the mechanical properties of such materials: (i) the morphology and dimensions of the nanoparticles, (ii) the processing method, and (iii) the microstructure of the matrix and matrix-filler interactions. With regard to the morphology and dimensions, for rod-like particles the geometrical aspect ratio is an important factor since it determines the percolation threshold value. In addition, flexibility and the possibility of tangling the nanofibers play an important role [721–723]. Regarding processing methods, slow processes such as casting/evaporation have been reported as producing materials with the highest mechanical performance. This effect was ascribed to the probable orientation of the rod-like nanoparticles during film processing resulting from shear stress induced by freeze-drying/molding and freeze-drying/extrusion/molding [724]. The microstructure of the matrix and the resulting competition between matrix-filler and filler-filler interactions also affects the mechanical behavior of the nanoparticles-reinforced nanocomposites. Apart from the mechanical properties, thermal properties like dimensional stability, heat distortion temperature (HDT), and thermal stability dictate the widespread applicability of polymeric materials. For instance, the low thermal deformation tolerance of PLA, a widely marketed biodegradable polymer, has restricted its application in electronics, microwavable packaging, etc. Therefore, it is important to understand and resolve these issues to widen the applicability of polymeric materials. First, the dimensional stability of polymeric materials during molding is a key parameter, particularly in automobile applications, where polymers with essentially high coefficients of thermal expansion (CTE) are integrated with metals, which have much lower CTE [725]. In the case of layered particles into polymer matrices, an enhancement of their thermal stability [726] was generally detected. The increase in thermal stability may be due to the layers hindering the diffusion of oxygen and volatile products throughout the polymer, as well as to the formation of a char layer after thermal decomposition of the organic matrix. In the case of cellulosic-based materials, thermal behavior was reported to be function of filler-matrix interaction in the case of chemically modified nanocrystals [727], to the anchoring effect of the

cellulosic filler, which probably act as a nucleating agent in presence of a chemical surface modification [702]. Besides, main properties such as mechanical and thermal performance of nanocomposites, the improvement of the electrical properties is another important characteristic of the thermoplastic matrices that has been extensively investigated. As an example, the addition of MWCNT to polyethylene (PE) via twin-screw extrusion has been reported to improve the electrical conductivity from 10^{-20} to 10^{-4} S/cm with a percolation threshold of about 7.5 wt%, which is higher than that of similar systems [728]. In fact, the addition of 1 wt% MWCNT to polypyrrole (PPy) increases the electrical conductivity by an order of magnitude. Barrier properties, which are of prime importance in bottling, food packaging, protective coating industries, can be indeed improved with incorporation of nanofillers: in general, it has been found that incorporating up to 5 wt% nanofiller can greatly reduce the permeability to oxygen and water [729]. In comparison with other physical and mechanical properties of polymer/clay nanocomposites, which have mixed results, barrier properties are mostly positive, that is, dramatic decreases in permeability to different media can be achieved at relatively low loadings of nanoparticles (particularly with high-aspect-ratio fillers like layered silicates) in contrast to the neat polymers and polymer micro-composites. This is due to the high aspect ratios of reinforcements that force the gas or liquid molecules to traverse a tortuous path in the polymer matrix surrounding these silicate particles. This obviously increases the effective path length for diffusion [730,731]. It is evident that aspect ratio, loading, orientation, and degree of dispersion have a significant effect on barrier properties. In addition, many factors, like the surface treatment of the nanoparticles, processing techniques, and the degree of crystallinity and cross-linking of the polymer, can have an indirect bearing on the barrier properties of these materials. One successful application for improvement of barrier properties is the one related to the use of cellulosic nanoparticles in barrier membranes [732,733], where the nano-sized fillers form a dense percolating network held together by strong inter-particle bonds, which reinforce their use as barrier films. The same effect can be found when nanofillers are introduced in the polymeric matrix for fire retardancy: it is well known that flame retardant additives such as inorganic metal oxides/hydroxides or halogens with or without phosphorous and nitrogen-containing materials are required in conventional methods to modify flammable thermoplastic materials. However, large amounts of additives (>30%) are necessary and in many cases a reduction of mechanical properties, such as toughness, melt flow, etc. and/or release of smoke and toxic emissions, occurs when the modified thermoplastic is burning. The incorporation of nanoparticles has been shown to be an effective approach, since small amounts of nanoparticles (<7%) are required to prepare nanocomposites that exhibit enhanced flammability properties when compared with the modified thermoplastic processed by conventional methods. Moreover, the resulting nanocomposites exhibit enhanced mechanical properties such as high strength/modulus, moisture resistance, higher heat deflection temperature, etc. Besides these analyzed main properties and few works that analyze minor properties such dielectric and optical properties, there are many other properties of polymer nanocomposites, which are important in many commercial applications: these include biodegradability, optical properties, corrosion, photo-degradation resistance, etc.

Thermoplastic nanocomposites are promising functional materials, as they have potential applications in different industrial sectors such as energy production and storage (photovoltaics, batteries, fuel cells), medicine (drug delivery, biomaterials, imaging), functional coatings, environment and safety (membranes, fire resistance), nano- and microelectronics, optics, etc.

Carbon based conductive fillers can, as an example, convert insulating plastic materials to electrically conductive materials. Near the percolation threshold, high values of conductivity and the dielectric constant can be achieved with these composites, which means they can be used in charge-storage devices, such as their high dissipation factor makes them suitable for decoupling capacitor applications. In applications in which the fire resistance is required, different products such as cables and construction panels can be produced using organo-layered silicates filled nanocomposites to meet the increasingly more stringent ratings of the low-smoke zero-halogen classification with reduced contents of mineral flame-retardants [734–736]. In the specific case of clay-filled polyolefins, applications of nanocomposites include water-storage systems, automotive injection-molded parts, and even foams. Moreover, in polyolefin packaging, films, bottles, and cups can be produced with improved mechanical, barrier, and rheological properties, resulting in better thermo-forming properties. Looking at the use of metal nanoreinforcements, a variety of metal nanoparticles has been incorporated for a wide range of applications, for example gold, copper, silver, palladium and cobalt. Metal nanoparticles have been added to polymers for uses such as chemical sensors, photocatalysis [737], microelectronic devices, biosensors [738], memory devices [739], photovoltaic cells [740]. There are also a number of optical and photonic applications for metal nanoparticles embedded into suitable polymers as plasmon waveguides, stable light filters and eye and sensor protection. In recent years, silver has been also incorporated into polymers for its antimicrobial properties [741,742]. Making specific reference to thermoplastic nanocomposites based on biopolymeric matrices, neat bioplastics suffer from main disadvantages like narrow processing window, poor gas and water barrier properties, unbalanced mechanical properties, low softening temperature and weak resistivity that have limited their use in a wide range of applications. Therefore, nanofillers can help in improving the above discussed properties, leading to an extension of the final applications of these materials [743]. In electronics, sensor and energy applications, polymer nanocomposites receive extensive attention in developing various devices and as a result, applications of bioplastics and their composites in electronic products are increasing due to their biodegradability and renewability with less environmental impact/carbon footprint [744]. The versatility and adaptability of bionanocomposites enable these materials to be utilized also for biomedical applications. An essential characteristic of medical biomaterials is biocompatibility, the ability to function appropriately in the human body to produce the desired clinical outcome, without causing adverse effects [745]: bionanocomposites that combine the tissue compatibility of natural polymers and bio-derived polymers along with the physical and chemical properties of nanoreinforcements have find widespread use in clinical medicine. In particular, three emerging areas of medical applications for bionanocomposites are tissue engineering, drug delivery, and gene therapy. Looking at the ever-growing produced literature in which the structure/property relationship in polymeric nanocomposites is continuously reported, it is clear how nanofillers have excellent potential to revolutionize the utilization of polymeric matrices and expand their use in high value applications.

5. Processing of advanced composites with nanostructured matrices

The terms advanced composites with nanostructure matrices are mainly referred to long fiber/thermosetting matrices based composites. Although considerable progress has been also obtained in the last few years in the field of the long fiber/thermoplastic counterpart, this section will focus mainly on the former group. It is important to

point out that the production of fiber-reinforced composites (FRP) based on nanocomposite matrices is generally performed using the same techniques commonly employed for commercial FRP based on the neat matrices. These techniques may be very different, although the aim is always to obtain a finite part combining high performance fibers with a polymeric matrix [746,747]. FRP can perform and behave very differently depending on the production technology, which affects the performances, the fiber content and the cost. It must be pointed out that the performances of FRP are strongly affected by the degree of impregnation of the fibers that has to be high and no unwetted fibers are tolerated in the case of high performance composites.

In the last 20 years, several progresses have been made to obtain well-impregnated composites, with high fiber volume fraction, without the need of using high cost processes (i.e. autoclave) and expensive product precursors. This is due to the evolution of the so-called "Liquid Molding Processes" [748,749]; these processes are derived from the resin transfer molding (RTM), schematized in Fig. 23, having as a common characteristic, the fact that the impregnation of the fiber preform and the production of the composite laminate, is performed at the same time. A dry fibrous reinforcement is therefore impregnated by the polymeric liquid matrix in a closed mold. The polymer precursor is able to flow around the fiber tows (inter-tow flow) and within the tow (intra-tow flow) impregnating each single filament constituting the tow itself. Pressure, in cavity vacuum, or the combination of both are the main driving forces for the matrix flow in this process. The other two factors controlling the matrix flow are strictly dependent on the material properties: the thermoset precursor viscosity and the fibrous reinforcement permeability. After the impregnation, the system is thermally cured inside the mold and subsequently demolded.

Thermosetting liquid precursors containing homogeneously disperse nanofillers are commonly more viscous than the neat counterparts. The high viscosity may create pitfalls in the processing that can lead to a poor quality fiber-reinforced laminates. A heterogeneous dispersion throughout the laminate, a re-agglomeration of the nanoparticles and a poor impregnation of the fibers are some of the most common problems that a composite manufacturer could face [750].

The application of nano-reinforced matrices in the hand lay-up technique does not generally cause significant problems in the realization of the composite/nanocomposite structure, unless the matrix viscosity becomes too high because of the nanofillers presence [751,752]. Many processing techniques are significantly affected by the employment of nanoreinforced liquid precursors used as matrix for the realization of high fiber volume fraction

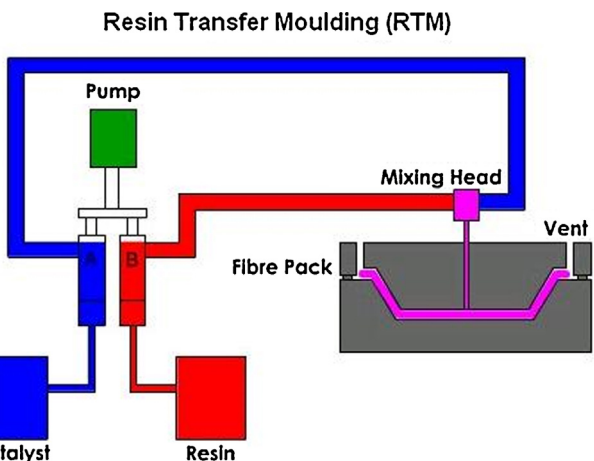


Fig. 23. RTM process schematization. (Courtesy of British Plastic Federation—Plastech Thermoset Tectonics).

composites. Liquid molding techniques, such as resin transfer molding (RTM), vacuum assisted resin transfer molding (VARTM) and Seemann composites resin infusion molding process (SCRIMP), could be strongly affected by the presence of nanoparticles in the matrix.

As just said, the main problem in the employment of nanofilled matrices in liquid molding techniques is the increase of the related viscosity. In fact, low viscosity polymer precursors can completely and homogeneously wet the fibers and create an effective interface between the matrix and the fibers, allowing the composite to perform its best properties. On the other hand, too viscous monomers could lead to a significant interface detriment and a loss of the material properties.

The increase in viscosity depends on many factors: filler morphology, filler nature, compatibility of filler with the matrix and weight amount. High filler loads can be the main cause of processing problems because filler clusters and agglomerates can be filtered by the fibers yielding a non-homogeneous dispersion. On the other hand, a good dispersion of filler generally increases the viscosity, leading to a difficult impregnation of the fiber fabric.

Many studies have been conducted on fiber-reinforced composites based on nanomodified matrices produced by liquid molding techniques. Gojny et al. [542] developed a glass fiber composite where the matrix was constituted by an epoxy with amino-functionalized double-wall carbon nanotubes. In spite of the increase in viscosity that they observed, the production of a laminate via RTM with an epoxy containing 0.3 wt% CNT was achieved. Torre et al. [753] analyzed composite laminates based on crosslinked epoxy matrix filled with 3 wt% of organo-modified montmorillonite, and 50% in volume of a carbon fiber. Despite the relatively high amount of fibers and the presence of an intercalated and not perfectly exfoliated layered phyllosilicate, the RTM process was effectively carried out with no significant changes in the process parameters in comparison to the composites based on the neat matrix. Moreover no detriments in the nanocomposite matrix based laminate occurred. Tests on this composite/nanocomposite material showed higher mechanical strength than those based on the neat matrix.

Monti et al. [553,754], showed the possibility to effectively process low viscosity precursor, containing different kinds of

conductive nanoparticles, both employing the RTM and the SCRIMP techniques (Fig. 24). To this purpose, a successful employment of carbon nanofibers as a filler in the unsaturated polyester matrix of a glass fiber reinforced polymer (GFRP) was reported [553]. Because of the high aspect ratio of carbon nanofibers, very small amount of these particles (1 wt%) were sufficient to significantly modify the electrical properties of the obtained glass fiber composites. As anticipated, the composite was effectively processed by mean of a RTM technique. SCRIMP technology was on the other hand, used to produce a glass fiber composite based on an epoxy monomer filled with a different amount of CNT as a matrix [754]. A small amount of nanotubes (0.5 wt%) allowed to obtain a sufficiently conductive composites with no filtration problems and inhomogeneities during the infusion stage.

Wichmann et al. [755] added different fillers (CNT, carbon blacks, and fumed silica nanoparticles) to the epoxy matrix to produce a RTM-based glass fiber composite. They found that nanoparticles significantly changed the matrix viscosity complicating the RTM process, an extension of the degassing and the injection time was necessary to obtain good quality of impregnation. In the case of electrically active fillers, the mold was modified to apply an electrical field during the curing process, in order to induce a preferred orientation of the CNT perpendicular to the fiber plane. Even in this study, they could not observe any filtering effect of the glass fiber bundles on the nanoparticles, although, especially in the case of CNT, they found a re-agglomeration behavior during the RTM injection.

Thostenson and Chou in their studies [756–758] successfully produced multiwall carbon nanotubes (MWCNT)-based glass fiber-reinforced polymer (GFRP) via vacuum-assisted resin transfer molding (VARTM), adding a precursor distribution layer to assist infiltration and hermetically sealing the layup in a vacuum bag. In order to compensate the increase of the viscosity due to the presence of the nanotubes, they heated the nanocomposite matrix up to 60 °C.

Haque et al. [759], using a process similar to the vacuum assisted resin infusion method (VARIM), showed large improvement of the mechanical properties of S2-glass fiber/epoxy laminates and at very low layered silicate content, indicating a good dispersion of filler. Other authors [760] used RTM and resin

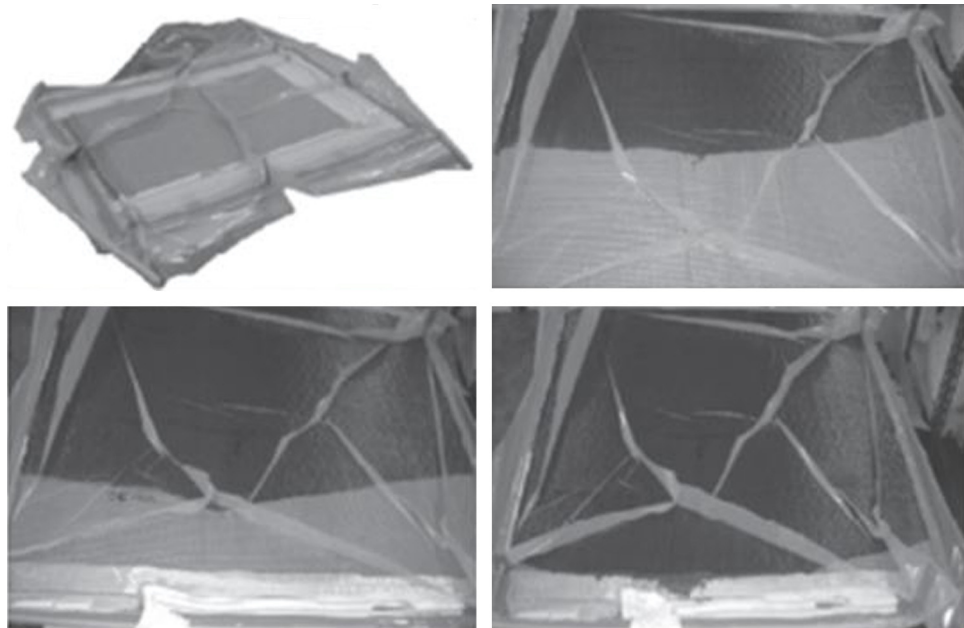


Fig. 24. Liquid molding process of CNT-epoxy matrix during the impregnation of a glass fiber laminate.

infusion under flexible tool (RIFT) for the processing of glass fabric epoxy laminates with 5 wt% of silica nanoparticles in the epoxy matrix. They found that high fiber fraction reinforcement filtered the silica nano-aggregates, stopping the in-plane liquid precursor infiltration in RTM just at the beginning of the filling stage. On the contrary, laminates with lower fiber fraction were successfully produced by RIFT.

In order to verify if the introduction of a kind of nanofiller could help the dispersion of another one, Sene and co-workers [761] introduced multi-walled carbon nanotubes and clays in an epoxy precursor to produce long fibers reinforced nanocomposites through RTM. Two types of montmorillonite clays were used: natural (MMT-Na) and organophilic (MMT-30B). In this investigation, higher viscosity was obtained for the mixture with MMT-30B and it was observed that this clay did not perform as well as the MMT-Na in helping the dispersion of the carbon nanotubes. It was verified by TEM analysis that more homogeneous dispersions and more intercalated structures were obtained with the MMT-30B than with the MMT-Na.

Kchit et al. [762] introduced nanoclays in an unsaturated polyester/glass fibers reinforced system with a liquid molding technique; the best dispersion route of nanoparticles was found to be the sonication of the nanoparticles in styrene, followed by the addition of the unsaturated polyester matrix. The blend was mechanically mixed letting the excess of styrene to evaporate.

Another important technique to produce composite materials is filament winding. This process is employed for the production of pipes and other hollow parts. In the filament winding process, fiber filaments are wetted by a liquid matrix precursor and then wound around a rotating mandrel at various angles to meet mechanical requirements. The structure is then thermally cured and, after curing, the mandrel is removed. This technique can also be used with a nanocomposite matrix. At this purpose, Hussain et al. [560] developed a filament wound glass/epoxy composite with 10 wt% of nanosized alumina; despite the increased viscosity, the possibility of producing a work-piece of good quality was the same of the one with the neat epoxy. Spindler-Ranta and Bakis [763] used an epoxy with 1 wt% single-wall nanotubes to produce a carbon fiber filament-wound composite. The presence of CNT did not produce any particular effect on the processing behavior of the composite that was successfully produced.

Many papers have been published on fiber-reinforced nanocomposites using pre-impregnated fabrics, (prepregs). Thermoset matrix prepregs, in which the monomer is only partially cured to allow easy handling, are usually used for the realization of fiber-reinforced composites in autoclave. This advanced composite process produces denser, void free materials because higher heat and pressure are used during curing. Autoclave is widely used in the aerospace industry to produce high strength/weight ratio parts from pre-impregnated high strength fibers for aircraft, spacecraft and missiles. Autoclaves are essentially heated pressure vessels usually equipped with vacuum systems into which the bagged lay-up on the mold is placed for the cure cycle. Curing pressures are generally in the range of 50 to 100 psi and cure cycles normally involve many hours. The method accommodates higher temperature crosslinked matrices such as epoxies, having higher properties than the conventional matrices.

Yokozeki et al. [764] studied nanocomposite laminates manufactured from prepregs that consisted in traditional carbon fibers and epoxy matrix filled with the CNT. Although they did not mention the experimental details on the prepregs processing, they were able to obtain a three-phase composite with increased fracture toughness and decreased residual thermal strain. Chen et al. [765] worked on the development of basalt fibers/epoxy prepregs with functionalized CNT embedded in the matrix, observing an enhancement of the mechanical properties. Srikan-

et al. [766] produced prepregs based on nano silica-modified phenolic matrices for enhancing ablation resistance of carbon fiber reinforced composites. Viscosity of the mixture was controlled adding ethanol and each composition was applied to the carbon fabric with a brush and allowed to dry at room temperature to form the prepregs. It is very interesting, from this base point, to analyze the European Patent EP2000494A1 [767], published in 10/12/2008 (Application number: 07380334.8), whose inventors developed several methods aimed to the production of prepregs based on nanofilled (with nanofibers and carbon nanotubes) matrices. At this purpose, four nanofillers embodiment techniques were developed, but the preferred one comprised many processing stages:

- Nanoreinforcement mixing with precursor and subsequent dispersing in a solvent;
- Adding of the solvent containing the nanoreinforcement to the monomer;
- Solvent evaporation and subsequent adding of the hardener;
- Manufacturing of the nanoreinforcement based mixture to produce the prepregs.

The obtained product comprised an amount of nanostructures between 0.0001% and 80% by weight. Moreover, the thickness was comprised between 0.05 mm and 2.0 mm and its density was comprised between 0.5 and 3.0 g/cm³.

Garcia et al. [768] developed an interlaminar reinforcement using aligned carbon nanotubes applied to prepregs for unidirectional carbon tape composites. At this purpose, aligned CNT were grown at high temperature and then printed to prepregs at room temperature, maintaining CNT alignment in the through thickness direction. Moreover, these results show that the employed fabrication methods are compatible with existing manufacturing processes and have the potential to enhance the structural and multifunctional properties of advanced composite laminates.

Sometimes, due to the difficulty in the effective mixing of nanofillers with viscous matrices, the nanoparticles can be directly sprayed over the prepreg surface. Adhikari et al. [769] reported this approach on prepregs based on an epoxy/graphite fibers system sprayed with carbon nanotubes. The process can be considered scalable, the results related to inter-laminar shear stress, showed that air spray processing had minimal effect on the quality of the laminates. Scanning electron microscopy studies showed that CNT were distributed uniformly in the plane of the laminate but not in the thickness direction due to low polymer flow during cure. At high concentrations (>1 wt%), the combination of a rather thick band of CNT and low matrix flow caused lack of polymer inside of CNT bundles. The in-plane shear strength, interlaminar fracture toughness, compressive strength and electrical conductivity improved in correspondence of low CNT loadings.

As it has been said, improvements of the properties in fiber-reinforced nanocomposites can be obtained only if an adequate dispersion of nanoparticles in the polymer matrix is obtained. However good dispersion implies always an increase of the viscosity, therefore the research devoted to solve this problem is still active and new ideas are already available. One interesting perspective would be to have the possibility to spray up the nanoparticles directly on the preform and inject the precursor in a second step. Interesting attempts are reported by Zhou et al. [770] and Khattab et al. [771], who reported an improvement of the properties of the final composites by spraying directly on the fiber reinforcement a solution of nanofibers in a binder and then impregnated the performs. Khattab et al. obtained an increase of 12% of the strength and of 28% of the modulus by spray coating the fiber with a solution of carbon nanofibers at different concentrations. They claimed that the small carbon nanofibers coating on the

fibers had positively affected the fiber-matrix interfacial bonding and therefore the properties depending on the interface were improved.

6. Summary and perspectives

This report has reviewed the processing behavior of nanostructured polymers and nanocomposites. These materials have gained popularity in the last two decades due to their exciting bulk and surface properties. Indeed, nanocomposites based on polymeric matrices gained significant interest after one of the first industrial applications when Toyota reported the use of nanoclays in nylon-6 matrix in 1993 [772]. However, the actual mention of the nanocomposite term was first found in the work on Lan and Pinnavaia [773] reported one year later. It is clear from the review reported here that the control of the nanostructure of polymers and the addition of nanoparticles has led to structural and functional property enhancements in a number of polymer systems as a material answer to continuous requirements from advanced industrial sectors. The availability of new nanoparticles with extraordinary properties (i.e. carbon nanotubes, graphenes, but also nanoclays, nanocellulose, metals and ceramics) have determined new and exciting possibilities for a continuous enlargement of polymer markets. However, it is also evident that the potentialities of these new materials are still strongly dependent on the development and scaling-up of reliable processing routes. Through this review it has been demonstrated how the efficient exploitation of the theoretical excellent properties of polymer nanocomposites requires the homogeneous and complete dispersion of the nanoparticles in the matrix and the consequent development of a huge interfacial area. For this reason, most of the research efforts in polymer nanotechnologies have been focused on developing rational processing strategies for nanostructured polymers and nanocomposites and in promoting better matrix-particle interactions reviewed in this report.

In particular, bottom-up and top-down approaches have been reviewed evidencing that typical processing technologies are clear top-down processes where ingredients (polymer and nanoparticles) are introduced and macroscopically melt mixed in the equipment. On the other hand, bottom-up self-assembling is not easily achieved in polymer materials due to the complex morphology of the polymer chains and to their complex interaction with nanoparticles. In this report, some bottom-up approaches are reviewed. They typically regard polymer and block copolymer nanostructuration by phase separation and reactive processing, with very few real applications.

Following the results of this review report, it is clear that the continuous growth of the applications of nanostructured polymers and nanocomposites requires continuous and intense efforts on the different aspects controlling the processing behavior of polymers and nanofillers. First, the huge potentiality of different nanoparticles (CNT, graphenes, carbon nanofibers, nanocellulose, metal and ceramic nanoparticles) can be properly exploited only through a solid functionalization strategy, eventually associated to reactive processes where functionalization and processing of polymers and nanofillers can be simultaneously achieved. The development of new matrices, eventually nanostructured, is not a current priority in the agenda of the most important polymer industries although few interesting results are available at the most active international research centers. Finally, the modernization of processing infrastructures at transformation companies is still incipient and most of the technical efforts are dedicated to the modification and updating of the current equipment with very few real innovations in processing machinery.

Current trends in the processing of polymer nanocomposites include also some particular techniques and approaches, not

focused and reviewed here, but with relevant potential for specialty nanocomposites. In first term, the modification of traditional processes for the elimination of environmental aggressive solvents must be mentioned. In particular, the use of ionic liquids and supercritical fluids as “green solvents” has attracted strong research interests in last years. Ionic liquids have been used either as compatibilizers for different nanofillers (i.e. clays, carbon nanotubes, graphenes) [779–784] and as “green solvents” in different processing strategies (i.e. solvent processing of thermoplastics, reactive processing, electrospinning) [784–787]. On the other hand, the use of supercritical fluids has been extensively reported for the environmental benign processing of thermoplastic matrix nanocomposites [788–793].

The processing of organic-inorganic hybrids has been also an interesting research area since many years mainly in the fields of tissue engineering and photoactive polymer nanocomposites. Mature processing strategies with still strong scientific interest and several applications in the nanocomposites field are based on the development of interpenetrating networks and sol-gel processes [794–800]. Other processing strategies of polymer nanocomposites that should be mentioned here include the microwave assisted processes [459,801,802], the frontal polymerization [803–808], the processing of foams [809,810] and aerogels [811–813]. In all these processes, the presence of the nanofillers and the interaction with the matrix represent again relevant factors for the processing behavior and the final properties of the nanocomposites obtained.

Another relevant sector of interest of the processing of nanocomposites is the use of the functional properties of the nanofillers for fluid control during processing operations. This is the case of the use of electrical fields for the orientation of carbon nanotubes and other conductive nanoparticles leading to nanocomposites with anisotropic electrical properties [119,814–816] or the use of magnetic fields for the orientation of magnetic nanoparticles [817,818].

Regarding composite materials, a growing interest strategy is the transfer of the use of fiber preforms to the nanocomposite fields. In fact, some recent developments are focused on the preparation of nanofiber preforms for successive impregnation with reactive monomers allowing higher nanofiller loadings in the final nanocomposite [819,820]. Evidently, the monomer flow through the preform and the wettability of the nanofibers are the bottlenecks of this new approach.

Finally, it should be mentioned that while strong research efforts were dedicated few decades ago to the modelling of the processing behavior of polymer matrix composites, similar attention has not been devoted to polymer nanocomposites. In fact, very few scientific reports can be found on the fundamental mass, heat and momentum transfer phenomena applied to the processing of polymer matrix nanocomposites [821–825].

In spite of the fact that the optimization of the processing of polymer nanocomposites has not been yet reached, there is an increasing number of reports on the application of nanostructured polymers and polymer composites in several industrial sectors, taking advantage of the multifunctional properties provided for innovative materials solutions [767–825]. Continuous publications in scientific papers are approaching these perspectives providing a clear proof of the continuous interest of academia, research centers and industry. Therefore, the tendency is to fill gradually the gap between nanotechnologies development and the market always avid of technological innovation. In fact, in a recent industrial and commercial report analysts from BCC Research have estimated that the global nanotechnology market is currently growing at an yearly rate of 19% and will reach 49 billion \$ in 2017. Currently, the car and food packaging industries in particular represent the main market for polymer nanocomposites, and in the next decades they

will continue to lead the way but other markets are now growing fast as for example electronic appliances, photovoltaic devices, packaging of inedible products and a range of other long-life product markets.

The basic principles applied more than 20 years ago by Toyota with their first nylon nanocomposites in automobile applications have since then been applied to other polymeric systems in various industrial sectors. This has pushed manufacturers in all parts of the polymer industry – from rubber to thermoplastics and thermosetting resins – to consider how nanocomposite technologies can be applied to existing polymeric systems on the market. Research results have shown that not all polymers are equally suitable for nanocomposites and that polymer matrices and nanoparticles must be designed for effective nanostructuration and nanocompounding. On the other hand, safety questions are still associated to the use of nanofillers. There is a generalized concern about the environmental impact of nanofillers and the risks to the human health leading to intense research activities in nanosafety around the world. However, this question is far to be solved and few regulations already exist in some countries. Therefore, the increased marketing of polymer nanotechnologies will be certainly associated to combined research efforts on processing–structure–properties relationships and on safe procedures for manipulation and disposal of nanoparticles.

Acknowledgments

We are indebted to the Spanish Ministry of Economy and Competitiveness (MINECO) for their economic support of this research (MAT2013-48059-C2-1-R). LP acknowledges the support of a JAEDoc grant from CSIC cofinanced by FSE. JMK acknowledges the support of the Russian Ministry of Education and Science within State Contract No. 14.Z50.31.0002.

References

- [1] E.P. Giannelis, *Adv. Mater.* 8 (1996) 29–35, <http://dx.doi.org/10.1002/adma.19960080104>.
- [2] E. Manias, A. Touny, L. Wu, K. Strawhecker, B. Lu, T.C. Chung, *Chem. Mater.* 13 (2001) 3516–3523, <http://dx.doi.org/10.1021/cm010627>.
- [3] S. Sinha Ray, M. Okamoto, *Prog. Polym. Sci.* 28 (2003) 1539–1641.
- [4] E.T. Thostenson, C. Li, T.W. Chou, *Compos. Sci. Technol.* 65 (2005) 491–516.
- [5] X.L. Xie, Y.W. Mai, X.P. Zhou, *Mater. Sci. Eng. R* 49 (2005) 89–112.
- [6] F. Hussain, M. Hojjati, M. Okamoto, R.E. Gorga, *J. Compos. Mater.* 40 (2006) 1511–1575, <http://dx.doi.org/10.1177/0021998306067321>.
- [7] V. Viswanathan, T. Laha, K. Balani, A. Agarwal, S. Seal, *Mater. Sci. Eng. R* 54 (2006) 121–285.
- [8] R.A. Vaia, J.F. Maguire, *Chem. Mater.* 19 (2007) 2736–2751, <http://dx.doi.org/10.1021/cm062693>.
- [9] D.R. Paul, L.M. Robeson, *Polymer* 49 (2008) 3187–3204.
- [10] S. Pavlidou, C.D. Papaspyrides, *Prog. Polym. Sci.* 33 (2008) 1119–1198.
- [11] Z. Spitalsky, D. Tasis, K. Papagelis, C. Galiotis, *Prog. Polym. Sci.* 35 (2010) 357–401.
- [12] I. Siró, D. Plackett, *Cellulose* 17 (2010) 459–494.
- [13] P.C. Ma, N.A. Siddiqui, G. Marom, J.K. Kim, *Compos., A—Appl. Sci. Manuf.* 41 (2010) 1345–1367.
- [14] C. Oueiny, S. Berlioz, F.-X. Perrin, *Prog. Polym. Sci.* 39 (2014) 707–748.
- [15] D. Vennerberg, Z. Rueger, M.R. Kessler, *Polymer* 55 (2014) 1854–1865.
- [16] G. Mittal, V. Dhand, K.Y. Rhee, S.-J. Park, W.R. Lee, J. Ind. Eng. Chem. (2014), <http://dx.doi.org/10.1016/j.jiec.2014.03.022>, in press.
- [17] K.K. Sadasivuni, D. Ponnamma, S. Thomas, Y. Grohens, *Prog. Polym. Sci.* 39 (2014) 749–780.
- [18] K. Hu, D.D. Kulkarni, I. Choi, V.V. Tsukruk, *Prog. Polym. Sci.* 39 (2014), <http://dx.doi.org/10.1016/j.progpolymsci.2014.03.001>, in press.
- [19] A.A. Azeez, K.Y. Rhee, S.J. Park, D. Hui, *Composites, B: Eng.* 45 (2013) 308–320.
- [20] A.I. Alateyah, H.N. Dhakal, Z.Y. Zhang, *Adv. Polym. Technol.* 32 (2013) 21368, <http://dx.doi.org/10.1002/adv>. 21368.
- [21] M.T. Albdry, B.F. Yousif, H. Ku, K.T. Lau, *J. Comp. Mat.* 47 (2013) 1093–1115.
- [22] J.K. Pandey, K.R. Reddy, A.K. Mohanty, M. Misra (Eds.), *Handbook of Polymer Nanocomposites. Processing, Performance and Application*, Springer, Berlin, Heidelberg, 2014, p. 538, ISBN: 978-3-642-38648-0.
- [23] D. Fleury, J.A.S. Bomfim, A. Vignes, C. Girard, S. Metz, F. Muñoz, B. R'Mili, A. Ustache, A. Guiot, J.X. Bouillard, *J. Cleaner Prod.* 53 (2013) 22–36.
- [24] P.C. LeBaron, Z. Wang, T.J. Pinnavaia, *Appl. Clay Sci.* 15 (1999) 11–29.
- [25] D. Schmidt, D. Shah, E.P. Giannelis, *Curr. Opin. Solid State Mater. Sci.* 6 (2002) 205–212.
- [26] M. Alexandre, Ph. Dubois, *Mater. Sci. Eng. R* 28 (2000) 1–63.
- [27] F. Uddin, *Metall. Mater. Trans. A* 39 (a) (2008) 2804–2814.
- [28] H.A. Patel, R.S. Soman, H.C. Bajaj, R.V. Jasra, *Bull. Mater. Sci.* 29 (2006) 133–145.
- [29] (<http://www.rockwoodadditives.com/nanoclay/pdfs/consistency.pdf>) (1/12/2013).
- [30] T. McNally, W.R. Murphy, C.Y. Lew, R.J. Turner, G.P. Brennan, *Polymer* 44 (2003) 2761–2772.
- [31] M.J. Solomon, A.S. Almusallam, K.F. Seefeldt, A. Somwangthanaroj, P. Varadan, *Macromolecules* 34 (2001) 1864–1872.
- [32] M. Zanetti, S. Lomakina, G. Camino, *Macromol. Mater. Eng.* 279 (2000) 1–9.
- [33] J.B. Dixon, *Appl. Clay Sci.* 5 (1991) 489–503.
- [34] E. Manias, A. Touny, L. Wu, K. Strawhecker, B. Lu, T.C. Chung, *Chem. Mater.* 13 (2001) 3516–3523.
- [35] I. Chin, T. Thurn-Albrechta, H. Kima, T.P. Russella, J. Wang, *Polymer* 42 (2001) 5947–5952.
- [36] L. Torre, M. Chieruzzi, J.M. Kenny, *J. Appl. Polym. Sci.* 115 (2010) 3659–3666.
- [37] H. Ishida, S. Campbell, J. Blackwell, *Chem. Mater.* 12 (2000) 1260–1267.
- [38] H.R. Dennis, D.L. Hunter, D. Chang, S. Kim, J.L. White, J.W. Cho, *Polymer* 42 (2001) 9513–9522.
- [39] K. Varlot, E. Reynaud, M.H. Kloppfer, G. Vigier, J. Varlet, *J. Polym. Sci. Pol. Phys.* 39 (2001) 1360–1370.
- [40] N. Ogata, S. Kawakage, T. Ogihara, *J. Appl. Polym. Sci.* 66 (1997) 573–581.
- [41] R. Levy, C.W. Francis, *J. Colloid Interface Sci.* 50 (1975) 442–450.
- [42] J. Billingham, C. Breen, J. Yarwood, *Vib. Spectrosc.* 14 (1997) 19–34.
- [43] A.B. Morgan, J.W. Gilman, *J. Appl. Polym. Sci.* 87 (2003) 1329–1338.
- [44] R.A. Vaia, E.P. Giannelis, *Macromolecules* 30 (1997) 8000–8009.
- [45] I. Ab Rahman, V. Padavattan, *J. Nanomater.* (2012), <http://dx.doi.org/10.1155/2012/132424>, Article ID 132424.
- [46] P.M. Ajayan, L.S. Schadler, P.V. Braun, *Nanocomposite Science and Technology*, Wiley-VCH Verlag, Weinheim, Germany, 2003.
- [47] P. Raveendran, J. Fu, S.L. Wallen, *J. Am. Chem. Soc.* 125 (2003) 13940–13941.
- [48] V. Kumar, S.K. Yadav, *J. Chem. Tech. Biotech.* 84 (2009) 151–157.
- [49] K.N. Thakkar, S.S. Mhatre, R.Y. Parikh, *Nanomed.-Nanotechnol.* 6 (2010) 257–262.
- [50] D.G. Shchukin, G.B. Sukhorukov, *Adv. Mater.* 16 (2004) 671–682.
- [51] C.L. Sajti, R. Sattari, B.N. Chichkov, S. Barcikowski, *J. Phys. Chem. C* 114 (2010) 2421–2427.
- [52] S. Barcikowski, A. Hahn, A.V. Kabashin, B.N. Chichkov, *Appl. Phys. A—Mater. Sci. Process* 87 (2007) 47–55.
- [53] D.K. Agrawal, *Curr. Opin. Solid State Mater. Sci.* 3 (1998) 480–485.
- [54] D. Vollath, D.V. Szabó, J. Haußelt, *J. Eur. Ceram. Soc.* 17 (1997) 1317–1324.
- [55] R. Chaim, *Mater. Sci. Eng. A* 443 (2006) 25–32.
- [56] M.T. Swihart, *Curr. Opin. Colloid Interface Sci.* 8 (2003) 127–133.
- [57] M. Hirasawa, H. Shirakawa, H. Hamamura, Y. Egashira, *J. Appl. Phys.* 82 (1997) 1404–1407.
- [58] Y.W. Su, C.S. Wu, C.C. Chen, C.D. Chen, *Adv. Mater.* 15 (2003) 49–51.
- [59] C. Kaya, J.Y. He, X. Gu, E.G. Butler, *Microporous Mesoporous Mater.* 54 (2002) 37–49.
- [60] L.Y. Cao, C.B. Zhang, J.F. Huang, *Ceram. Int.* 31 (2005) 1041–1044.
- [61] D.L. Zhang, *Prog. Mater. Sci.* 49 (2004) 537–560.
- [62] S.E. Pratsinis, *Prog. Energy Combust.* 24 (1998) 197–219.
- [63] L. Mädler, H.K. Kammler, R. Mueller, S.E. Pratsinis, *J. Aerosol. Sci.* 33 (2002) 369–389.
- [64] E. Reverchon, *Ind. Eng. Chem. Res.* 41 (2002) 2405–2411.
- [65] F.E. Kruis, H. Fissan, A. Peled, *J. Aerosol. Sci.* 29 (1998) 511–535.
- [66] R. Mueller, L. Mädler, S.E. Pratsinis, *Chem. Eng. Sci.* 58 (2003) 1969–1976.
- [67] G. Garnweinertner, M. Niederberger, *J. Am. Chem. Soc.* 89 (2006) 1801–1808.
- [68] J. Zhang, S. Xu, E. Kumacheva, *J. Am. Chem. Soc.* 126 (2004) 7908–7914.
- [69] L. Nicolais, G. Carotenuto (Eds.), *Metal-Polymer Nanocomposites*, John Wiley & Sons, Inc., Hoboken, NJ, USA, 2005.
- [70] P. Pachfule, B.K. Balan, S. Kurungot, R. Banerjee, *Chem. Commun.* 48 (2012) 2009–2011.
- [71] K. Sim, S.J. Sung, E.A. Jung, D.H. Son, D.H. Kim, J.K. Kang, K.Y. Cho, *Nanoscale Res. Lett.* 7 (2012) 46–48, <http://dx.doi.org/10.1186/1556-276X-7-46>.
- [72] A.C. Balazs, T. Emrick, T.P. Russell, *Science* 314 (2006) 1107–1110.
- [73] R.A. Vaia, C.L. Dennis, L.V. Natarajan, V.P. Tondiglia, D.W. Tonlin, T.J. Bunning, *Adv. Mater.* 13 (2001) 1570–1574.
- [74] C. Sanchez, B. Julian, P. Belleville, M. Popall, *J. Mater. Chem.* 15 (2005) 3559–3592.
- [75] R. Gangopadhyay, A. De, *Chem. Mater.* 12 (2000) 608–622, <http://dx.doi.org/10.1021/cm990537f>.
- [76] B.C. Sih, M.O. Wolf, *Chem. Commun.* 27 (2005) 3375–3384, <http://dx.doi.org/10.1039/B501448D>.
- [77] P. Dallas, V.K. Sharma, R. Zboril, *Adv. Colloid Interface Sci.* 166 (1–2) (2011) 119–135.
- [78] N. Ciolfi, L. Torsi, N. Ditaranto, G. Tantillo, Lina Ghibelli, L. Sabbatini, T. Bleve-Zacheo, M. D'Alessio, P.G. Zambonin, E. Traversa, *Chem. Mater.* 17 (2005) 5255–5262, <http://dx.doi.org/10.1021/cm0505244>.
- [79] J.L. Wilson, P. Poddar, N.A. Frey, H. Srikanth, *J. Appl. Phys.* 95 (2004) 1439–1443, <http://dx.doi.org/10.1063/1.1637705>.
- [80] R.M. Crooks, M. Zhao, L. Sun, V. Chechik, L.K. Yeung, *Acc. Chem. Res.* 34 (2001) 181–190, <http://dx.doi.org/10.1021/ar000110a>.
- [81] J.L. Leblanc, *Filled Polymers: Science and Industrial Applications*, CRC Press Taylor Francis Group, Boca Raton, FL, USA, 2010.

- [82] Z. Peng, L.X. Kong, S.D. Li, Y. Chen, M.F. Huang, *Compos. Sci. Technol.* 67 (2007) 3130–3139.
- [83] J. Xiao, W. Chen, F. Wang, J. Du, *Macromolecules* 46 (2013) 375–383.
- [84] A. Becheri, M. Dürr, P. Lo Nostro, P. Baglioni, *J. Nanopart. Res.* 10 (2008) 679–689.
- [85] G. Fu, P.S. Vary, C.T. Lin, *J. Phys. Chem. B* 109 (2005) 8889–8898.
- [86] B. Tan, Y. Wu, *J. Phys. Chem. B* 110 (2006) 15932–15938.
- [87] I.P. Parkin, R.G. Palgrave, *J. Mater. Chem.* 15 (2005) 1689–1695.
- [88] M.I. Katsnelson, *Mat. Today* 10 (2007) 20–27.
- [89] L. Pauling, *The Nature of the Chemical Bond*, Cornell University Press, Ithaca, NY, 1960.
- [90] R.F. Curl, *Rev. Mod. Phys.* 69 (1997) 691–702.
- [91] H. Kroto, *Rev. Mod. Phys.* 69 (1997) 703–722.
- [92] R.E. Smalley, *Rev. Mod. Phys.* 69 (1997) 723–730.
- [93] S. Iijima, *Nature* 354 (1991) 56–58.
- [94] K.S. Novoselov, D. Jiang, F. Schedin, T.J. Booth, V.V. Khotkevich, S.V. Morozov, A.K. Geim, *Proc. Nat. Acad. Sci. U.S.A.* 102 (2005) 10451–10453.
- [95] M.S. Dresselhaus, G. Dresselhaus, K. Sugihara, I.L. Spain, H.A. Goldberg, *Graphite Fibers and Filaments*, Springer-Verlag, Berlin, 1988.
- [96] T.G.S. Durkop, E. Cobas, M.S. Fuhrer, *Nano Lett.* 4 (2004) 35–39.
- [97] J.W.W. Mintmire, C.T. White, *Phys. Rev. Lett.* 81 (1998) 2506–2509.
- [98] S.D.D. Saito, G. Dresselhaus, M.S. Dresselhaus, *Physics Properties of Carbon Nanotubes*, Imperial College Press, London, 1998.
- [99] C.M.E. Kane, L. Balents, M.P.A. Fisher, *Phys. Rev. Lett.* 79 (1997) 5086–5089.
- [100] E.S. Snow, J.P. Novak, P.M. Campbell, D. Park, *Appl. Phys. Lett.* 82 (2003) 2145–2147.
- [101] J.S. Bunch, S.S. Verbridge, J.S. Alden, S. Jonathan, A.M. van der Zande, M. Arend, J.M. Parpia, H.G. Craighead, P.L. McEuen, *Nano Lett.* 8 (2008) 2458–2462.
- [102] E. Belyarova, M.E. Itkis, N. Cabrera, B. Zhao, A.P. Yu, J.B. Gao, R.C.J. Haddon, *Am. Chem. Soc.* 127 (2005) 5990–5995.
- [103] A.B. Kaiser, V. Skakalova, S. Roth, *Physica E* 40 (2008) 2311–2318.
- [104] J. Wu, H.A. Becerril, Z. Bao, Z. Liu, *Appl. Phys. Lett.* 92 (2008) 263302–263304.
- [105] Q. Cao, S.H. Hur, Z.T. Zhu, Y.G. Sun, C.J. Wang, M.A. Meitl, M. Shim, J.A. Rogers, *Adv. Mater.* 18 (2006) 304–308.
- [106] C. Oshima, A. Nagashima, *J. Phys.: Condens. Matter* 9 (1997) 1–20.
- [107] A.K. Geim, K.S. Novoselov, *Nat. Mater.* 6 (2007) 183–191, <http://dx.doi.org/10.1038/nmat1849>.
- [108] J.C. Charlier, P.C. Eklund, J. Zhu, A.C. Ferrari, *Topics Appl. Phys.* 111 (2008) 673–709.
- [109] M.S. Toshiaki Enoki, M. Endo, *Graphite Intercalation Compounds and Applications*, Oxford University Press, Oxford, 2003.
- [110] F.D.M. Haldane, *Phys. Rev. Lett.* 61 (1988) 2015–2018.
- [111] K.F. Mak, M.Y. Sfeir, Y. Wu, C.H. Lui, J.A. Misewich, T.F. Heinz, *Phys. Rev. Lett.* 101 (2008) 196405–196408.
- [112] W.A. Fowler, *Rev. Mod. Phys.* 56 (1984) 149–179.
- [113] C. Lee, X. Wei, J.W. Kysar, J. Hone, *Science* 321 (2008) 385–388.
- [114] S. Stankovich, D.A. Dikin, G.H. Dommett, K.M. Kohlhaas, E.J. Zimney, E.A. Stach, R.D. Piner, S.T. Nguyen, R.S. Ruoff, *Nature* 442 (2006) 282–286.
- [115] H.K. Jeong, H.J. Shin, K.K. Kim, A. Benayad, S.M. Yoon, H.K. Park, I.S. Jung, M.H. Jin, H.K. Jeong, J.M. Kim, J.Y. Choi, Y.H. Lee, *J. Am. Chem. Soc.* 130 (2008) 1362–1366.
- [116] S. Stankovich, D.A. Dikin, R.D. Piner, K.A. Kohlhaas, A. Kleinhammes, Y. Jia, Y. Wu, S.T. Nguyen, R.S. Ruoff, *Carbon* 45 (2007) 1558–1565.
- [117] S. Bittolo Bon, M. Piccini, A. Mariani, J.M. Kenny, L. Valentini, *Diamond Relat. Mater.* 20 (2011) 871–874.
- [118] J.W. Hill, R.H. Petrucci, *General Chemistry*, third ed., Prentice Hall, New Jersey, 2002.
- [119] K. Min, T.H. Han, J. Kim, J. Jung, C. Jung, S.M. Hong, C.M. Koo, *J. Colloid Interface Sci.* 383 (2012) 36–42.
- [120] D.A. Dikin, S. Stankovich, E.J. Zimney, R.D. Piner, G.H.B. Dommett, G. Evmenenko, S.T. Nguyen, R.S. Ruoff, *Nature* 448 (2007) 457–460.
- [121] A.C. Ferrari, J. Robertson, *Philos. Trans. R. Soc. London, Ser. A* 362 (2004) 2477–2512.
- [122] G. Eda, M. Chhowalla, *Nano Lett.* 9 (2009) 814–818.
- [123] S. Watcharotone, D.A. Dikin, S. Stankovich, R. Piner, I. Jung, S.-F. Chen, C.-P. Liu, S.T. Nguyen, R.S. Ruoff, *Nano Lett.* 7 (2007) 1888–1892.
- [124] Y. Hernandez, V. Nicolosi, M. Lotya, F.M. Blighe, Z.Y. Sun, I.T. McGovern, B. Holland, M. Byrne, Y. Gunko, *Nat. Nanotechnol.* 3 (2008) 563–568.
- [125] D. Nuvoli, V. Alzari, R. Sanna, S. Scognamillo, M. Piccinni, L. Peponi, J.M. Kenny, A. Mariani, *Nanoscale Res. Lett.* 7 (2012) 1–7.
- [126] M. Lotya, Y. Hernandez, P.J. King, R.J. Smith, V. Nicolosi, L.S. Karlsson, F.M. Blighe, S. De, Z. Wang, I.T. McGovern, G.S. Duesberg, J.N. Coleman, *J. Am. Chem. Soc.* 131 (2009) 3611–3620.
- [127] S. Gilje, S. Han, M. Wang, K.L. Wang, R.B. Kaner, *Nano Lett.* 7 (2007) 3394–3398.
- [128] T. Ramanathan, A.A. Abdala, S. Stankovich, D.A. Dikin, M. Herrera-Alonso, R.D. Piner, D.H. Adamson, H.C. Schniepp, X. Chen, R.S. Ruoff, S.T. Nguyen, I.A. Aksay, R.K. Prud'Homme, L.C. Brinson, *Nat. Nanotechnol.* 3 (2008) 327–331.
- [129] M. Cardinali, L. Valentini, J.M. Kenny, I. Mutlay, *Polym. Int.* 61 (2012) 1079–1083.
- [130] Z. Mo, Y. Zhao, J. Zhang, T. Xie, *Mater. Manuf. Proc.* 27 (2012) 1324–1328.
- [131] H. Kim, A.A. Abdala, C.W. Macosko, *Macromolecules* 43 (2010) 6515–6530.
- [132] S. Gilberto, J. Bras, A. Dufresne, *Polymers* 2 (2010) 728–765.
- [133] H. Zhu, Y. Yuan, D. Ha, S. Zhu, C. Preston, Q. Chen, Y. Li, X. Han, S. Lee, G. Chen, T. Li, J. Munday, J. Huang, L. Hu, *Nano Lett.* (2014), <http://dx.doi.org/10.1021/nl404101p>.
- [134] TAPPI Standard WI-3021: Standard Terms and Their Definition for Cellulose Nanomaterials, (<http://www.tappi.org/content/hide/draft3.pdf>), draft.
- [135] I. Oke, *SURG* 3 (2010) 77–80.
- [136] S. Kalia, B.S. Kaith, I. Kaur, *Cellulose Fibers: Bio- and Nano-Polymer Composites*, Springer, Berlin, Heidelberg, 2011.
- [137] E. Fortunati, F. Luzi, D. Puglia, A. Terenzi, M. Vercellino, L. Visai, C. Santulli, L. Torre, J.M. Kenny, *Carbohydr. Polym.* 97 (2013) 837–848.
- [138] A. Samir, M.A. Said, F. Alloin, Al. Dufresne, *Biomacromolecules* 6 (2005) 612–626.
- [139] I.M. Saxena, R.M. Brown, *Ann. Bot.* 96 (2005) 9–21.
- [140] D.Z. Min, J.F. Revol, D.G. Gray, *Cellulose* 5 (1998) 19–32.
- [141] S. Beck-Candanedo, M. Roman, D.G. Gray, *Biomacromolecules* 6 (2005) 1048–1054.
- [142] N. Ljungberg, C. Bonini, F. Bortolussi, C. Boisson, L. Heux, J.Y. Cavaillé, *Biomacromolecules* 6 (2005) 2732–2739.
- [143] A.J. Uddin, J. Araki, Y. Gotoh, *Biomacromolecules* 12 (2011) 617–624.
- [144] Y. Habibi, L.A. Lucia, O.J. Rojas, *Chem. Rev.* 6 (2010) 3479–3500.
- [145] E. Fortunati, D. Puglia, M. Monti, C. Santulli, M. Maniruzzaman, J.M. Kenny, *J. Appl. Polym. Sci.* 128 (2013) 3220–3230.
- [146] C. Zhou, Q. Wu, in: Sudheer Neralla (Ed.), *Nanotechnology and Nanomaterials: Nanocrystals—Synthesis, Characterization and Applications*, InTech, 2012, <http://dx.doi.org/10.5772/48727>, ISBN: 978-953-51-0714-9.
- [147] I. Siro, D. Plackett, *Cellulose* 17 (2010) 459–494.
- [148] N. Lavoine, I. Desloges, A. Dufresne, J. Bras, *Carbohydr. Polym.* 90 (2012) 735–764.
- [149] M. Pääkkö, M. Ankerfors, A. Kosonen, A. Nykänen, S. Ahola, M. Osterberg, J. Ruokolainen, J. Laine, P.T. Larsson, O. Ikkala, T. Lindström, *Biomacromolecules* 8 (2007) 1934–1941.
- [150] M. Henriksson, G. Henriksson, L.A. Berglund, T. Lindström, *Eur. Polym. J.* 43 (2007) 3434–3441.
- [151] T. Saito, Y. Nishiyama, J.L. Putaux, M. Vignon, A. Isogai, *Biomacromolecules* 7 (2006) 1687–1691.
- [152] P. Tingaut, C. Eyholzer, T. Zimmermann, Functional polymer nanocomposite materials from microfibrillated cellulose, in: A. Hashim (Ed.), *Advances in Nanocomposite Technology*, InTech, 2011, <http://dx.doi.org/10.5772/20817>, ISBN: 978-953-307-347-7.
- [153] K. Missoum, M. Naceur Belgacem, J. Bras, *Materials* 6 (2013) 1745–1766, <http://dx.doi.org/10.3390/ma6051566>.
- [154] M. Iguchi, S. Yamanaka, A. Budhiono, J. Mater. Sci. 35 (2000) 261–270.
- [155] N. Butchosa, C. Brown, P.T. Larsson, L.A. Berglund, V. Bulone, Q. Zhou, *Green Chem.* 15 (2013) 3404–3413.
- [156] K.Y. Lee, T. Tammelin, K. Schuftler, H. Kiiskinen, J. Samela, A. Bismarck, *ACS Appl. Mater. Interfaces* 4 (2012) 4078–4086.
- [157] M.P.G. Laborie, in: L.A. Lucia, O.J. Rojas (Eds.), *Nanoscience and Technology of Renewable Biomaterials*, John Wiley & Sons, Ltd., Chichester, UK, 2009, <http://dx.doi.org/10.1002/9781444307479ch9>.
- [158] M. Terrones, O. Martín, M. González, J. Pozuelo, B. Serrano, J.C. Cabanelas, S.M. Vega-Díaz, J. Baselga, *Adv. Mater.* 23 (2011) 5302–5310.
- [159] S. Bittolo Bon, L. Valentini, R. Verdejo, J.L. García Fierro, L. Peponi, M.A. Lopez-Manchado, J.M. Kenny, *Chem. Mater.* 21 (2009) 3433–3438.
- [160] S. Osuna, M. Torrent-Sucarrat, M. Solà, P. Gearlings, C.P. Ewels, G.V. Lier, *J. Phys. Chem. C* 114 (2010) 3340–3345.
- [161] B. Wang, B.J. Cooley, S. Cheng, K. Zou, Q.Z. Hao, F. Okino, J. Sofo, N. Samarth, J. Zhu, *APS March Meeting Abstracts*, American Physical Society, 2010.
- [162] J.O. Sofo, A.S. Chaudhari, G.D. Barber, *Phys. Rev. B: Condens. Matter* 75 (2007) 153401–153404.
- [163] A.K. Geim, K.S. Novoselov, D.C. Elias, R.R. Nair, T.M.G. Mohiuddin, S.V. Morozov, P. Blake, M.P. Halsall, A.C. Ferrari, D.W. Boukhvalov, M.I. Katsnelson, *Science* 323 (2009) 610–613.
- [164] S. Park, R.S. Ruoff, *Nat. Nanotechnol.* 4 (2009) 217–224.
- [165] E.T. Thostenson, Z. Ren, T.W. Chou, *Compos. Sci. Technol.* 61 (2001) 1899–1912.
- [166] R. Andrews, D. Jacques, D. Qian, T. Rantell, *Acc. Chem. Res.* 35 (2002) 1008–1017.
- [167] N. Nakashima, Y. Tomonari, H. Murakami, *Chem. Lett.* 31 (2002) 638–639.
- [168] M.F. Islam, E. Rojas, D.M. Bergey, A.T. Johnson, A.G. Yodh, *Nano Lett.* 3 (2003) 269–273.
- [169] N.O. Plank, G.A. Forrest, R. Cheung, A.J. Alexander, *J. Phys. Chem. B* 109 (2005) 22096–22101.
- [170] Y.Q. Wang, P.M.A. Sherwood, *Chem. Mater.* 16 (2004) 5427–5436.
- [171] L. Zhang, V.U. Kiny, H. Peng, J. Zhu, R.F. Lobo, J.L. Margrave, V.N. Khabashesku, *Chem. Mater.* 16 (2004) 2055–2061.
- [172] P.E. Pehrsson, W. Zhao, J.W. Baldwin, C. Song, J. Liu, S. Kooi, B. Zheng, *J. Phys. Chem. B* 107 (2003) 5690–5695.
- [173] J.L. Stevens, A.Y. Huang, H. Peng, I.W. Chiang, V.N. Khabashesku, J.L. Margrave, *Nano Lett.* 3 (2003) 331–336.
- [174] V.N. Khabashesku, W.E. Billups, J.L. Margrave, *Acc. Chem. Res.* 35 (2002) 1087–1095.
- [175] L. Valentini, J. Macan, I. Armentano, F. Mengoni, J.M. Kenny, *Carbon* 44 (2006) 2196–2201.
- [176] L. Valentini, D. Puglia, F. Carniato, E. Boccaleri, L. Marchese, J.M. Kenny, *Compos. Sci. Technol.* 68 (2008) 1008–1014.
- [177] B.N. Khare, P. Wilhite, M. Meyyappan, *Nanotechnology* 15 (2004) 1650–1654.
- [178] A. Felten, C. Bittencourt, J.J. Pireaux, *J. Appl. Phys.* 98 (2005) 074308–074309.
- [179] L. Valentini, D. Puglia, I. Armentano, J.M. Kenny, *Chem. Phys. Lett.* 403 (2005) 385–388.
- [180] L. Valentini, I. Armentano, F. Mengoni, D. Puglia, G. Pennelli, J.M. Kenny, *J. Appl. Phys.* 97 (2005) 114320–114325.
- [181] M. Roohani, Y. Habibi, N.M. Belgacem, G. Ibrahim, A.N. Karimi, A. Dufresne, *Eur. Polym. J.* 44 (2008) 2489–2498.
- [182] T. Abitbol, T. Johnstone, T.M. Quinn, D.G. Gray, *Soft Matter* 7 (2011) 2373–2379.
- [183] M. Roman, W.T. Winter, *Biomacromolecules* 5 (2004) 1671–1677.
- [184] N. Wang, E. Ding, R.R. Cheng, *Polymer* 48 (2007) 3468–3493.

- [185] A. Dufresne, in: Walter De Gruyter Incorporated (Ed.), *Nanocellulose: From Nature to High Performance Tailored Materials*, Walter De Gruyter Incorporated, Berlin, 2012, pp. 147–192.
- [186] C. Goussé, H. Chanzy, G. Excoffier, L. Soubeyrand, E. Fleury, *Polymer* 43 (2002) 2645–2651.
- [187] M. Hasani, E.D. Cranston, G. Westman, D.G. Gray, *Soft Matter* 4 (2008) 2238–2244.
- [188] S.P. Dong, M. Roman, *J. Am. Chem. Soc.* 129 (2007) 13810–13811.
- [189] Y. Habibi, H. Chanzy, M. Vignon, *Cellulose* 13 (2006) 679–687.
- [190] H. Lönnberg, L. Fogelström, M.A.S.A. Samir, L. Berglund, E. Malmström, A. Hult, *Eur. Polym. J.* 44 (2008) 2991–2997.
- [191] G. Morandi, L. Heath, W. Thielemans, *Langmuir* 25 (2009) 8280–8286.
- [192] S. Rebouillat, F. Pla, *J. Biomat. Nanobiotech.* 4 (2013) 165–188.
- [193] Y. Habibi, A. in, S. Dufresne, L.A. Thomas, Pothen (Eds.), *Chemical Modification of Nanocelluloses, in Biopolymer Nanocomposites: Processing, Properties, and Applications*, John Wiley & Sons, Inc., Hoboken, NJ, 2013, <http://dx.doi.org/10.1002/8.978111860995ch16>.
- [194] C. Yan, K.S. Kim, S.K. Lee, S.H. Bae, B.H. Hong, J.H. Kim, H.J. Lee, J.H. Ahn, *ACS Nano* 6 (2012) 2096–2103.
- [195] T.J. Ha, J. Lee, S.F. Chowdhury, D. Akinwande, P.J. Rossky, A. Dodabalapur, *ACS Appl. Mater. Interfaces* 5 (2013) 16–20.
- [196] W.H. Lee, J.W. Suk, J. Lee, Y.F. Hao, J. Park, J.W. Yang, H.W. Ha, S. Murali, H. Chou, D. Akinwande, K.S. Kim, S. Ruoff, *ACS Nano* 6 (2012) 1284–1290.
- [197] C.Y. Lin, C.S. Chang, J.H. Lin, C.C. Hsu, F.S. Chien, *Appl. Phys. Lett.* 102 (2013) 013505–013505.
- [198] T.T. Gao, X.L. Wang, B. Yu, Q.B. Wei, Y.Q. Xia, F. Zhou, *Langmuir* 29 (2013) 1054–1060.
- [199] B.J. Kim, H. Jang, S.K. Lee, B.H. Hong, J.H. Ahn, J.H. Cho, *Nano Lett.* 10 (2010) 3464–3466.
- [200] S.S. Sabri, J. Guillemette, A. Guermoune, M. Siaj, T. Szkopek, *Appl. Phys. Lett.* 100 (2012) 1131061–1131064.
- [201] J.W. Colson, A.R. Wöll, A. Mukherjee, M.P. Levendorf, E.L. Spitler, V.B. Shields, M.G. Spencer, J. Park, W.R. Dichtel, *Science* 332 (2011) 228–231.
- [202] J. Zhu, M. Yudasaka, M. Zhang, D. Kasuya, S. Iijima, *Nano Lett.* 3 (2003) 1239–1243.
- [203] A.M. Rao, E. Richter, S. Bandow, B. Chase, P.C. Eklund, K.A. Williams, S. Fang, K.R. Subbaswamy, M. Menon, A. Theiss, R.E. Smalley, G. Dresselhaus, M.S. Dresselhaus, *Science* 275 (1997) 187–191.
- [204] M.J. O'Connell, S.M. Bachilo, C.B. Huffman, V.C. Moore, M.S. Strano, E.H. Haroz, K.L. Rialon, P.J. Boul, W.H. Noon, C. Kittrell, J. Ma, R.H. Hauge, R.B. Weisman, R.E. Smalley, *Science* 297 (2002) 593–596.
- [205] K. Yurekli, C.A. Mitchell, R. Krishnamoorti, *J. Am. Chem. Soc.* 126 (2004) 9902–9903.
- [206] X.Y. Gong, J. Liu, S. Baskaran, R.D. Voise, J.S. Young, *Chem. Mater.* 12 (2000) 1049–1052.
- [207] J.-F. Sassi, H. Chancy, *Cellulose* 2 (1995) 111–127.
- [208] S. Spoljarić, A. Genovese, R.A. Shankts, *Composites, A—Appl. Sci. Manuf.* 40 (2009) 791–799.
- [209] S. Padalkar, J.R. Capadona, S.J. Rowan, C. Weder, Y.H. Won, L.A. Stanciu, R.J. Moon, *Langmuir* 26 (2010) 8497–8502, <http://dx.doi.org/10.1021/la904439p>.
- [210] L. Heux, G. Chauve, C. Bonini, *Langmuir* 16 (2000) 8210–8212.
- [211] E. Fortunati, M. Peltzer, I. Armentano, L. Torre, A. Jiménez, J.M. Kenny, *Carbohydr. Polym.* 90 (2012) 948–956.
- [212] Q. Guo, K. Wang, L. Chen, S. Zheng, P.J. Halley, *J. Appl. Polym. Sci., B: Polym. Phys.* 44 (2006) 975–985.
- [213] M. Lazzari, G. Liu, S. Lecommandoux, *Block Copolymers in Nanoscience*, VCH-Wiley, Weinheim, 2006.
- [214] N. Hadjichristidis, S. Pispas, G.A. Floudas, *Block Copolymers. Synthetic Strategies, Physical Properties and Applications*, John Wiley & Sons, New Jersey, 2003.
- [215] J. Ahn, Y. Shin, S. Kim, J. Lee, *Polymer* 44 (2003) 3847–3854.
- [216] F.J. Hua, Y.L. Yang, *Polymer* 42 (2001) 1361–1368.
- [217] I.W. Hamley, in: I.W. Hamley (Ed.), *Developments in Block Copolymer Science and Technology*, John Wiley & Sons, Chichester, UK, 2004, ISBN: 0-470-84335-7.
- [218] C.D. Han, J. Kim, J.K. Kim, *Macromolecules* 22 (1989) 383–394.
- [219] F.S. Bates, *Science* 251 (1991) 898–905, <http://dx.doi.org/10.1126/science.251.4996898>.
- [220] G. Hild, J. Lamps, *Polymer* 39 (1998) 2637–2649.
- [221] L. Peponi, I. Navarro-Baena, A. Sonseca, E. Gimenez, A. Marcos-Fernandez, J.M. Kenny, *Eur. Polym. J.* 49 (2013) 893–903.
- [222] M. Szwarc, M. Levy, R. Milkovich, J. Am. Chem. Soc. 78 (1956) 2656–2657.
- [223] M. Kato, M. Kamigaito, M. Sawamoto, T. Higashimura, *Macromolecules* 28 (1995) 1721–1723, <http://dx.doi.org/10.1021/ma90010a056>.
- [224] J. Wang, K. Matyjaszewski, *J. Am. Chem. Soc.* 117 (1995) 5614–5615, <http://dx.doi.org/10.1021/ja50012a035>.
- [225] K. Matyjaszewski, *Israel J. Chem.* 52 (2012) 206–220.
- [226] K.A. Davis, K. Matyjaszewski, *Macromolecules* 34 (2001) 2101–2107.
- [227] L. Peponi, I. Navarro-Baena, J.E. Baez, J.M. Kenny, A. Marcos-Fernandez, *Polymer* 53 (2012) 4561–4568.
- [228] H.T. Lee, D.S. Lee, *Macromol. Res.* 10 (2002) 359–364.
- [229] A.P. Dove, *Chem. Commun.* 48 (2008) 6446–6470.
- [230] J.C. Chen, J.M. Xiang, Z. Cai, H. Yong, H. Wang, L. Zhang, W. Luo, H. Min, J. Macromol. Sci. Pure Appl. Chem. 47 (2010) 655–662, <http://dx.doi.org/10.1080/10601325.2010.483350>.
- [231] M. Hillmyer, *Curr. Opin. Solid State Mater. Sci.* 4 (1999) 559–564.
- [232] C.Y. Li, F.J. Xu, W.T. Yang, *Langmuir* 29 (2013) 1541–1550.
- [233] Y. Mai, A. Eisenberg, *Chem. Soc. Rev.* 41 (2012) 5969–5985, <http://dx.doi.org/10.1039/c2cs35115c>.
- [234] M. Gomoll, H. Siede, *Plaste Kautsch* 16 (1969) 412–415.
- [235] F.S. Bates, G.H. Fredrickson, *Annu. Rev. Chem.* 41 (1990) 525–557, <http://dx.doi.org/10.1146/annurev.pc.41.100190.002521>.
- [236] G. Floudas, S. Pispas, N. Hadjichristidis, T. Pakula, I. Erkhhimovich, *Macromolecules* 29 (1996) 4142–4154, <http://dx.doi.org/10.1021/ma62v9517>.
- [237] T.P. Lodge, *Macromol. Chem. Phys.* 204 (2003) 265–273, <http://dx.doi.org/10.1002/macp.200290073>.
- [238] P.J. Flory, *Principles of Polymer Chemistry*, Cornell University Press, Ithaca, NY, 1953.
- [239] T.P. Lodge, B. Pudil, K.J. Hanley, *Macromolecules* 35 (2002) 4707–4717, <http://dx.doi.org/10.1021/ma0200975>.
- [240] E. Helfand, *Macromolecules* 8 (1975) 552–556, <http://dx.doi.org/10.1021/ma6004a032>.
- [241] E. Helfand, Z.R. Wasserman, *Macromolecules* 9 (1976) 879–888, <http://dx.doi.org/10.1021/ma46005a001>.
- [242] E. Helfand, Z.R. Wasserman, in: I. Goodman (Ed.), *Developments in Block Copolymers 1, Applied Science*, London, 1982, p. 99.
- [243] L. Leibler, *Macromolecules* 13 (1980) 1602–1617, <http://dx.doi.org/10.1021/ma86007a0047>.
- [244] T.P. Lodge, *Macromol. Chem. Phys.* 204 (2003) 265–273, <http://dx.doi.org/10.1002/macp.200290073>.
- [245] M.I. Malik, H. Pasch, *Prog. Polym. Sci.* 39 (2014) 87–123.
- [246] H.-Y. Mi, X. Jing, M.R. Salick, W.C. Crone, X.F. Peng, L.-S. Turng, *Adv. Polym. Technol.* 33 (2014) 21380, <http://dx.doi.org/10.1002/adv.21380>.
- [247] Y. Li, G.A. Thouas, Q.-Z. Chen, *RSC Adv.* 2 (2012) 8229–8242.
- [248] M.W. Matsen, *Eur. Phys. J. E* 36 (2013) 9857.
- [249] M. Banaszak, S. Wołoszczuk, T. Pakula, S. Jurga, *Phys. Rev. E: Stat. Phys. Plasmas Fluids Relat. Interdisciplin. Top.* 66 (2002) 031804.
- [250] T. Gemma, A. Hatano, T. Dotera, *Macromolecules* 35 (2002) 3225–3237.
- [251] J. Cai, J.M. Prausnitz, *J. Chem. Phys.* 119 (2003) 1223–1231.
- [252] T.M. Beardsley, M.W. Matsen, *Eur. Phys. J. E* 32 (2010) 255–264, <http://dx.doi.org/10.1140/epje/i2010-10651-x>.
- [253] T.M. Beardsley, M.W. Matsen, *Macromolecules* 44 (2011) 6209–6219, <http://dx.doi.org/10.1021/ma200966a>.
- [254] K. Lewandowski, M. Banaszak, *Phys. Rev. E: Stat. Phys. Plasmas Fluids Relat. Interdisciplin. Top.* 84 (2011) 011806–011809, <http://dx.doi.org/10.1103/PhysRevE.84.011806>.
- [255] F.J. Martínez-Veraocoecha, F.A. Escobedo, *Macromolecules* 38 (2005) 8522–8531, <http://dx.doi.org/10.1021/ma14+0512>.
- [256] F.J. Martínez-Veraocoecha, F.A. Escobedo, *J. Chem. Phys.* 125 (2006) 104907.
- [257] M.W. Matsen, G.H. Griffiths, R.A. Wickham, O.N. Vassiliou, *J. Chem. Phys.* 124 (2006) 024904.
- [258] S. Wołoszczuk, M. Banaszak, P. Knychała, M. Radosz, *Macromolecules* 41 (2008) 5945–5951, <http://dx.doi.org/10.1021/ma0718346>.
- [259] J.H. Song, T.F. Shi, Y. Li, J. Chen, L. An, *J. Chem. Phys.* 129 (2008) 054906–054907, <http://dx.doi.org/10.1063/1.2957463>.
- [260] V. Hugouvieux, M.A.V. Axelos, M. Kolb, *Soft Matter* 7 (2011) 2580–2591, <http://dx.doi.org/10.1039/COSM01018A>.
- [261] B. Abu-Sharkh, A. AlSunaidi, *Macromol. Theory Simul.* 15 (2006) 507–515, <http://dx.doi.org/10.1002/mats.200600014>.
- [262] S.H. Chou, D.T. Wu, H.K. Tsao, Y.J. Sheng, *Soft Matter* 7 (2011) 9119–9129, <http://dx.doi.org/10.1039/C1SM05808H>.
- [263] X.D. Guo, J.P.K. Tan, L.J. Zhang, M. Khan, S.Q. Liu, Y.Y. Yang, Y. Qian, *Chem. Phys. Lett.* 473 (2009) 336–342, <http://dx.doi.org/10.1016/j.cplett.2009.04.009>.
- [264] C.I. Huang, H.T. Yu, *Polymer* 48 (2007) 4537–4546, <http://dx.doi.org/10.1016/j.polymer.2007.06.002>.
- [265] M. Han, M. Hong, E. Sim, J. *Chem. Phys.* 134 (2011) 204901.
- [266] A.R. Khokhlov, P.G. Khalatur, *Chem. Phys. Lett.* 461 (2008) 58–63, <http://dx.doi.org/10.1016/j.cplett.2008.06.054>.
- [267] Y. Xu, J. Feng, H. Liu, Y. Hu, *Mol. Simul.* 34 (2008) 559–565.
- [268] E. Yıldırım, M. Yurtseven, *J. Theor. Comput. Chem.* 12 (2013) 1250100–1250117, <http://dx.doi.org/10.1142/S0219633612501003>.
- [269] I.W. Hamley, *The Physics of Block Copolymers*, Oxford University Press, Oxford, 1998.
- [270] M.W. Matsen, *Curr. Opin. Colloid Interface Sci.* 3 (1998) 40–47.
- [271] G. Widawski, M. Rawiso, B. Francois, *Nature* 369 (1994) 387–389, <http://dx.doi.org/10.1038/873693a0>.
- [272] M. Park, C. Harrison, P.M. Chaikin, R.A. Register, D.H. Adamson, *Science* 276 (1997) 1401–1404, <http://dx.doi.org/10.1126/science.276.5317.1401>.
- [273] C. Harrison, M. Park, P.M. Chaikin, R.A. Register, D.H. Adamson, *J. Vac. Sci. Technol. B* 16 (1998) 544–552.
- [274] K. Liu, S.M. Baker, M. Tuominen, T.P. Russell, I.K. Schuller, *Phys. Rev. B: Condens. Matter* 63 (2001) 060403(R), <http://dx.doi.org/10.1103/PhysRevB.63.060403>.
- [275] G. Holden, N.R. Legge, R. Quirk, H.E. Schroeder, *Thermoplastic Elastomers*, second ed., Hanser/Gardner Publications, Cincinnati, OH, 1996.
- [276] M.R. Bockstaller, R.A. Mickiewicz, E.L. Thomas, *Adv. Mater.* 17 (2005) 1331–1349, <http://dx.doi.org/10.1002/adma.200500167>.
- [277] L. Peponi, A. Marcos-Fernández, J.M. Kenny, *Nanoscale Res. Lett.* 7 (2012) 103–109, <http://dx.doi.org/10.1186/1556-276X-7-103>.
- [278] K.R. Li, Y. Cao, *Soft Matter* 8 (2010) 226–238, <http://dx.doi.org/10.1080/1539445X.2010.495616>.
- [279] X. Wu, Y.J. Qiao, H. Yang, J.B. Wang, *J. Colloid Interface Sci.* 349 (2010) 560–564, <http://dx.doi.org/10.1016/j.jcis.2010.05.093>.

- [280] J. Houdayer, M. Muller, *Macromolecules* 37 (2004) 4283–4295, <http://dx.doi.org/10.1021/ma035814p>.
- [281] L.F. Zhang, A. Eisenberg, *Polym. Adv. Technol.* 9 (1998) 677–699.
- [282] L.F. Zhang, A. Eisenberg, *Macromolecules* 32 (1999) 2239–2249.
- [283] G. Rizis, T.G.M. van de Ven, A. Eisenberg, *Soft Matter* 10 (2014) 2825–2835.
- [284] T.P. Lodge, B. Pudil, K.J. Hanley, *Macromolecules* 35 (2002) 4707–4717, <http://dx.doi.org/10.1021/ma0200975>.
- [285] K.J. Hanley, T.P. Lodge, C.I. Huang, *Macromolecules* 33 (2000) 5918–5931, <http://dx.doi.org/10.1021/ma000318b>.
- [286] J.E. Glass (Ed.), *Water-soluble Polymers: Beauty with Performance*, vol. 213, American Chemical Society, Washington, DC, 1986.
- [287] I.R. Schmolka, in: P.J. Tarcha (Ed.), *Polymers for Controlled Drug Delivery*, CRC Press, Boston, MA, 1991.
- [288] M.W. Edens, in: V.N. Nace (Ed.), *Nonionic Surfactants. Polyoxalkylene Block Copolymers*, vol. 60, Marcel Dekker, New York, NY, 1996, p. 185.
- [289] M. Malmsten, in: P. Alexandridis, B. Lindman (Eds.), *Amphiphilic Block Copolymers: Self-assembly and Applications*, Elsevier, Amsterdam, 2000.
- [290] J. Zipfel, P. Lindner, M. Tsianou, P. Alexandridis, W. Richtering, *Langmuir* 15 (1999) 2599–2602, <http://dx.doi.org/10.1021/la981666y>.
- [291] T. Riley, S. Stolnik, C.R. Heald, C.D. Xiong, M.C. Garnett, L. Illum, S.S. Davis, S.C. Purkiss, R.J. Barlow, P.R. Gellert, *Langmuir* 17 (2001) 3168–3174.
- [292] M.V. Seregina, L.M. Bronstein, O.A. Platonova, D.M. Chernyshov, P.M. Valetsky, J. Hartmann, E. Wenz, M. Antonietti, *Chem. Mater.* 9 (1997) 923–931, <http://dx.doi.org/10.1021/cm960469m>.
- [293] L.M. Bronstein, S.N. Sidorov, P.M. Valetsky, J. Hartmann, H. Colfen, M. Antonietti, *Langmuir* 15 (1999) 6256–6262, <http://dx.doi.org/10.1021/la990146f>.
- [294] I.W. Hamley, C. Daniel, W. Mingvanish, S.M. Mai, C. Booth, L. Messe, A.J. Ryan, *Langmuir* 16 (2000) 2508–2514, <http://dx.doi.org/10.1021/la991035>.
- [295] I.W. Hamley, J.P.A. Fairclough, A.J. Ryan, C.Y. Ryu, T.P. Lodge, A.J. Gleeson, J.S. Pedersen, *Macromolecules* 31 (1998) 1188–1196, <http://dx.doi.org/10.1021/ma970831y>.
- [296] H.E.H. Meijer, R.W. Venderbosch, J.G.P. Goossens, P.J. Lemstra, *High Perform. Polym.* 8 (1996) 133–167.
- [297] L. Ruiz-Pérez, G.J. Royston, J.P.A. Fairclough, A.J. Ryan, *Polymer* 49 (2008) 4475–4488.
- [298] M. Tiitua, A. Talob, O. Forsenb, O. Ikkala, *Polymer* 46 (2005) 6855–6861.
- [299] G. Holden, N.R. Legge, R. Quirk, H.E. Schroeder, *Thermoplastic Elastomers*, second ed., Hanser/Gardner Publications, Cincinnati, OH, 1996.
- [300] D. Cohn, A.F. Salomon, *Biomaterials* 26 (2005) 2297–2305, <http://dx.doi.org/10.1016/j.biomaterials.2004.07.052>.
- [301] C. Giacomelli, V. Schmidt, K. Aïssou, R. Borsali, *Langmuir* 26 (2010) 15734–15744, <http://dx.doi.org/10.1021/la100641j>.
- [302] A. Capretti, F. Auriemma, C. De Rosa, R. Di Girolamo, C. Forestiere, G. Miano, G.P. Pepe, Proc SPIE, 8771, Metamaterials VIII, 87710V, 2013, <http://dx.doi.org/10.1117/12.2018492>.
- [303] I. Choi, D.D. Kulkarni, W. Xu, C. Tsitsilianis, V.V. Tsukruk, *Langmuir* 29 (2013) 9761–9769, <http://dx.doi.org/10.1021/la401597p>.
- [304] A. Horechyy, B. Nandan, N.E. Zafeiropoulos, P. Formanek, U. Oertel, N.C. Bigall, A. Eychmüller, M. Stamm, *Adv. Funct. Mater.* 23 (2013) 483–490, <http://dx.doi.org/10.1002/adfm.201201452>.
- [305] B. Finnigan, D. Martin, P. Halley, R. Truss, K. Campbell, *Polymer* 45 (2004) 2249–2260.
- [306] A.F. Osman, G.A. Edwards, T.L. Schiller, Y. Andriani, K.S. Jack, I.C. Morrow, P.J. Halley, D.J. Martin, *Macromolecules* 45 (2012) 198–210.
- [307] S. Niu, R.F. Saraf, *Nanotechnology* 18 (2007), Art No. 125607.
- [308] I. Szleifer, R. Yerushalmi-Rozen, *Polymer* 46 (2005) 7803–7818, <http://dx.doi.org/10.1016/j.polymer.2005.05.104>.
- [309] J.W. Zhu, Y. Qin, Y. Zhang, *Electrochim. Commun.* 11 (2009) 1684–1687, <http://dx.doi.org/10.1016/j.electcom.06.2009.025>.
- [310] L. Peponi, A. Tercjak, L. Torre, J.M. Kenny, I. Mondragon, J. Nanosci. Nanotechnol. 9 (2009) 2128–2139, <http://dx.doi.org/10.1166/jnn.2009.437>.
- [311] R. Adhikari, W. Brostow, T. Datashvili, S. Henning, B. Menard, K.P. Menard, G.H. Michler, *Mater. Res. Innov.* 16 (2012) 19–24, <http://dx.doi.org/10.1179/1433075X11Y.0000000019>.
- [312] S. Horiochi, Y. Nakao, *Curr. Nanosci.* 3 (2007) 206–214.
- [313] S.K. Bae, S.Y. Lee, S.C. Hong, *React. Funct. Polym.* 71 (2011) 187–194, <http://dx.doi.org/10.1016/j.reactfunctopolym.12.2010.002>.
- [314] C.W. Hu, Y. Huang, R.C.C. Tsiang, J. Nanosci. Nanotechnol. 9 (2009) 3084–3091, <http://dx.doi.org/10.1166/jnn.2009.003>.
- [315] M. Haupt, S. Miller, S. Miller, R. Glass, M. Arnold, R. Sauer, K. Thonke, M. Möller, J.P. Spatz, *Adv. Mater.* 15 (2003) 829–831, <http://dx.doi.org/10.1002/adma.200304688>.
- [316] L. Peponi, A. Tercjak, L. Torre, I. Mondragon, J.M. Kenny, *J. Mat. Sci.* 44 (2009) 1287–1293, <http://dx.doi.org/10.1007/s10853-009-32772>.
- [317] S.J. Zhou, T. Sakamoto, J. Wang, A. Sugawara-Narutaki, A. Shimojima, T. Okubo, *Langmuir* 28 (2012) 13181–13188, <http://dx.doi.org/10.1021/la302443f>.
- [318] R. Suntivich, I. Choi, M.K. Gupta, C. Tsitsilianis, V.V. Tsukruk, *Langmuir* 27 (2011) 10730–10738, <http://dx.doi.org/10.1021/la2022566>.
- [319] J. Gutierrez, A. Tercjak, I. Garcia, I. Mondragon, *Nanotechnology* 20 (2009) 225603, <http://dx.doi.org/10.1088/0957-4484/20/22/225603>.
- [320] E. Buzdugan, P. Ghioca, *Mat. Plast.* 39 (2002) 87–95.
- [321] Y. Zhao, K. Saito, M. Takenaka, S. Koizumi, T. Hashimoto, *Macromolecules* 42 (2009) 5272–5277, <http://dx.doi.org/10.1021/ma900342v>.
- [322] Y. Zhao, K. Saito, T. Hashimoto, *Macromolecules* 46 (2013) 957–970, <http://dx.doi.org/10.1021/ma302070>.
- [323] L. Peponi, A. Tercjak, L. Torre, J.M. Kenny, I. Mondragon, *Compos. Sci. Technol.* 68 (2008) 1631–1636, <http://dx.doi.org/10.1016/j.compscitech.2008.02.032>.
- [324] L. Peponi, A. Tercjak, L. Torre, J.M. Kenny, I. Mondragon, *J. Nanostruct. Polym. Nanocomp.* 4 (2008) 76–83.
- [325] L. Peponi, A. Tercjak, L. Martin, L. Torre, I. Mondragon, J.M. Kenny, *Express Polym. Lett.* 5 (2011) 104–118, <http://dx.doi.org/10.3144/expresspolymlett.2011.12>.
- [326] L. Peponi, A. Tercjak, J. Gutierrez, H. Stadler, L. Torre, J.M. Kenny, I. Mondragon, *Macromol. Mater. Eng.* 293 (2008) 568–573, <http://dx.doi.org/10.1002/mame.200800033>.
- [327] J. Gutierrez, A. Tercjak, L. Peponi, I. Mondragon, *J. Phys. Chem. C* 113 (2009) 8601–8605, <http://dx.doi.org/10.1021/jp900858f>.
- [328] A.A. Askari, L. Rahimi, A.R. Bahrampour, G.P. Pepe, *Eur. Phys. J. B* 86 (2013) 150–158, <http://dx.doi.org/10.1140/epjb/e2013-31055-y>.
- [329] I. Garcia, A. Tercjak, J. Gutierrez, L. Rueda, I. Mondragon, *J. Phys. Chem. C* 112 (2008) 14343–14347, <http://dx.doi.org/10.1021/jp802345q>.
- [330] J. Huh, V.V. Ginzburg, A.C. Balazs, *Macromolecules* 33 (2000) 8085–8096, <http://dx.doi.org/10.1021/ma000708y>.
- [331] M. Fermeglia, S. Prich, *Comput. Chem. Eng.* 33 (2009) 1701–1710, <http://dx.doi.org/10.1016/j.compchemeng.2009.04.006>.
- [332] J. Albuquer, A. Boschetto-de-Fierro, C. Abetz, D. Fierro, V. Abetz, *Adv. Eng. Mater.* 13 (2011) 803–810, <http://dx.doi.org/10.1002/adem.201000291>.
- [333] J.H. Zou, L.W. Liu, H. Chen, S.I. Khondaker, R.D. Mc Cullough, Q. Huo, L. Zhai, *Adv. Mater.* 20 (2008) 2055–2060, <http://dx.doi.org/10.1002/adma.20070199555>.
- [334] J.H. Zou, S.I. Khondaker, Q. Huo, L. Zhai, *Adv. Funct. Mater.* 19 (2009) 479–483, <http://dx.doi.org/10.1002/adfm.200800542>.
- [335] J. Zou, H. Chen, A. Chunder, Y. Yu, Q. Huo, L. Zhai, *Adv. Mater.* 20 (2008) 3337–3341, <http://dx.doi.org/10.1002/adma.200703094>.
- [336] R.D. Bennett, G.H. Xiong, Z. Ren, R. Cohen, *Chem. Mater.* 16 (2004) 5589–5595.
- [337] W. Brostow, G. Broza, T. Datashvili, H.E. Hagg Lobland, A. Kopyniecka, *J. Mater. Res.* 27 (2012) 1815–1823.
- [338] A.N. Chakoli, J. Wan, J.T. Feng, M. Amirian, J.H. Sui, W. Cai, *Appl. Surf. Sci.* 256 (2009) 170–177, <http://dx.doi.org/10.1016/j.apsusc.2009.07.103>.
- [339] Z.M. Chen, Y. Liu, C. Yao, G. Yang, *Polym. Eng. Sci.* 53 (2013) 914–922, <http://dx.doi.org/10.1002/pen.23337>.
- [340] V. Datsyuk, C. Guerret-Piecourt, S. Dagreou, L. Billon, J.C. Dupin, E. Flahaut, A. Peigney, C. Laurent, *Carbon* 43 (2005) 873–876, <http://dx.doi.org/10.1016/j.carbon.2004.10.052>.
- [341] K.J. Gilmore, S.E. Moulton, G.G. Wallace, *Carbon* 45 (2007) 402–410, <http://dx.doi.org/10.1016/j.carbon.2006.09.015>.
- [342] C.X. Li, J.C. Hsu, K. Sugiyama, A. Hirao, W.C. Chen, R. Mezzenga, *Macromolecules* 42 (2009) 5793–5801, <http://dx.doi.org/10.1021/ma900861s>.
- [343] L. Peponi, L. Valentini, L. Torre, I. Mondragon, J.M. Kenny, *Carbon* 47 (2009) 2474–2480, <http://dx.doi.org/10.1016/j.carbon.2009.04.039>.
- [344] L. Peponi, A. Tercjak, J. Gutierrez, M. Cardinali, I. Mondragon, L. Valentini, J.M. Kenny, *Carbon* 48 (2010) 2590–2595, <http://dx.doi.org/10.1016/j.carbon.2010.03.062>.
- [345] H. Garate, M.L. Fascio, I. Mondragon, N.B. D'Accorso, S. Goyanes, *Polymer* 52 (2011) 2214–2220, <http://dx.doi.org/10.1016/j.polymer.2011.03.032>.
- [346] J.J. Hernandez, M.C. Garcia-Gutierrez, A. Nogales, D.R. Rueda, A. Sanz, I. Sics, B.S. Hsiao, Z. Roslaniec, G. Broza, T.A. Ezquerro, *Polymer* 48 (2007) 3286–3293, <http://dx.doi.org/10.1016/j.polymer.2007.03.070>.
- [347] H. Acharya, J. Sung, S. Hye-in, P. Soo-Young, M.B. Gil, P. Cheolmin, *React. Funct. Polym.* 69 (2009) 552–557, <http://dx.doi.org/10.1016/j.reactfunctpoly.2009.01.006>.
- [348] A. Eniotiadis, K. Litina, D. Gournis, S. Rangou, A. Avgeropoulos, P. Xidas, K. Triantafyllidis, *J. Phys. Chem. B* 117 (2013) 907–915, <http://dx.doi.org/10.1021/jp309361b>.
- [349] D. Becker, L.A.F. Coelho, *Curr. Org. Chem.* 17 (2013) 1844–1857, <http://dx.doi.org/10.2174/13852728113179990086>.
- [350] R. Adhikari, C. Damm, G.H. Michler, H. Münschedt, F.J. Baltá-Calleja, *Compos. Interface* 15 (2008) 453–463, <http://dx.doi.org/10.1163/156855408784655283>.
- [351] A. Ganguly, M. De Sarkar, A.K. Bhowmick, J. Polym. Sci., B–Polym. Phys. 45 (2007) 52–66, <http://dx.doi.org/10.1002/polb.20973>.
- [352] M. Ganss, B.K. Satapathy, M. Thunga, U. Staudinger, R. Weidisch, D. Jehnichen, J. Hempel, M. Rettenmayr, A. Garcia-Marcos, H.H. Goertz, *Eur. Polym. J.* 45 (2009) 2549–2563, <http://dx.doi.org/10.1016/j.europolymj.2009.05.021>.
- [353] Y.H. Ha, E.L. Thomas, *Macromolecules* 35 (2002) 4419–4428.
- [354] A. Vazquez, M. Lopez, E. Serrano, A. Valea, N.E. Zafeiropoulos, I. Mondragon, *J. Appl. Polym. Sci.* 110 (2008) 3624–3637, <http://dx.doi.org/10.1002/app.28885>.
- [355] J. Choi, T.M. Hermans, B.G.G. Lohmeijer, R.C. Pratt, G. Dubois, J. Frommer, R.M. Waymouth, J.L. Hedrick, *Nano Lett.* 6 (2006) 1761–1764, <http://dx.doi.org/10.1021/nl0612906>.
- [356] L. Peponi, A. Tercjak, R. Verdejo, M.A. Lopez-Manchado, I. Mondragon, J.M. Kenny, *J. Phys. Chem. C* 113 (2009) 17973–17978, <http://dx.doi.org/10.1021/jpc9074527>.
- [357] Y.W. Cao, Z.L. Lai, J.C. Feng, P.Y. Wu, *J. Mater. Chem.* 21 (2011) 9271–9278, <http://dx.doi.org/10.1039/c1jm10420a>.
- [358] N. Chen, Y.T. Liu, X.M. Xie, X.Y. Ye, X. Feng, Y.F. Chen, Y.H. Wang, *Carbon* 50 (2012) 4760–4764, <http://dx.doi.org/10.1016/j.carbon.2012.05.054>.
- [359] X.L. Zheng, Q. Xu, L.H. He, N. Yu, S.S. Wang, Z.M. Chen, J.W. Fu, *J. Phys. Chem. B* 115 (2011) 5815–5826, <http://dx.doi.org/10.1021/jp2018082>.
- [360] D.B. Velusamy, S.K. Hwang, R.H. Kim, G. Song, S.H. Cho, I. Bae, C. Park, *J. Mater. Chem.* 22 (2012) 25183–25189, <http://dx.doi.org/10.1039/c2jm35539f>.
- [361] Z. Liu, J.Q. Liu, L. Cui, R. Wang, X. Luo, C.J. Barrow, W.R. Yang, *Carbon* 51 (2013) 148–155, <http://dx.doi.org/10.1016/j.carbon.2012.08.023>.

- [362] T. Skaltsas, N. Karousis, H.J. Yan, C.R. Wang, S. Pispas, N. Tagmatarchis, *J. Mater. Chem.* 22 (2012) 21507–21512, <http://dx.doi.org/10.1039/c2jm33245k>.
- [363] B.H. Kim, J.Y. Kim, S.J. Jeong, J.O. Hwang, D.H. Lee, D.O. Shin, S.Y. Choi, S.O. Kim, *ACS Nano* 4 (2010) 5464–5470, <http://dx.doi.org/10.1021/nn101491g>.
- [364] G.X. Liu, Y.Q. Wu, Y.M. Lin, D.B. Farmer, J.A. Ott, J. Bruley, A. Grill, P. Avouris, D. Pfeiffer, A.A. Balandin, C. Dimitrakopoulos, *ACS Nano* 6 (2012) 6786–6792, <http://dx.doi.org/10.1021/nn301515a>.
- [365] L. Levitt, C.W. Macosko, *Macromolecules* 32 (1999) 6270–6277, <http://dx.doi.org/10.1021/ma9814999>.
- [366] J.R. Bell, K. Chang, C.R. Lopez-Barron, C.W. Macosko, D.C. Morse, *Macromolecules* 43 (2010) 5024–5032, <http://dx.doi.org/10.1021/ma90 2805>.
- [367] D.R. Paul, S. Newman (Eds.), *Polymer Blends*, Academic, London, 1978.
- [368] M.J. Folkes, P.S. Hoppe (Eds.), *Polymeric Blends and Alloys*, Blackie, London, 1993.
- [369] S. Datta, D.J. Lohse, *Polymeric Compatibilizers: Uses and Benefits in Polymer Blends*, Hanser, Munich, 1996.
- [370] L.A. Utracki, *Commercial Polymer Blends*, Chapman and Hall, London, 1998.
- [371] D.R. Paul, C.B. Bucknall (Eds.), *Polymer Blends: Formulation and Performance*, John Wiley & Sons, Chichester, UK, 2000, ISBN: 978-0-471-24825-5.
- [372] T. Hashimoto, K. Yamasaki, S. Koizumi, H. Hasegawa, *Macromolecules* 26 (1993) 2895–2904.
- [373] S. Koizumi, H. Hasegawa, T. Hashimoto, *Macromolecules* 27 (1994) 6532–6540.
- [374] M.A. Hillmyer, W.W. Maurer, T.P. Lodge, F.S. Bates, *J. Phys. Chem. B* 103 (1999) 4814–4824, <http://dx.doi.org/10.1021/jp990089z>.
- [375] F.S. Bates, W.W. Maurer, P.M. Lipic, M.A. Hillmyer, K. Almdal, K. Mortensen, G.H. Fredrickson, T.P. Lodge, *Phys. Rev. Lett.* 79 (1997) 849–852.
- [376] J.H. Lee, N.P. Balsara, R. Krishnamoorti, H.S. Jeon, B. Hammouda, *Macromolecules* 34 (2001) 6557–6560.
- [377] P. Stepanek, T.L. Morkved, K. Krishnan, T.P. Lodge, F.S. Bates, *Physica A* 314 (2002) 411–418.
- [378] M.W. Matsen, *J. Chem. Phys.* 110 (1999) 4658–4667, <http://dx.doi.org/10.1063/1.478349>.
- [379] R.B. Thompson, M.W. Matsen, *J. Chem. Phys.* 112 (2000) 6863–6872.
- [380] H.E. Stanley, *Introduction to Phase Transitions and Critical Phenomena*, Oxford University Press, Oxford, 1971.
- [381] S. Koizumi, H. Hasegawa, T. Hashimoto, *Macromolecules* 27 (1994) 4371–4381, <http://dx.doi.org/10.1021/ma00093a044>.
- [382] D. Yamaguchi, M. Takenaka, H. Hasegawa, T. Hashimoto, *Macromolecules* 34 (2001) 1707–1719, <http://dx.doi.org/10.1021/ma0013152>.
- [383] H. Frielinghaus, N. Hermsdorf, K. Almdal, K. Mortensen, L. Messe, L. Corvazier, J.P.A. Fairclough, A.J. Ryan, P.D. Olmsted, I.W. Hamley, *Europhys. Lett.* 53 (2001) 680–686, <http://dx.doi.org/10.1209/epl/i2001-00205-7>.
- [384] H. Frielinghaus, N. Hermsdorf, R. Sigel, K. Almdal, K. Mortensen, I.W. Hamley, L. Messe, L. Corvazier, A.J. Ryan, D. van Dusschoten, M. Wilhelm, G. Floudas, G. Fytas, *Macromolecules* 34 (2001) 4907–4916, <http://dx.doi.org/10.1021/ma010233q>.
- [385] N. Lopez-Rodriguez, A. Lopez-Arraiza, E. Meaurio, J.R. Sarasua, *Polym. Eng. Sci.* 46 (2006) 1299–1308, <http://dx.doi.org/10.1002/pen.20609>.
- [386] C.L. Simoes, J.C. Viana, A.M. Cunha, *J. Appl. Polym. Sci.* 112 (2009) 345–352.
- [387] D. Wu, Y. Zhang, M. Zhang, W. Zhou, *Eur. Polym. J.* 44 (2008) 2171–2183.
- [388] J.-P. Pascault, R.J.J. Williams (Eds.), *Epoxy Polymers*, Wiley-VCH, 2010.
- [389] J.P. Pascault, H. Sautereau, J. Verdu, R.J.J. Williams, *Thermosetting Polymers*, Marcel Dekker, New York, NY, USA, 2002.
- [390] S. Elliniadis, J.S. Higgins, N. Clarke, T.C.B. McLeish, R.A. Choudhery, S.D. Jenkins, *Polymer* 38 (1997) 4855–4862, [http://dx.doi.org/10.1016/S0032-3861\(97\)00006-2](http://dx.doi.org/10.1016/S0032-3861(97)00006-2).
- [391] T. Fine, J.P. Pascault, *Macromol. Symp.Special Issue: World Polymer Congress—MACRO, 2006*, 375–385.
- [392] M.A. Hillmyer, P.M. Lipic, D.A. Hajduk, K. Almdal, F.S. Bates, *J. Am. Chem. Soc.* 119 (1997) 2749–2750, <http://dx.doi.org/10.1021/ja963622m>.
- [393] P.M. Lipic, F.S. Bates, M.A. Hillmyer, *J. Am. Chem. Soc.* 120 (1998) 8963–8970, <http://dx.doi.org/10.1021/ja981544s>.
- [394] J.L. Chen, F.C. Chang, *Macromolecules* 32 (1999) 5348–5356, <http://dx.doi.org/10.1021/ma98 1819>.
- [395] J.L. Chen, F.C. Chang, *Polymer* 42 (2001) 2193–2199, [http://dx.doi.org/10.1016/S0032-3861\(00\)00511-5](http://dx.doi.org/10.1016/S0032-3861(00)00511-5).
- [396] M. Larranaga, M.D. Martin, N. Gabilondo, G. Kortaberria, A. Eceiza, C.C. Riccardi, I. Mondragon, *Coll. Polym. Sci.* 284 (2006) 1403–1410, <http://dx.doi.org/10.1007/s00396-006-1512-9>.
- [397] F. Meng, S. Zheng, W. Zhang, H. Li, Q. Liang, *Macromolecules* 39 (2006) 711–719.
- [398] S. Ritzenthaler, F. Court, L. David, E. Girard-Reydet, L. Leibler, J.P. Pascault, *Macromolecules* 35 (2002) 6245–6254, <http://dx.doi.org/10.1021/ma0121868>.
- [399] C. Ocando, E. Serrano, A. Tercjak, C. Pena, G. Kortaberria, C. Calberg, B. Grignard, R. Jerome, P.M. Carrasco, D. Mecerreyres, I. Mondragon, *Macromolecules* 40 (2007) 4068–4074, <http://dx.doi.org/10.1021/ma070585i>.
- [400] A. Tercjak, E. Serrano, I. Mondragon, *Macromol. Rapid Commun.* 28 (2007) 937–941, <http://dx.doi.org/10.1002/marc.200600893>.
- [401] Z. Xu, S. Zheng, *Polymer* 48 (2007) 6134–6144.
- [402] H.E. Romeo, I.A. Zucchi, M. Rico, C.E. Hoppe, R.J.J. Williams, *Macromolecules* 46 (2013) 4854–4861.
- [403] R.B. Grubbs, J.M. Dean, M.E. Broz, F.S. Bates, *Macromolecules* 33 (2000) 9522–9534.
- [404] R.B. Grubbs, M.E. Broz, J.M. Dean, F.S. Bates, *Macromolecules* 33 (2000) 2308–2310.
- [405] E. Serrano, M. Larranaga, P.M. Remiro, I. Mondragon, P.M. Carrasco, J.A. Pomposo, D. Mecerreyres, *Macromol. Chem. Phys.* 205 (2004) 987–996, <http://dx.doi.org/10.1002/macp.200300123>.
- [406] E. Serrano, A.D. Martin, A. Tercjak, J.A. Pomposo, D. Mecerreyres, I. Mondragon, *Macromol. Rapid. Commun.* 26 (2005) 982–985, <http://dx.doi.org/10.1002/marc.200500131>.
- [407] E. Serrano, A. Tercjak, C. Ocando, M. Larranaga, M.D. Parellada, S.C. Galvan, D. Mecerreyres, N.E. Zafeiropoulos, M. Stamm, I. Mondragon, *Macromol. Chem. Phys.* 208 (2007) 2281–2292.
- [408] E. Serrano, A. Tercjak, G. Kortaberria, J.A. Pomposo, D. Mecerreyres, N.E. Zafeiropoulos, M. Stamm, I. Mondragon, *Macromolecules* 39 (2006) 2254–2261, <http://dx.doi.org/10.1021/ma0515477>.
- [409] S.M. George, D. Puglia, J.M. Kenny, V. Caussin, P. Jyotishkumar, S. Thomas, *Ind. Eng. Chem. Res.* 52 (2013) 9121–9129.
- [410] C. Ocando, R. Fernández, A. Tercjak, I. Mondragon, A. Eceiza, *Macromolecules* 46 (2013) 3444–3451, <http://dx.doi.org/10.1021/ma400152g>.
- [411] C. Ocando, A. Tercjak, I. Mondragon, *Compos. Sci. Technol.* 70 (2010) 1106–1112.
- [412] J. Gutierrez, A. Tercjak, I. Mondragon, *J. Phys. Chem. C* 114 (2010) 22424–22430, <http://dx.doi.org/10.1021/jp1070902>.
- [413] E. Serrano, P. Gerard, F. Lortie, J.P. Pascault, D. Portinha, *Macromol. Mater. Eng.* 293 (2008) 820–827.
- [414] R.N. Mahaling, M. Vayer, S. Guillot, C. Sinturel, *Eur. Polym. J.* 47 (2011) 2277–2282.
- [415] X. Li, W. Fu, Y. Wang, T. Chen, X. Liu, H. Lin, P. Sun, Q. Jin, D. Ding, *Polymer* 49 (2008) 2886–2897.
- [416] C. Sinturel, M. Vayer, R. Erre, H. Amenitsch, *Macromolecules* 40 (2007) 2532–2538, <http://dx.doi.org/10.1021/ma06 2849>.
- [417] D.H. Builes, A. Tercjak, I. Mondragon, *Polymer* 53 (2012) 3669–3676, <http://dx.doi.org/10.1016/j.polymer.2012.06.018>.
- [418] M. Messori, M. Toselli, F. Polati, C. Tonelli, *Polymer* 42 (2001) 9877–9885, [http://dx.doi.org/10.1016/S0032-3861\(01\)00521-3](http://dx.doi.org/10.1016/S0032-3861(01)00521-3).
- [419] D.H. Builes, H. Hernandez, I. Mondragon, A. Tercjak, *J. Phys. Chem. C* 117 (2013) 3563–3571, <http://dx.doi.org/10.1021/jp3097617>.
- [420] X. Kornmann, H. Lindberg, L.A. Berglund, *Polymer* 42 (2001) 1303–1310.
- [421] T. Lan, T.J. Pinnavaia, *Chem. Mater.* 6 (1994) 2216–2219.
- [422] X. Kornmann, L.A. Berglund, J. Sterte, *Polym. Eng. Sci.* 38 (1998) 1351–1359.
- [423] T. Lan, P.D. Kaviratna, T.J. Pinnavaia, *Chem. Mater.* 7 (1995) 2144–2150.
- [424] L. Jiankun, K. Yucai, Q. Zongneng, Y. Xiao-Su, *J. Polym. Sci. Polym. Phys.* 39 (2001) 115–120.
- [425] P.B. Messersmith, E.P. Giannelis, *Chem. Mater.* 6 (1994) 1719–1725.
- [426] B. Bittmann, F. Haupert, A.K. Schlarb, *Ultrason. Sonochem.* 16 (2009) 622–628.
- [427] H.T. Kahraman, H. Gevgilili, D.M. Kalyon, E. Pehlivan, *J. Appl. Polym. Sci.* 129 (2013) 1773–1783, <http://dx.doi.org/10.1002/app.38867>.
- [428] K. Dean, J. Krstina, W. Tian, R.J. Varley, *Macromol. Mater. Eng.* 292 (2007) 415–427.
- [429] S.C.R. Sriraman, R.P. Singh, *J. Mat. Sci.* 41 (2006) 2219–2228.
- [430] M. Natali, J.M. Kenny, L. Torre, *Compos. Sci. Technol.* 70 (2010) 571–577.
- [431] A. Yasmin, L. Jandri, L. Abot, I.M. Daniel, *Scripta Mater.* 49 (2003) 81–86.
- [432] X. Xie, Y. Mai, X. Zhou, *Mat. Sci. Eng. R.* 49 (2005) 89–112.
- [433] E.T. Thostenson, Z. Ren, T. Chou, *Compos. Sci. Technol.* 61 (2001) 1899–1912.
- [434] P.C. Ma, N.A. Siddiqui, G. Marom, J.K. Kim, *Compos., A—Appl. Sci.* 41 (2010) 1345–1367.
- [435] Y.Y. Huang, E.M. Terentjev, *Polymers* 4 (2012) 275–295.
- [436] T.R. Frømyr, F.K. Hansen, T. Olsen, *J. Nanotechnol.* (2012), Article ID 545930, <http://dx.doi.org/10.1155/2012/545930>.
- [437] N. Hameed, N.V. Salim, T.L. Hanley, M. Sona, B.L. Fox, Q. Guo, *Phys. Chem. Chem. Phys.* 15 (2013) 11696–11703.
- [438] P. Miadet, S. Badaire, M. Maugey, A. Derre, V. Pichot, P. Launois, P. Poulin, C. Zakri, *Nano Lett.* 5 (2005) 2212.
- [439] Q.F. Cheng, J.W. Bao, J. Park, Z.Y. Liang, C. Zhang, B. Wang, *Adv. Funct. Mater.* 19 (2009) 3219.
- [440] D. Puglia, L. Valentini, J.M. Kenny, *Diamond Relat. Mater.* 12 (2003) 827–832.
- [441] L. Valentini, I. Armentano, D. Puglia, J.M. Kenny, *Carbon* 42 (2003) 323–329.
- [442] H. Xie, B. Liu, Z. Yuan, J. Shen, R. Cheng, *J. Pol. Sci., B—Polym. Phys.* 42 (2004) 3701–3712.
- [443] K. Tao, S. Yang, J.C. Grunlan, Y.-S. Kim, B. Dang, Y. Deng, R.L. Thomas, B.L. Wilson, X. Wei, *J. Appl. Polym. Sci.* 102 (2006) 5248–5254.
- [444] A. Martone, C. Formicola, M. Giordano, M. Zarrelli, *Compos. Sci. Technol.* 70 (2010) 1154–1160.
- [445] M.B. Bryning, M.F. Islam, J.M. Kikkawa, A.G. Yodh, *Adv. Mater.* 17 (2005) 1186–1191.
- [446] W.J. Ma, L.Q. Liu, Z. Zhang, R. Yang, G. Liu, T.H. Zhang, X.F. An, X.S. Yi, Y. Ren, Z.Q. Niu, J.Z. Li, H.B. Dong, W.Y. Zhou, P.M. Ajayan, S.S. Xie, *Nano Lett.* 9 (2009) 2855–2861.
- [447] J.N. Coleman, M. Cadek, R. Blake, V. Nicolosi, K.P. Ryan, C. Belton, A. Fonseca, J.B. Nagy, Y.K. Gun'ko, W.J. Blau, *Adv. Funct. Mater.* 14 (2004) 791–798.
- [448] J. Wu, D.D.L. Chung, *Carbon* 42 (2004) 3039–3042.
- [449] J. Bae, J. Jang, S.-H. Yoon, *Macromol. Chem. Phys.* 203 (2002) 2196–2204.
- [450] H. Kim, A.A. Abdala, C.W. Macosko, *Macromolecules* 43 (2010) 6515–6530.
- [451] S. Wang, M. Tamraparni, J. Qiu, J. Tipton, D. Dean, *Macromolecules* 42 (2009) 5251–5255.
- [452] J. Liang, Y. Wang, Y. Huang, Y. Ma, Z. Liu, J. Cai, C. Zhang, H. Gao, Y. Chen, *Carbon* 47 (2009) 922–925.
- [453] D.D.L. Chung, *J. Mater. Sci.* 39 (2004) 2645–2661.
- [454] S. Wang, M. Tamraparni, J. Qiu, J. Tipton, D. Dean, *Macromolecules* 42 (2009) 5251–5255.
- [455] L.M. Veca, M.J. Meziani, W. Wang, X. Wang, F. Lu, P. Zhang, Y. Lin, R. Fee, J.W. Connell, Y.-P. Sun, *Adv. Mater.* 21 (2009) 2088–2092.
- [456] S. Ganguli, A.K. Roy, D.P. Anderson, *Carbon* 46 (2008) 806–817.

- [457] R. Sengupta, M. Bhattacharya, S. Bandyopadhyay, A.K. Bhowmick, *Prog. Polym. Sci.* 36 (2011) 638–670.
- [458] R.J. Young, I.A. Kinloch, L. Gong, K.S. Novoselov, *Compos. Sci. Technol.* 72 (2012) 1459–1476.
- [459] B. Li, W. Zhong, *J. Mater. Sci.* 46 (2011) 5595–5614.
- [460] M. Raza, A. Westwood, C. Stirling, *Mater. Chem. Phys.* 132 (2012) 63–73.
- [461] M. Monti, M. Rallini, D. Puglia, L. Peponi, L. Torre, J.M. Kenny, *Compos. A—Appl. Sci. Manuf.* 46 (2013) 166–172.
- [462] S. Chandrasekaran, C. Seidel, K. Schulte, *Eur. Polym. J.* 49 (2013) 3878–3888.
- [463] W. Guo, G. Chen, *J. Appl. Polym. Sci.* (2014), <http://dx.doi.org/10.1002/APP.40565>, Available on line 6 MAR 2014.
- [464] L.M. Chiacciarelli, M. Rallini, M. Monti, D. Puglia, J.M. Kenny, L. Torre, *Compos. Sci. Technol.* 80 (2013) 73–79.
- [465] A. Tamburrano, F. Sarasini, G. De Bellis, A.G. D'Aloia, M.S. Sarto, *Nanotechnology* 24 (2014) 465702, <http://dx.doi.org/10.1088/0957-4484/24/46/465702>.
- [466] M.-Y. Shen, T.-Y. Chang, T.-H. Hsieh, Y.-L. Li, C.-L. Chiang, H. Yang, M.-C. Yip, *J. Nanomater.* 2013 (2013) 565401, <http://dx.doi.org/10.1155/2013/565401>.
- [467] L.J. Cote, R. Cruz-Silva, J. Huang, *J. Am. Chem. Soc.* 131 (2009) 11027–11032.
- [468] K.S. Subrahmanyam, P. Kumar, A. Nag, C.N.R. Rao, *Solid State Commun.* 150 (2010) 1774–1777.
- [469] Y. Matsuo, K. Tahara, Y. Sugie, *Carbon* 35 (1997) 113–120.
- [470] B. Das, K.E. Prasad, U. Ramamurtty, C.N.R. Rao, *Nanotechnology* 20 (2009), 125705/1.
- [471] A.V. Raghu, Y.R. Lee, H.M. Jeong, C.M. Shin, *Macromol. Chem. Phys.* 209 (2008) 2487–2493.
- [472] J.R. Potts, D.R. Dreyer, C.W. Bielawski, R.S. Ruoff, *Polymer* 52 (2011) 5–25.
- [473] G.I. Titelman, V. Gelman, S. Bron, R.L. Khalfin, Y. Cohen, H. Bianco-Peled, *Carbon* 43 (2005) 641–649.
- [474] M. Hirata, T. Gotou, S. Horiuchi, M. Fujiwara, M. Ohba, *Carbon* 42 (2004) 2929–2937.
- [475] S. Stankovich, R.D. Piner, S.T. Nguyen, R.S. Ruoff, *Carbon* 44 (2006) 3342–3347.
- [476] S. Park, J. An, R.D. Piner, I. Jung, D. Yang, A. Velamakanni, S.T. Nguyen, R.S. Ruoff, *Chem. Mater.* 20 (2008) 6592–6594.
- [477] H.-L. Guo, X.-F. Wang, Q.-Y. Qian, F.-B. Wang, X.-H. Xia, *ACS Nano* 3 (2009) 2653–2659.
- [478] G. Eda, M. Chhowalla, *Adv. Mater.* 22 (2010) 2392–2415.
- [479] Yu.M. Shul'ga, V.N. Vasilets, S.A. Baskakov, V.E. Muradyan, E.A. Skryleva, Yu.N. Parkhomenko, *High Energy Chem.* 46 (2012) 117–121.
- [480] G. Williams, B. Seger, P.V. Kamat, *ACS Nano* 2 (2008) 1487–1491.
- [481] A. Yeltik, G. Kucukayan-Dogu, B. Guzelturk, S. Fardindooost, Y. Kelestemur, H.V. Demir, *J. Phys. Chem. C* 117 (2013) 25298–25304.
- [482] B. Weng, S. Liu, N. Zhang, Z.-R. Tang, Y.-J. Xu, *J. Catal.* 309 (2014) 146–155.
- [483] Y. Matsumoto, M. Koinuma, S.Y. Kim, Y. Watanabe, T. Taniguchi, K. Hatakeyama, H. Tateishi, S. Ida, *ACS Appl. Mater. Interfaces* 2 (2010) 3461–3466.
- [484] R.S. Davidson, *Exploring the Science, Technology and Applications of U. V and E.B. Curing*, SITA Technology Ltd., London, 1998.
- [485] M. Sangermann, S. Marchi, L. Valentini, S. Bittolo Bon, P. Fabbri, *Macromol. Mater. Eng.* 296 (2011) 401–407.
- [486] R. Auvergne, S. Caillol, G. David, B. Boutevin, J.-P. Pascault, *Chem. Rev.* 114 (2014) 1082–1115.
- [487] M. Matos Ruiz, J.Y. Cavaille, A. Dufresne, C. Graillat, J.F. Gerard, *Macromol. Symp.* 169 (2001) 211–222.
- [488] L. Tang, C. Weder, *ACS Appl. Mater. Interfaces* 2 (2010) 1073–1080.
- [489] N.E. Marcovich, M.L. Auad, N.E. Bellesi, S.R. Nutt, M.I. Aranguren, *J. Mater. Res.* 21 (2006) 870–881.
- [490] Y. Li, A.J. Ragauskas, in: Boreddy Reddy (Ed.), *Cellulose Nano Whiskers as a Reinforcing Filler in Polyurethanes, Advances in Diverse Industrial Applications of Nanocomposites*, InTech, 2011, <http://dx.doi.org/10.5772/14240>.
- [491] S.H. Park, K.W. Oh, S.H. Kim, *Compos. Sci. Technol.* 86 (2013) 82–88.
- [492] A. Saralegi, L. Rueda, L. Martin, A. Arbelaitz, A. Eceiza, M.A. Corcuer, *Compos. Sci. Technol.* 88 (2013) 39–47.
- [493] L. Rueda, A. Saralegi, B. Fernández d'Arlas, Q. Zhou, L.A. Berglund, M.A. Corcuer, I. Mondragon, A. Eceiza, *Carbohydr. Polym.* 92 (2013) 751–757.
- [494] Y. She, H. Zhang, S. Song, Q. Lang, J. Pu, *BioResources* 8 (2013) 2594–2604.
- [495] A.N. Nakagaito, H. Yano, *Appl. Phys. A* 78 (2004) 547–552.
- [496] H. Liu, M.P.G. Laborie, *Cellulose* 18 (2011) 619–630.
- [497] A.N. Nakagaito, H. Yano, *Cellulose* 15 (2008) 323–331.
- [498] A. Turcova, J.R. Davies, S.J. Eichhorn, *Biomacromolecules* 6 (2005) 1055–1061.
- [499] J. Lu, P. Askeland, L.T. Drzal, *Polymer* 49 (2008) 1285–1296.
- [500] M.M. Ruiz, J.Y. Cavaille, A. Dufresne, J.F. Gerard, C. Graillat, *Compos. Interfaces* 7 (2000) 117–131.
- [501] H. Takagi, A.N. Nakagaito, K. Uchida, *WIT Trans. Built. Env.* 114 (2012) 379–386.
- [502] R. Masoodi, R.F. El-Hajjar, K.M. Pillai, R. Sabo, *Mater. Des.* 36 (2012) 570–576.
- [503] K.-Y. Lee, L.L.C. Wong, J.J. Blaker, J.M. Hodgkinson, A. Bismarck, *Green Chem.* 13 (2011) 3117–3123.
- [504] M. Shibata, K. Nakai, *J. Polym. Sci. B: Polym. Phys.* 48 (2010) 425–433.
- [505] V.M. Wik, M.I. Aranguren, M.A. Mosiewicki, *Polym. Eng. Sci.* 51 (2011) 1389–1396.
- [506] S. Lin, J. Huang, P.R. Chang, S. Wei, Y. Xu, Q. Zhang, *Carbohydr. Polym.* 95 (2013) 91–99.
- [507] L. Pranger, R. Tannenbaum, *Macromolecules* 41 (2008) 8682–8687.
- [508] L.A. Pranger, G.A. Nunnery, R. Tannenbaum, *Compos. B: Eng.* 43 (2012) 1139–1146.
- [509] H. Fischer, *Mater. Sci. Eng. C* 23 (2003) 763–772.
- [510] G. Lagaly, *Appl. Clay Sci.* 15 (1999) 1–9.
- [511] T.D. Fornes, D.R. Paul, *Polymer* 44 (2003) 4993–5013.
- [512] K. Wang, L. Chen, J. Wu, M.L. Toh, C. He, A.F. Yee, *Macromolecules* 38 (2005) 788–800.
- [513] J. Pappas, K. Patel, E.B. Nauman, *J. Appl. Polym. Sci.* 95 (2005) 1169–1174.
- [514] M.L. Auad, S.R. Nutt, V. Pettarin, P.M. Frontini, *Express Polym. Lett.* 1 (2007) 629–639.
- [515] M.-W. Ho, C.-K. Lam, K.-T. Lau, D.H.L. Ng, D. Hui, *Compos. Struct.* 75 (2006) 415–421.
- [516] B. Qi, Q.X. Zhang, M. Bannister, Y.-W. Mai, *Compos. Struct.* 75 (2006) 514–519.
- [517] J. Liu, H.-J. Sue, Z.J. Thompson, F.S. Bates, M. Dettloff, G. Jacob, N. Vergheese, H. Pham, *Macromolecules* 41 (2008) 7616–7624.
- [518] Z.J. Thompson, M.A. Hillmyer, J. Liu, H.-J. Sue, M. Dettloff, F.S. Bates, *Macromolecules* 42 (2009) 2333–2335.
- [519] J. Liu, H.-J. Sue, Z.J. Thompson, F.S. Bates, M. Dettloff, G. Jacob, N. Vergheese, H. Pham, *Acta Materialia* 57 (2009) 2691–2701.
- [520] S. Ritzenthaler, F. Court, E. Girard-Reydet, L. Leibler, J.P. Pascault, *Macromolecules* 36 (2003) 118–126, <http://dx.doi.org/10.1021/ma0211075>.
- [521] L. Wang, K. Wang, L. Chen, Y. Zhang, C. He, *Composites, A—Appl. Sci. Manuf.* 37 (2006) 1890–1896.
- [522] W. Liu, S.V. Hoa, M. Pugh, *Compos. Sci. Technol.* 65 (2005) 2364–2373.
- [523] A.S. Zerda, A.J. Lesser, *J. Polym. Sci. Polym. Phys.* 39 (2001) 1137–1146.
- [524] B. Wetzel, P. Rosso, F. Haupert, K. Friedrich, *Eng. Fract. Mech.* 73 (2006) 2375–2398.
- [525] J.T. Han, K. Cho, *J. Mater. Sci.* 41 (2006) 4239–4245.
- [526] G. Ragosta, M. Abbate, P. Musto, G. Scarinzi, L. Mascia, *Polymer* 46 (2005) 10506–10516.
- [527] B. Wetzel, F. Hupert, M.Q. Zhang, *Compos. Sci. Technol.* 63 (2003) 2055–2067.
- [528] P. Kardar, M. Ebrahimi, S. Bastani, *Prog. Org. Coat.* 62 (2008) 321–325.
- [529] F.H. Gojny, M.H.G. Wichmann, U. Köpke, B. Fiedler, K. Schulte, *Comp. Sci. Technol.* 64 (2004) 2363–2371.
- [530] H. Miyagawa, L.T. Drzal, *Polymer* 45 (2004) 5163–5170.
- [531] M.A. Rafiee, J. Rafiee, Z. Wang, H. Song, Z.Z. Yu, N. Koratkar, *ACS Nano* 3 (2009) 3884–3890, <http://dx.doi.org/10.1021/nm09010472>.
- [532] W. Bauhofer, J.Z. Kovacs, *Compos. Sci. Technol.* 69 (2009) 1486–1498.
- [533] H.N. Alamus, H. Fukunaga, S. Atobe, Y. Liu, J. Li, *Sensors* 11 (2011) 10691–10723.
- [534] Y.-J. Kim, J.Y. Cha, H. Ham, H. Huh, D.-S. So, I. Kang, *Curr. Appl. Phys.* 11 (2011) S350–S352.
- [535] J.K.W. Sandler, J.E. Kirk, I.A. Kinloch, M.S.P. Shaffer, A.H. Windle, *Polymer* 44 (19) (2003) 5893–5899.
- [536] J. Sandler, M.S.P. Shaffer, T. Prasse, W. Bauhofer, K. Schulte, A.H. Windle, *Polymer* 40 (1999) 5967–5971.
- [537] G.T. Pham, Y.-B. Park, Z. Liang, C. Zhang, B. Wang, *Composites, B: Eng.* 39 (2008) 209–216.
- [538] M.H. Al-Saleh, U. Sundararaj, *Carbon* 47 (2009) 2–22.
- [539] L.M. Chiacciarelli, M. Rallini, M. Monti, D. Puglia, J.M. Kenny, L. Torre, *Compos. Sci. Technol.* 80 (2013) 73–79.
- [540] J. Njuguna, K. Pielichowski, J.R. Alcock, *Adv. Eng. Mater.* 9 (2007) 835–847.
- [541] V.P. Veedu, A. Cao, X. Li, K. Ma, C. Soldano, S. Kar, S.P.M. Ajayan, M.N. Ghasemi-Nejad, *Nat. Mater.* 5 (2006) 457–470.
- [542] F.H. Gojny, M.H.G. Wichmann, B. Fiedler, W. Bauhofer, K. Schulte, *Composites, A—Appl. Sci. Manuf.* 36 (2005) 1525–1535.
- [543] M.H.G. Wichmann, J. Sumfleth, F.H. Gojny, M. Quaresimin, B. Fiedler, K. Schulte, *Eng. Fract. Mech.* 73 (2006) 2346–2359.
- [544] D.L. Zhao, R.H. Qiao, C.Z. Wang, Z.M. Shen, in: *Proceedings of the Asian International Conference on Advanced Materials (AICAM 2005)*, 2005, pp. 517–520.
- [545] K. Hsiao, J. Alms, S.G. Advani, *Nanotechnology* 14 (2003) 791–801.
- [546] S.A. Meguid, Y. Sun, *Mater. Des.* 25 (2004) 289–298.
- [547] Y. Iwahori, S. Ishiwata, T. Sumizawa, T. Ishikawa, *Composites, A—Appl. Sci. Manuf.* 36 (2005) 1430–1439.
- [548] M. Joshi, A. Bhattacharyya, *Composites, NSTI—Nanotech.* 3 (2004) 308–311.
- [549] J. Cho, J.Y. Chen, I.M. Daniel, *Scr. Mater.* 56 (2007) 685–688.
- [550] J. Oh, K. Oh, C. Kim, C. Hong, *Composites, B: Eng.* 35 (2004) 49–56.
- [551] K. Park, S. Lee, C. Kim, J. Han, *Comp. Struct.* 81 (2007) 401–406.
- [552] B. Fiedler, F.H. Gojny, M.H.G. Wichmann, W. Bauhofer, K. Schulte, *Ann. Chim. Sci. Mat.* 29 (2004) 81–94.
- [553] M. Monti, M. Natali, R. Petrucci, J.M. Kenny, L. Torre, *Polym. Compos.* 32 (2011) 766–775.
- [554] X. Kornmann, M. Rees, Y. Thomann, A. Necola, M. Barbezat, R. Thomann, *Compos. Sci. Technol.* 65 (2005) 2259–2268.
- [555] F.H. Chowdhury, M.V. Hosur, S. Jeelani, *Mater. Sci. Eng. A* 421 (2006) 298–306.
- [556] L. Linn, J. Lee, C. Hong, G. Yoo, S.G. Advani, *Compos. Sci. Technol.* 66 (2006) 2116–2125.
- [557] K. Wang, L. Chen, J. Wu, M.L. Toh, C. He, A.F. Yee, *Macromolecules* 38 (2005) 788–798.
- [558] N.A. Siddiqui, R.S.C. Woo, J. Kim, C.C.K. Leung, A. Munir, *Composites, A—Appl. Sci. Manuf.* 38 (2007) 449–460.
- [559] G. Zhou, S. Movva, L.J. Lee, *J. Appl. Polym. Sci.* 108 (2008) 3720–3726.
- [560] M. Hussain, A. Nakahira, K. Niijhara, Mater. Lett. 26 (1996) 185–191.
- [561] Q.H. Wang, X.R. Zhang, X. Pei, Mater. Des. 31 (2010) 1403–1409.
- [562] J. Lin, C.M. Ma, W. Tai, W. Chang, C. Tsai, *Polym. Compos.* 27 (2000) 305–311.
- [563] F. Hossain, D. Dean, A. Haque, M. Shamsuzzoha, J. Adv. Mater. 37 (2005) 16–27.
- [564] B. Finnigan, D. Martin, P. Halley, R. Truss, K. Campbell, *Polymer* 45 (2004) 2249–2260.
- [565] A.F. Osman, G.A. Edwards, T.L. Schiller, Y. Andriani, K.S. Jack, I.C. Morrow, P.J. Halley, D.J. Martin, *Macromolecules* 45 (2012) 198–210.
- [566] C. Hongxiang, Z. Danlin, X. Xiaoqin, Z.G. Maosheng, K. Changmei, L. Yanjun, *Mat. Sci. Eng. A—Struct.* 528 (2011) 1656–1661.

- [567] H.X. Chen, M.S. Zheng, H.Y. Sun, Q.M. Jia, *Mat. Sci. Eng. A—Struct.* 445 (2007) 725–730.
- [568] J.H. Chang, Y.U. An, *J. Polym. Sci., B—Polym. Phys.* 40 (2002) 670–677.
- [569] J.C. Wang, Y.H. Chen, R.J. Chen, *J. Polym. Sci., B—Polym. Phys.* 45 (2007) 519–531.
- [570] C. Mc Clory, T. McNally, G.P. Brennan, *J. Appl. Polym. Sci.* 105 (2007) 1003–1011.
- [571] C. Dubois, D. Rajabian, Rodriguez, *Polym. Eng. Sci.* 46 (2006) 360–371.
- [572] S. Chen, J.J. Sui, L. Chen, *Coll. Polym. Sci.* 283 (2004) 66–73.
- [573] D.Y. Cai, K. Yusoh, M. Song, *Nanotechnology* 20 (2009) 085712.
- [574] S. Stankovich, R.D. Piner, S.T. Nguyen, R.S. Ruoff, *Carbon* 44 (2006) 3342–3347.
- [575] G. Gorras, M. Tortora, V. Vittoria, *J. Polym. Sci., B—Polym. Phys.* 43 (2005) 2454–2467.
- [576] M. Tortora, G. Gorras, V. Vittoria, G. Galli, S. Ritrovati, E. Chiellini, *Polymer* 43 (2002) 6147–6157.
- [577] Y.I. Tien, K.H. Wei, *Macromolecules* 34 (2001) 9045–9052.
- [578] Y.I. Tien, K.H. Wei, *Polymer* 42 (2001) 3213–3221.
- [579] Z. Wang, T.J. Pinnavaia, *Chem. Mater.* 10 (1998) 3769–3771.
- [580] K.J. Yao, M. Song, D.J. Hourston, D.Z. Luo, *Polymer* 43 (2002) 1017–1020.
- [581] S.V. Levchik, G. Camino, M.P. Luda, L. Costa, G. Muller, B. Costes, Y. Henry, *Polym. Adv. Technol.* 7 (1996) 7823–7832.
- [582] J.H. Troitzsch, *Chem. Today* 16 (1998) 1–18.
- [583] F. Laoutid, L. Bonnau, M. Alexandre, J.M. Lopez-Cuesta, Ph. Dubois, *Mater. Sci. Eng. R* 63 (2009) 100–125.
- [584] S.V. Levchik, E.D. Weil, *Polym. Int.* 53 (2004) 1901–1929.
- [585] B.K. Kandola, W. Pornwannachai, *J. Fire Sci.* 28 (2010) 357–381.
- [586] W. Liu, R.J. Varley, G.P. Simon, *Polymer* 47 (2006) 2091–2098.
- [587] G. Camino, G. Tartaglione, A. Frache, C. Manferti, G. Costa, *Polym. Degrad. Stabil.* 90 (2005) 354–362.
- [588] M. Bartholomai, B. Schartel, *Polym. Adv. Technol.* 15 (2004) 355–364.
- [589] J.W. Gilman, *Appl. Clay Sci.* 15 (1999) 31–49.
- [590] O. Becker, R.J. Varley, G.P. Simon, *Eur. Polym. J.* 40 (2004) 187–195.
- [591] J. Zhu, F.M. Uhl, A.B. Morgan, C.A. Wilkie, *Chem. Mater.* 13 (2001) 4649–4654.
- [592] M. Lewin, *Polym. Adv. Technol.* 17 (2006) 758–763.
- [593] T. Kashiwagi, F. Du, J.F. Douglas, K.I. Winey, R.H. Harris, J.R. Shields, *Nat. Mater.* 4 (2005) 928–933.
- [594] P. Kiliaris, C.D. Papaspyrides, *Prog. Polym. Sci.* 35 (2010) 902–958.
- [595] B. Schartel, A. Wei, H. Sturm, M. Kleemeier, A. Hartwig, C. Vogt, R.X. Fischer, *Polym. Adv. Technol.* 22 (2010) 1581–1592.
- [596] M. Zanetti, P. Bracco, L. Costa, *Polym. Degrad. Stabil.* 85 (2004) 657–665.
- [597] S. Bandyopadhyay, R. Chen, E.P. Giannelis, J. Macromol. Sci. Rev. 81 (1999) 159–160.
- [598] A. Guo, G. Liang, *Polym. Degrad. Stabil.* 80 (2003) 383–391.
- [599] M. Zammarrano, in: A.B. Morgan, C.A. Wilkie (Eds.), *Flame Retardant Polymer Nanocomposites*, John Wiley & Son, Hoboken, NJ, 2007, pp. 235–285.
- [600] B. Schartel, U. Knoll, A. Hartwig, D. Putz, *Polym. Adv. Technol.* 17 (2006) 281–293.
- [601] T. Kashiwagi, J.W. Gilman, K. Butler, R.H. Harris, J.R. Shields, *Fire Mater.* 24 (2000) 277–289.
- [602] T. Kashiwagi, J.R. Shields, R.H. Harris, R.D. Davis, *J. Appl. Polym. Sci.* 87 (2003) 1541–1553.
- [603] G.H. Hsieh, Y.L. Liu, H.H. Liao, *J. Polym. Sci., A* 39 (2001) 986–996.
- [604] M. Natali, M. Monti, J.M. Kenny, L. Torre, *J. Appl. Polym. Sci.* 120 (2011) 2632–2640.
- [605] L. Tibiletti, C. Longuet, L. Ferry, P. Coutelen, A. Mas, J.J. Robin, J.M. Lopez-Cuesta, *Polym. Degrad. Stabil.* 96 (2011) 67–75.
- [606] Y. Liu, C. Hsu, W. Wei, R. Jeng, *Polymer* 44 (2003) 5159–5167.
- [607] J.T. Saavedra, J. Lo Beceiro, S. Naya, R. Artiaga, *Polym. Degrad. Stabil.* 93 (2008) 2133–2137.
- [608] A. Afzal, H.M. Siddiqi, N. Iqbal, Z. Ahmad, *J. Therm. Anal. Calorim.* 111 (2013) 247–252.
- [609] T. Kashiwagi, F. Du, K.I. Winey, K.M. Groth, J.R. Shields, S.P. Bellayer, H. Kim, J.F. Douglas, *Polymer* 46 (2005) 471–481.
- [610] S.S. Rahatekar, M. Zammarrano, S. Matko, K.K. Koziol, A.H. Windle, M. Nyden, T. Kashiwagi, J.W. Gilman, *Polym. Degrad. Stabil.* 95 (2010) 870–879.
- [611] J.H. Koo, *Polymer Nanocomposites Processing, Characterization and Applications*, McGraw-Hill, New York, NY, 2006.
- [612] Z. Wu, C. Zhou, R. Qi, *Polym. Compos.* 23 (2002) 634–643.
- [613] J.H. Koo, W.K. Chow, H. Stretz, A.C.K. Cheng, A. Bray, J. Weispfenning, in: *Proceedings SAMPE International Symposium, SAMPE, Covina, CA, (2003)*, pp. 954–963.
- [614] J.S. Tate, D. Kabakov, J.H. Koo, S.C. Lao, in: *Proceedings SAMPE International Symposium, Baltimore, MD, (2009)*, pp. 875–884.
- [615] A.R. Bahramian, M. Kokabil, M.H. Beheshty, M.H.N. Famili, *Iran Polym. J.* 16 (2007) 375–387.
- [616] M. Rallini, M. Natali, J.M. Kenny, L. Torre, *Polymer* 54 (2013) 5154–5165.
- [617] N. Ogata, S. Kawakage, T. Ogihara, *J. Appl. Polym. Sci.* 66 (1997) 573–581.
- [618] J. Billingham, C. Breen, J. Yarwood, *Vibr. Spectrosc.* 14 (1997) 19–34.
- [619] R. Levy, C.W. Francis, *J. Colloid Interface Sci.* 50 (1975) 442–450.
- [620] J. Wu, M.M. Lerner, *Chem. Mater.* 5 (1993) 835–838.
- [621] N. Ogata, G. Jimenez, H. Kawai, T. Ogihara, *J. Polym. Sci., B—Polym. Phys.* 35 (1997) 389–396.
- [622] G. Jimenez, N. Ogata, H. Kawai, T. Ogihara, *J. Appl. Polym. Sci.* 64 (1997) 2211–2220.
- [623] J. Tudor, L. Willington, D. O'Hare, B. Royan, *Chem. Commun.* 17 (1996) 2031–2032.
- [624] Ph. Dubois, M. Alexandre, F. Hindryckx, R. Jerome, *J. Macromol. Sci. R.M.C.* 38 (1998) 511–565.
- [625] H.R. Dennis, D. Hunter, D. Chang, S. Kim, D.R. Paul, *Polymer* 42 (2001) 9513–9522.
- [626] R.A. Vaia, K.D. Jant, E.J. Kramer, E.P. Giannelis, *Chem. Mater.* 8 (1996) 2628–2635.
- [627] A. Rehab, N. Salahuddin, *Mat. Sci. Eng. A—Struct.* 399 (2005) 368–376.
- [628] M. Kawasumi, M. Hasegawa, A. Usuki, A. Okada, *Macromolecules* 30 (1997) 6333–6338.
- [629] N. Hasegawa, M. Kawasumi, M. Kato, A. Usuki, A. Okada, *J. Appl. Polym. Sci.* 67 (1998) 87–92.
- [630] M. Kato, A. Usuki, A. Okada, *J. Appl. Polym. Sci.* 66 (1997) 1781–1785.
- [631] N. Hasegawa, H. Okamoto, M. Kato, A. Usuki, *J. Appl. Polym. Sci.* 78 (2000) 1918–1929.
- [632] D. Bikiaris, *Materials* 3 (2010) 2884–2946.
- [633] T. McNally, P. Potschke, *Polymer–Carbon Nanotube Composites—Preparation, Properties and Applications*, Woodhead Publishing Limited, Philadelphia, 2011.
- [634] N.G. Sahoo, S. Rana, J.W. Cho, L. Li, S.H. Chan, *Prog. Polym. Sci.* 35 (2010) 837–867.
- [635] A.M.K. Esawi, H.G. Salem, H.M. Hussein, A.R. Ramadan, *Polym. Compos.* 31 (2010) 772–780.
- [636] D. Bonduel, M. Mainil, M. Alexandre, F. Monteverde, Ph. Dubois, *Chem. Commun.* 6 (2005) 781–783.
- [637] V. Georgakilas, K. Kordatos, M. Prato, D. Guldi, M. Holzinger, A. Hirsch, *J. Am. Chem. Soc.* 124 (2002) 760–761.
- [638] J.N. Coleman, U. Khan, W.J. Blau, Y.K. Gunko, *Carbon* 44 (2006) 1624–1652.
- [639] A.L. Martínez-Hernández, C. Velasco-Santos, V.M. Castaño, *Curr. Nanosci.* 6 (2010) 12–39.
- [640] D. Baskaran, J. Mays, M. Bratcher, *Chem. Mater.* 17 (2005) 3389–3397.
- [641] N.R. Ravarikar, L.S. Schadler, A. Vijayaraghavan, Y. Zhao, B. Wei, P.M. Ajayan, *Chem. Mater.* 17 (2005) 974–983.
- [642] E.S. Choi, J.S. Brooks, D.L. Eaton, M.S. Al-Haij, M.Y. Hussaini, H. Garmestani, D. Li, K. Dahmen, *J. Appl. Phys.* 94 (2003) 6034–6039.
- [643] R.E. Gorga, R.E. Cohen, *J. Polym. Sci., B—Pol. Phys.* 42 (2004) 2690–2702.
- [644] F. Du, J.E. Fischer, K.I. Winey, *Phys. Rev. B: Condens. Matter* 72 (2005) 121404–121408.
- [645] P. Song, Z. Cao, Y. Cai, L. Zhao, Z. Fang, S. Fu, *Polymer* 52 (2011) 4001–4010.
- [646] P. Steurer, R. Wissert, R. Thomann, R. Mulhaupt, *Macromol. Rapid Commun.* 30 (2009) 316–327.
- [647] J.R. Potts, D.R. Dreyer, C.W. Bielawski, R.S. Ruoff, *Polymer* 52 (2011) 5–25.
- [648] A. Lerf, H. He, M. Forster, J. Klinowski, *J. Phys. Chem. B* 102 (1998) 4477.
- [649] Y. Matsuo, T. Miyabe, T. Fukutsuka, Y. Sugie, *Carbon* 45 (2007) 1005.
- [650] A.B. Bourlinos, D. Gournis, D. Petridis, T. Szabo, A. Szeri, I. Dekany, *Langmuir* 19 (2003) 6050.
- [651] Y. Matsuo, K. Watanabe, T. Fukutsuka, Y. Sugie, *Carbon* 41 (2003) 1545.
- [652] O.C. Compton, D.A. Dikin, K.W. Putz, L.C. Brinson, S.T. Nguyen, *Adv. Mater.* 22 (2010) 892.
- [653] A.B. Bourlinos, D. Gournis, D. Petridis, T. Szabo, A. Szeri, I. Dekany, *Langmuir* 19 (2003) 6050.
- [654] Y. Matsuo, T. Miyabe, T. Fukutsuka, Y. Sugie, *Carbon* 45 (2007) 1005.
- [655] D. Nuvoli, V. Alzari, R. Sanna, S. Scognamillo, M. Piccinini, L. Peponi, J.M. Kenny, A. Mariani, *Nanoscale Res. Lett.* 2012 (7) (2012) 674–680, <http://dx.doi.org/10.1186/1556-276X-7-674>.
- [656] B.L. Groenendaal, F. Jonas, D. Freitag, H. Pielartzik, J.R. Reynolds, *Adv. Mater.* 12 (2000) 481–494.
- [657] Y.F. Xu, Y. Wang, J.J. Liang, Y. Huang, Y.F. Ma, X.J. Wan, Y.S. Chen, *Nano Res.* 2 (2009) 343–348.
- [658] W.J. Hong, Y.X. Xu, G.W. Lu, C. Li, G.Q. Shi, *Electrochem. Commun.* 10 (2008) 1555–1558.
- [659] S. Bittolo Bon, L. Valentini, J.M. Kenny, *Chem. Phys. Lett.* 494 (2010) 264–268.
- [660] R.H. Baney, M. Itoh, A. Sakakibara, T. Suzuki, *Chem. Rev.* 95 (1995) 1409–1430.
- [661] A. Fina, O. Monticelli, G. Camino, *J. Mater. Chem.* 20 (2010) 9297–9305.
- [662] O. Monticelli, A. Fina, A. Ullah, P. Waghmare, *Macromolecules* 42 (2009) 6614–6623.
- [663] L. Valentini, S. Bittolo Bon, O. Monticelli, J.M. Kenny, *J. Mater. Chem.* 22 (2012) 6213.
- [664] Y. Xue, Y. Liu, F. Lu, J. Qu, H. Chen, L. Dai, *J. Phys. Chem. Lett.* 3 (2012) 1607.
- [665] M.S. Spector, E. Narango, S. Chiruvolu, J.A. Zasadzinski, *Phys. Rev. Lett.* 73 (1994) 2867–2870.
- [666] C. Wang, L. Feng, H. Yang, G. Xin, W. Li, J. Zheng, W. Tian, X. Li, *Phys. Chem. Chem. Phys.* 14 (2012) 13233–13238.
- [667] L. Zhang, Z. Wang, C. Xu, Y. Li, J. Gao, W. Wang, Y. Liu, *J. Mater. Chem.* 21 (2011) 10399–10406.
- [668] M. Fang, K. Wang, H. Lu, Y. Yang, S. Nutt, *J. Mater. Chem.* 19 (2009) 7098–7105.
- [669] H. Kim, Y. Miura, C.M. Macosko, *Chem. Mater.* 22 (2010) 3441–3450.
- [670] J.Y. Jang, M.S. Kim, H.M. Jeong, C.M. Shin, *Compos. Sci. Technol.* 69 (2009) 186–191.
- [671] N. Liu, F. Luo, H. Wu, Y. Liu, C. Zhang, J. Chen, *Adv. Funct. Mater.* 18 (2008) 1518–1525.
- [672] H.C. Schniepp, J.-L. Li, M.J. McAllister, H. Sai, M. Herrera-Alonso, D.H. Adamson, R.K. Prud'homme, R. Car, D.A. Saville, I.A. Aksay, *J. Phys. Chem. B* 110 (2006) 8535–8539.
- [673] M.J. McAllister, J.-L. Li, D.H. Adamson, H.C. Schniepp, A.A. Abdala, J. Liu, M. Herrera-Alonso, D.L. Milius, R. Car, R.K. Prud'homme, I.A. Aksay, *Chem. Mater.* 19 (2007) 4396–4404.
- [674] G. Wang, X. Shen, B. Wang, J. Yao, J. Park, *Carbon* 47 (2009) 1359–1364.
- [675] P. Liu, K. Gong, P. Xiao, M. Xiao, *J. Mater. Chem.* 10 (2000) 933–935.
- [676] W.-P. Wang, C.-Y. Pan, *Polym. Eng. Sci.* 44 (2004) 2335–2339.

- [677] Y.R. Lee, A.V. Raghu, H.M. Jeong, B.K. Kim, *Macromol. Chem. Phys.* 210 (2009) 1247–1254.
- [678] Y. Yang, J. Wang, J. Zhang, J. Liu, X. Yang, H. Zhao, *Langmuir* 25 (2009) 11808–11814.
- [679] H.J. Salavagione, M.A. Gomez, G. Martinez, *Macromolecules* 42 (2009) 6331–6334.
- [680] D.A. Nguyen, Y.R. Lee, A.V. Raghu, H.M. Jeong, C.M. Shin, B.K. Kim, *Polym. Int.* 58 (2009) 412–417.
- [681] R.K. Prud'homme, B. Ozbas, I.A. Aksay, R.A. Register, D.H. Adamson, W.O. Patent 2008045778 A1, 2008.
- [682] H. Kim, C.W. Macosko, *Polymer* 50 (2009) 3797–3809.
- [683] K. Wakabayashi, C. Pierre, D.A. Dikin, R.S. Ruoff, T. Ramanathan, L.C. Brinson, J.M. Torkelson, *Macromolecules* 41 (2008) 1905–1908.
- [684] S. Sun, Y. Cao, J. Feng, P. Wu, *J. Mater. Chem.* 20 (2010) 5605–5607.
- [685] E. Tkalya, M. Ghislandi, A. Alekseev, C. Koning, J. Loos, *J. Mater. Chem.* 20 (2010) 3035–3039.
- [686] R. Wissert, P. Steurer, S. Schopp, R. Thomann, R. Mülhaupt, *Macromol. Mater. Eng.* 295 (2010) 1107–1115.
- [687] X.Y. Qi, D. Yan, Z. Jiang, Y.K. Cao, Z.Z. Yu, F. Yavari, N. Koratkar, *ACS Appl. Mater. Interfaces* 3 (2011) 3130–3133.
- [688] V.H. Pham, T.V. Cuong, T.T. Dang, S.H. Hur, B.-S. Kong, E.J. Kim, E.W. Shina, J.S. Chung, *J. Mater. Chem.* 21 (2011) 11312–11316.
- [689] S. Bittolo Bon, L. Valentini, J.M. Kenny, *Express Polym. Lett.* 5 (2011) 819–824.
- [690] J.V. Seppala, *Express Polym. Lett.* 6 (2012) 257–344.
- [691] A. Bhatnagar, M. Sain, *J. Reinf. Plast. Comp.* 24 (2005) 1259–1268.
- [692] A.P. Mathew, A. Dufresne, *Biomacromolecules* 3 (2002) 609–617.
- [693] V. Favier, H. Chanzy, J.Y. Cavaille, *Macromolecules* 28 (1995) 6365–6367.
- [694] E. Ten, L. Jiang, M.P. Wolcott, in: K.H.M. Kan, J. Li, K. Wijesekera, E.D. Cranston (Eds.), *Functional Materials from Renewable Sources*, ACS Symposium Series, Vol. 1107, 2012, pp. 17–36, <http://dx.doi.org/10.1021/bk-2012-1107>.
- [695] I. Kvien, K. Oksman, *Appl. Phys. A—Mater. Sci. Process* 87 (2007) 641–643.
- [696] L. Petersson, I. Kvien, K. Oksman, *Compos. Sci. Technol.* 67 (2007) 2535–2544.
- [697] D. Bondeson, K. Oksman, *Compos., A: Appl. Sci.* 38 (2007) 2486–2492.
- [698] K. Okubo, T. Fujii, E.T. Thostenson, *Compos., A: Appl. Sci.* 40 (2009) 469–475.
- [699] J.R. Capadona, O. Van Den Berg, L.A. Capadona, M. Schroeter, S.J. Rowan, D.J. Tyler, *Nat. Nanotechnol.* 2 (2007) 765–769.
- [700] J.R. Capadona, K. Shamuganathan, S. Triftschuh, S. Seidel, S.J. Rowan, C. Weder, *Biomacromolecules* 10 (2009) 712–716.
- [701] O. Van den Berg, J.R. Capadona, C. Weder, *Biomacromolecules* 8 (2007) 1353–1357.
- [702] N. Ljungberg, J.Y. Cavaille, L. Heux, *Polymer* 47 (2006) 6285–6292.
- [703] A.J. De Menezes, G. Siqueira, A.A.S. Curvelo, A. Dufresne, *Polymer* 50 (2009) 4552–4563.
- [704] M. Grunert, W.T. Winter, *J. Polym. Environ.* 10 (2002) 27–30.
- [705] Y. Habibi, A.L. Goffin, N. Schiltz, E. Duquesne, Ph. Dubois, A. Dufresne, *J. Mater. Chem.* 18 (2008) 5002–5010.
- [706] K.H.M. Kan, J. Li, K. Wijesekera, E.D. Cranston, *Biomacromolecules* 14 (2013) 3130–3139.
- [707] G. Siqueira, J. Bras, A. Dufresne, *Langmuir* 26 (2010) 402–411.
- [708] M.A. Hubbe, O.J. Rojas, L.A. Lucia, M. Sain, *Bioresources* 3 (2008) 929–980.
- [709] R.J. Moon, A. Martini, J. Nairn, J. Simonsen, J. Youngblood, *Chem. Soc. Rev.* 40 (2011) 3941–3994.
- [710] E. Fortunati, F. Luzzi, D. Puglia, A. Terenzi, M. Vercellino, L. Visai, C. Santulli, L. Torre, J.M. Kenny, *Carbohydr. Polym.* 97 (2013) 837–848.
- [711] M. Jonoobi, J. Harun, A.P. Mathew, K. Oksman, *Compos. Sci. Technol.* 70 (2010) 1742–1747.
- [712] E. Fortunati, M. Peltzer, I. Armentano, L. Torre, A. Jiménez, J.M. Kenny, *Carbohydr. Polym.* 90 (2012) 948–956.
- [713] E. Fortunati, I. Armentano, Q. Zhou, A. Iannoni, E. Saino, L. Visai, L.A. Berglund, J.M. Kenny, *Carbohydr. Polym.* 87 (2012) 1596–1605.
- [714] K. Kalaitzidou, F. Hukushima, L.T. Drzal, *Compos. Sci. Technol.* 67 (2010) 2045–2051.
- [715] D. Lentz, R. Pyles, R. Hedden, *Polym. Eng. Sci.* 50 (2010) 120–127.
- [716] J. Gou, J. Zhuge, F. Liang, Processing of polymer nanocomposites, in: S.G. Advani, K.-T. Hsiao (Eds.), in: *Manufacturing techniques for polymer matrix composites*, Woodhead Publishing, Sawston, Cambridge, UK, 2012, pp. 95–115.
- [717] J.M. Garces, D.J. Moll, J. Bicerano, R. Fibiger, D.G. McLeod, *Adv. Mater.* 12 (2000) 1835–1839.
- [718] W. Zhao, M. Li, H.X. Peng, *Macromol. Mater. Eng.* 295 (2010) 838–845.
- [719] E. Ritzraupt-Kleissl, J. Boehm, J. Hausselt, T. Hanemann, *Mater. Sci. Eng.* 26 (2006) 1067–1071.
- [720] K.P. Ryan, M. Cadek, V. Nicolosi, D. Blond, M. Ruether, G. Armstrong, H. Swan, A. Fonseca, J.B. Nagy, W.K. Maser, W.J. Blau, J.N. Coleman, *Compos. Sci. Technol.* 67 (2007) 1640–1649.
- [721] M.A.S. Azizi Samir, F. Alloin, M. Paillet, A. Dufresne, *Macromolecules* 37 (2004) 4313–4316.
- [722] A. Bendahou, Y. Habibi, H. Kaddami, A. Dufresne, *J. Biobased Mater. Biol.* 3 (2009) 81–90.
- [723] D.M. Panaitescu, A.N. Frone, M. Ghiurea, C.I. Spataru, C. Radovici, M. Doina Iorga, in: Brahim Attaf (Ed.), *Properties of Polymer Composites with Cellulose Microfibrils. Advances in Composite Materials—Ecodesign and Analysis*, 2011, ISBN: 978-953-307-150-3.
- [724] A. Dufresne, *Can. J. Chem.* 86 (2008) 484–494.
- [725] D.R. Paul, L.M. Robeson, *Polymer* 49 (2008) 3187–3204.
- [726] G. Malucelli, F. Carosio, J. Alongi, A. Fina, A. Frache, G. Cammino, *Mater. Sci. Eng. R* 84 (2014) 1–20.
- [727] G. Siqueira, J. Bras, N. Follain, S. Belbekhouche, S. Marais, A. Dufresne, *Carbohydr. Polym.* 91 (2013) 711–717.
- [728] T. McNally, P. Potschke, P. Halley, M. Murphy, D. Martin, S. Bell, G. Brennan, D. Bein, P. Lemoine, J.P. Quinn, *Polymer* 46 (2005) 8222–8232.
- [729] J. Lange, Y. Wyser, *Packag. Technol. Sci.* 16 (2003) 149–158.
- [730] L.E. Nielsen, J. *Macromol. Sci. Chem. A* 1 (5) (1967) 929–942.
- [731] S.S. Ray, M. Okamoto, *Prog. Polym. Sci.* 28 (2003) 1539–1641.
- [732] H.M.C. Azeredo, H.L.C. Mattoso, R.J. Avena-Bustillos, G. Ceotto Filho, M.L. Mumford, D. Wood, T.H. McHugh, *J. Food. Sci.* 75 (2010) N1–N7.
- [733] P.R. Chang, R. Jian, P. Zheng, J. Yu, X. Ma, *Carbohydr. Polym.* 79 (2010) 301–305.
- [734] A.G. Gibson, A.P. Mouritz (Eds.), *Fire Properties of Polymer Composite Materials*, Series: Solid mechanics and its applications, vol. 143, Springer, Berlin, Heidelberg, 2007.
- [735] L. Wang, X. He, C.A. Wilkie, *Materials* 3 (2010) 4580–4606.
- [736] S. Bourbigot, S. Duquesne, G. Fontaine, S. Bellayer, T. Turf, F. Samyna, *Mol. Cryst. Liq. Cryst.* 486 (2008) 325–339.
- [737] A. O'Mullane, S. Dale, J. Macpherson, P.R. Unwin, *Chem. Commun.* 21 (2004) 1606–1607.
- [738] R. Ngece, N. West, M. Ndangili, R. Olowu, A. Williams, N. Hendricks, S. Mailu, P. Baker, E. Iwuoha, *Int. J. Electrochem. Sci.* 6 (2011) 1820–1834.
- [739] R. Tseng, J. Huang, J. Ouyang, R. Kaner, Y. Yang, *Nano Lett.* 5 (2005) 1077–1080.
- [740] P. Kishore, B. Viswanathan, T. Varadarajan, *Nanoscale Res. Lett.* 3 (2007) 14–20.
- [741] P. Dallas, V.K. Sharma, R. Zboril, *Adv. Colloid Interface Sci.* 166 (2011) 119–135.
- [742] H. Monteiro Cordeiro de Azeredo, L.H. Capparelli Mattoso, T. Habig McHugh, in: Boredy Reddy (Ed.), *Nanocomposites in Food Packaging—A Review*, Advances in Diverse Industrial Applications of Nanocomposites, 2011, ISBN: 978-953-307-202-9.
- [743] M.M. Reddy, S. Vivekanandhan, M. Misra, S.K. Bhatia, A.K. Mohanty, *Prog. Polym. Sci.* 38 (2013) 1653–1689.
- [744] M. Nogi, H. Yano, *Adv. Mater.* 20 (2008) 1849–1852.
- [745] B.D. Ratner, A.S. Hoffman, F.J. Schoer, J.E. Lemons, *Biomaterials Science: An Introduction to Materials in Medicine*, Elsevier Academic Press, London, 2004.
- [746] A.B. Strong, *Fundamentals of Composites Manufacturing: Materials, Methods and Applications*, second ed., SME, Dearborn, MI, 2008.
- [747] P.K. Mallick, *Fiber-Reinforced Composites*, third ed., CRC Press, New York, 2008.
- [748] P. Ermanni, C. Di Fratta, F. Trochu, in: L. Nicolais, A. Borzacchiello (Eds.), *Wiley Encyclopedia of Composites*, second ed., John Wiley & Sons, Inc., Chichester, UK, 2012.
- [749] W.J. Benjaminn, S.W. Beckwitt, *Resin Transfer Molding*, SAMPE Monograph no. 3, SAMPE Press, Covina, CA, USA, 1998.
- [750] M. Monti, M. Natali, R. Petrucci, D. Puglia, A. Terenzi, L. Valentini, J.M. Kenny, in: L. Nicolais, A. Borzacchiello (Eds.), *Wiley Encyclopedia of Composites*, second ed., John Wiley & Sons, Inc., Chichester, UK, 2012.
- [751] M. Norkhairunnisa, A. Bakar Azhar, C. Wen Shyang, *Polym. Int.* 56 (2007) 512–517.
- [752] L.N. Chang, W.S. Chow, *J. Comp. Mater.* 12 (2010) 1421–1434.
- [753] L. Torre, R. Petrucci, J.M. Kenny, SAMPE e Conference, Long Beach, CA, 2008.
- [754] M. Monti, M. Natali, R. Petrucci, J.M. Kenny, L. Torre, *J. App. Polym. Sci.* 122 (2011) 2829–2836.
- [755] M.H.G. Wichmann, J. Sumfleth, F.H. Gojny, M. Quaresimin, B. Fiedler, K. Schulte, *Eng. Fract. Mech.* 73 (2006) 2346–2359.
- [756] E.T. Thostenson, T.W. Chou, *Adv. Mater.* 18 (2006) 2837–2841.
- [757] L.M. Gao, E.T. Thostenson, Z.G. Zhang, T.W. Chou, *Adv. Funct. Mater.* 19 (2009) 123–130.
- [758] E.T. Thostenson, T.W. Chou, *Nanotechnology* 19 (2008) 215713–215721.
- [759] A. Haque, M. Shamsuzzoha, F. Hussain, D. Dean, *J. Comp. Mater.* 37 (2003) 1821–1883.
- [760] C. Lekakou, A. Hearn, A.K. Murugesh, B. Le Page, *Mater. Sci. Technol.* 23 (2007) 487–491.
- [761] T.S. Sene, L.V. da Silva, S.C. Amico, D. Becker, A.M. Ramirez, L.A.F. Coelho, *Mat. Res.* 16 (2013) 1128–1133.
- [762] N. Kchit, F. Bensadoun, T. Carrozani, C. Billotte, E. Ruiz, F. Trochu, 10th International Conference on Flow Processes in Composite Materials (FPCM10), July 11–15, Monte Verità, Ascona, CH, 2010.
- [763] S. Spindler-Ranta, C.E. Bakis, in: *Proceedings of 47th International SAMPE Symposium*, 47, 2002, pp. 1775–1884.
- [764] T. Yokozeki, Y. Iwahori, S. Ishiwata, *Composites, A—Appl. Sci. Manuf.* 38 (2007) 917–924.
- [765] W. Chen, H. Shen, M.L. Auad, C. Huang, S. Nutt, *Composites, A—Appl. Sci. Manuf.* 40 (2009) 1082–1089.
- [766] I. Srikanth, A. Daniel, S. Kumar, N. Padmavathi, V. Singh, P. Ghosal, A. Kumar, G. Rohini Devi, *Scr. Mater.* 63 (2010) 200–203.
- [767] Miravete de Marco A., Guzman de Villoria R. Nanoreinforcement prepreg method and product thus obtained, European Patent EP2000494A1, 2007.
- [768] J.E. Garcia, B.L. Wardle, A.J. Hart, *Composites, A—Appl. Sci. Manuf.* 39 (2008) 1065–1070.
- [769] K. Adhikari, P. Hubert, B. Simard, A. Johnston, 47th AIAA structures, dynamics, and materials conference proceedings, May 1–4, Newport, RI, 2006 [AIAA-2006-1855-604].
- [770] G. Zhou, S. Mowa, L.J. Lee, *Polym. Comp.* 30 (2009) 860–865.
- [771] A. Khattab, P. Zhang, W. Shou, M.J. Khattak, *Polym. Comp.* 34 (2013), <http://dx.doi.org/10.1002/polc.22816> (2013) article first published online 28 DEC.
- [772] A. Usuki, A.Y. Kojima, M. Kawasumi, A. Okada, Y. Fukushima, T. Kurauchi, O. Kamigaito, *J. Mater. Res.* 8 (1993) 1179–1184.
- [773] T. Lan, T. Pinnavaia, *Chem. Mater.* 6 (1994) 2216–2219.
- [774] T. Tanaka, G.C. Montanari, R. Mulhaupt, *IEEE Trans.* 11 (2004) 763–784.

- [775] A. Sorrentino, G. Gorrasí, V. Vittoria, *Trends Food Sci. Technol.* 18 (2007) 84–95.
- [776] M.J.A. Hore, R.J. Composto, *Macromolecules* (2014), <http://dx.doi.org/10.1021/ma79w4021>.
- [777] J. Njuguna (Ed.), *Structural Nanocomposites, Perspectives for Future Applications*, Series: *Engineering Materials*, VIII, 2013, 269 p. ISBN: 978-3-642-40322-4.
- [778] I. Armentano, M. Dottori, E. Fortunati, S. Mattioli, J.M. Kenny, *Polym. Degrad. Stabil.* 95 (2010) 2126–2146.
- [779] N.H. Kim, S.V. Malhotra, M. Xanthos, *Microporous Mesoporous Mater.* 96 (2006) 29–35.
- [780] S. Livi, G. Sar, V. Bugatti, E. Espuche, J. Duchet-Rumeau, *RSC Adv.* (2014), <http://dx.doi.org/10.1039/C4RA02143F> (2014) available online 04 Jun.
- [781] B. Dervaux, F. Meyer, J.-M. Raquez, A. Olivier, F.E. Du Prez, P. Dubois, *Macromol. Chem. Phys.* 213 (2012) 1259–1265.
- [782] S.P. Lonkar, A. Bobenrieth, J. De Winter, P. Gerbaux, J.-M. Raquez, P. Dubois, *J. Mater. Chem.* 22 (2012) 18124–18126, <http://dx.doi.org/10.1039/C2JM4323>.
- [783] Y.-K. Yang, C.-E. He, R.-G. Peng, A. Baji, X.-S. Du, Y.-L. Huang, X.-L. Xie, Y.-W. Mai, *J. Mater. Chem.* 22 (2012) 5666–5675, <http://dx.doi.org/10.1039/C2JM6D1600>.
- [784] D. Mecerreyres, *Prog. Polym. Sci.* 36 (2011) 1629–1648.
- [785] L. Zhao, Y. Li, X. Cao, J. You, W. Dong, *Nanotechnology* 23 (2012) 255702, <http://dx.doi.org/10.1088/0957-4484/23/25/255702>.
- [786] N. Singh, K.K. Koziol, J. Chen, A.J. Patil, J.W. Gilman, P.C. Trulove, W. Kafienah, S.S. Rahatekar, *Green Chem.* 15 (2013) 1192–1202, <http://dx.doi.org/10.1039/C3GC37087A>.
- [787] C. Zhu, J. Chen, K.K. Koziol, J.W. Gilman, P.C. Trulove, S.S. Rahatekar, *Express Polym. Lett.* 8 (2014) 154–163, <http://dx.doi.org/10.3144/expresspolymlett.2014.19>.
- [788] D.L. Tomasko, X. Han, D. Liu, W. Gao, *Curr. Opin. Solid State Mater. Sci.* 7 (2003) 407–412.
- [789] S. Horsch, G. Serhatkulu, E. Gulari, R.M. Kannan, *Polymer* 47 (2006) 7485–7496.
- [790] T. Hasell, in: L. Nicolais, G. Carotenuto (Eds.), *Nanocomposites: In Situ Synthesis of Polymer-Embedded Nanostructures*, John Wiley & Sons, Inc., Hoboken, NJ, 2013, pp. 1–43, <http://dx.doi.org/10.1002/9781118742655.ch1>, in press.
- [791] A. Tsimpliaraki, I. Tsivintzelis, S.I. Marras, I. Zuburtikidis, C. Panayiotou, *J. Supercrit. Fluids* 81 (2013) 86–91.
- [792] A. Javadi, Y. Srithep, C.C. Clemons, L.-S. Turng, S. Gong, *J. Mater. Res.* 27 (2012) 1506–1517, <http://dx.doi.org/10.1557/jmr.2012.74>.
- [793] F. Yang, M. Manitius, R. Kriegel, R.M. Kannan, *Polymer* (2014), <http://dx.doi.org/10.1016/j.polymer.2014.05.020> (2014) available on line 1 June.
- [794] B.M. Novak, *Adv. Mater.* 5 (1993) 422–433, <http://dx.doi.org/10.1002/adma.19930050603>.
- [795] R. Vendamme, S.-Y. Onoue, A. Nakao, T. Kunitake, *Nat. Mater.* 5 (2006) 494–501, <http://dx.doi.org/10.1038/nmat1655>.
- [796] K. Vallé, P. Belleville, F. Pereira, C. Sanchez, *Nat. Mater.* 5 (2006) 107–111, <http://dx.doi.org/10.1038/nmat1570>.
- [797] S.-W. Kuo, F.-C. Chang, *Prog. Polym. Sci.* 36 (2011) 1649–1696.
- [798] L. Zhao, Z.-L. Zhou, Z. Guo, G. Gibson, J.A. Brug, S. Lam, J. Pei, S.S. Mao, *J. Mater. Res.* 27 (2012) 639–652.
- [799] G. Poologasundarampillai, B. Yu, O. Tsigkou, E. Valliant, S. Yue, P.D. Lee, R.W. Hamilton, M.M. Stevens, T. Kasuga, J.R. Jones, *Soft Matter* 8 (2012) 4822–4832, <http://dx.doi.org/10.1039/C2SM00033D>.
- [800] C. Stamatopoulou, P. Klonos, S. Koutsoumpis, V. Gun'ko, P. Pissis, L. Karabanova, *J. Polym. Sci. Pol. Phys.* 52 (2014) 397–408, <http://dx.doi.org/10.1002/polb.23427>.
- [801] W. Lin, K.-S. Moon, C.P. Wong, *Adv. Mater.* 21 (2009) 2421–2424, <http://dx.doi.org/10.1002/adma.200803548>.
- [802] S. Hatori, R. Matsuzaki, A. Todoroki, *Compos. Sci. Technol.* 92 (2014) 9–15.
- [803] S. Chen, J. Sui, L. Chen, A. John, Pojman, *J. Polym. Sci. Chem.* 43 (2005) 1670–1680, <http://dx.doi.org/10.1002/pola.20628>.
- [804] A. Mariani, V. Alzari, O. Monticelli, J.A. Pojman, G. Caria, *J. Polym. Sci. Chem.* 45 (2007) 4514–4521, <http://dx.doi.org/10.1002/pola.22185>.
- [805] A. Mariani, S. Bidali, G. Caria, O. Monticelli, S. Russo, J.M. Kenny, *J. Polym. Sci. Chem.* 45 (2007) 2204–2211, <http://dx.doi.org/10.1002/pola.21987>.
- [806] Y. Fang, L. Chen, C.-F. Wang, S. Chen, *J. Polym. Sci. Chem.* 48 (2010) 2170–2177, <http://dx.doi.org/10.1002/pola.23986>.
- [807] V. Alzari, D. Nuvoli, S. Scognamillo, M. Piccinini, E. Giuffredi, G. Malucelli, S. Marceddu, M. Sechi, V. Sanna, A. Mariani, *J. Mater. Chem.* 21 (2011) 8727–8733, <http://dx.doi.org/10.1039/C1JM11076D>.
- [808] V. Alzari, D. Nuvoli, R. Sanna, S. Scognamillo, M. Piccinini, J.M. Kenny, G. Malucelli, A. Mariani, *J. Mater. Chem.* 21 (2011) 16544–16549, <http://dx.doi.org/10.1039/C1JM12104A>.
- [809] V. Mittal, *Polymer Nanocomposite Foams*, CRC Press, Taylor & Francis Group, Boca Raton, FL, 2014.
- [810] K. Piechowski, J. Njuguna, S. Michałowski, in: J.K. Pandey, K.R. Reddy, A.K. Mohanty, M. Misra (Eds.), *Handbook of Polymer Nanocomposites. Processing, Performance and Application. Volume A: Layered Silicates*, Springer, Berlin, Heidelberg, 2014, pp. 453–479, ISBN: 4 978-3-642-38648-0.
- [811] S. Longo, M. Mauro, C. Daniel, M. Galimberti, G. Guerra, *Front. Chem.* 13 (2013) 1–28, <http://dx.doi.org/10.3389/fchem.2013.00028>.
- [812] R. Hernández, A. Nogales, M. Sprung, C. Mijangos, T.A. Ezquerro, *J. Chem. Phys.* 140 (2014) 024909, <http://dx.doi.org/10.1063/1.4861043>.
- [813] D.J. Boday, P.Y. Keng, B. Muriathi, J. Pyun, D.A. Loy, *J. Mater. Chem.* 20 (2010) 6863–6865, <http://dx.doi.org/10.1039/C0JM01448F>.
- [814] Z.-M. Huang, Y.-Z. Zhang, M. Kotakic, S. Ramakrishnab, *Compos. Sci. Technol.* 63 (2003) 2223–2253.
- [815] M. Cakmak, S. Batra, B. Yalcin, *Polym. Eng. Sci.* (2014), <http://dx.doi.org/10.1002/pen.23861> (2014) available online 6 FEB.
- [816] J. Marzouk, B. Lucas, T. Trigaud, A. Pothier, J. Bouclé, B. Ratier, *Polym. Int.* (2014), <http://dx.doi.org/10.1002/pi.4686> (2014) available on line 6 FEB.
- [817] D. Fragouli, A. Das, C. Innocenti, Y. Guttikonda, S. Rahman, L. Liu, V. Caramia, C.M. Megaridis, A. Athanassiou, *ACS Appl. Mater. Interfaces* 6 (2014) 4535–4541, <http://dx.doi.org/10.1021/am500335u>.
- [818] F. Perineau, C. Rosticher, L. Rozes, C. Chanéac, C. Sanchez, D. Constantin, I. Dozov, P. Davidson, C. Rochas, *ACS Appl. Mater. Interfaces* 6 (2014) 1583–1588, <http://dx.doi.org/10.1021/am404313s>.
- [819] K.J. Green, D.R. Dean, U.K. Vaidya, E. Nyairo, *Composites, A—Appl. Sci. Manuf.* 40 (2009) 1470–1475.
- [820] A.N. Karwa, T.J. Barron, V.A. Davis, B.J. Tatarchuk, *Nanotechnology* 23 (2012) 185601, <http://dx.doi.org/10.1088/0957-4484/23/18/185601>.
- [821] A. Terenzi, C. Vedova, G. Lelli, J. Mijovic, L. Torre, L. Valentini, J.M. Kenny, *Compos. Sci. Technol.* 68 (2008) 1862–1868.
- [822] G. Lelli, A. Terenzi, J.M. Kenny, L. Torre, *Polym. Compos.* 30 (2009) 1–12, <http://dx.doi.org/10.1002/pc.20517>.
- [823] J. Liu, Y. Gao, D. Cao, L. Zhang, Z. Guo, *Langmuir* 27 (2011) 7926–7933, <http://dx.doi.org/10.1021/la201073>.
- [824] W. Bahloul, O. Oddes, V. Bounor-Legaré, F. Mélis, P. Cassagnau, B. Vergnes, *AIChE J.* 57 (2011) 2174–2184, <http://dx.doi.org/10.1002/aic.12425>.
- [825] J.R. Potts, O. Shankar, L. Du, R.S. Ruoff, *Macromolecules* 45 (2012) 6045–6055, <http://dx.doi.org/10.1021/ma300706k>.